MASTERARBEIT | MASTER'S THESIS

Titel | Title

DNA Methylation Analysis of MGMT Enhancers in Brain Metastases

verfasst von | submitted by

Benno Daniel Fehringer BSc

angestrebter akademischer Grad | in partial fulfilment of the requirements for the degree of

Master of Science (MSc)

Wien | Vienna, 2025

Studienkennzahl lt. Studienblatt | Degree programme code as it appears on the student record sheet:	UA 066 862
Studienrichtung lt. Studienblatt | Degree programme as it appears on the student record sheet:	Masterstudium Chemie
Betreut von | Supervisor:	Univ.-Prof. Mag. Dr. Margit Cichna-Markl

Abstract

This study addresses the correlation between O6-methylguanine-DNA-methyltransferase (MGMT) enhancer methylation and MGMT protein expression. A profound understanding of such biological interplay can lead to improvements in personalised therapy for various cancer types using cytostatic agents such as temozolomide (TMZ). This is because MGMT can interfere with the response to these agents by repairing alkylation lesions that are intended to destroy cancer cells. The goal is to predict MGMT expression based on enhancer methylation to determine the optimal treatment strategy.

Since patients with brain metastases respond less effectively to TMZ than, for example, patients with glioblastoma, a deeper understanding of the underlying processes is required. For this reason, melanoma brain metastasis samples with different MGMT expression levels were analysed using pyrosequencing methods targeting MGMT enhancer regions. In total, 92 different cytosine-phosphate-guanine dinucleotide sites located in intergenic and intragenic enhancers were analysed.

Notably, a significant difference between these two genomic regions was observed. For intergenic enhancers, methylation levels were distributed evenly. However, the analysis of intragenic enhancers revealed much higher methylation levels in MGMT-expressing samples compared to non-expressing ones. Moreover, a significant positive correlation between MGMT expression and MGMT intragenic enhancer methylation was observed.

These findings, together with the MGMT promoter methylation status, could be used to predict TMZ responses more accurately, thereby improving treatment efficiency and preventing unnecessary side effects.

Additionally, this study investigated and compared two different methods for detecting 5-hydroxymethylcytosine: on the one hand, oxidative bisulfite sequencing and on the other hand chemically assisted pyridine borane sequencing. This modification of cytosine is formed through the oxidation of 5-methylcytosine and has significant implications in epigenetics, gene regulation, and cancer biology. For the comparison, both methods were applied to a set of standards containing cytosine, 5-methylcytosine, or 5-hydroxymethylcytosine. The results suggest that bisulfite-free chemically assisted pyridine borane sequencing is the more accurate and less complex method. While it does not rely on a second method like oxidative bisulfite sequencing, there is also no need to first optimise temperature settings for the base conversion.

Zusammenfassung

Diese Arbeit befasst sich mit der Korrelation zwischen der Methylierung von O6-Methylguanin-DNA-Methyltransferase (MGMT) Enhancern und der MGMT-Proteinexpression. Ein fundiertes Verständnis dieses biologischen Zusammenspiels kann zu einer Verbesserung personalisierter Therapie bei verschiedenen Krebsarten unter Verwendung von Zytostatika wie zum Beispiel mit Temozolomid beitragen. Dies liegt daran, dass MGMT die Wirkung dieser Medikamente abschwächen kann, indem es Alkylierungsschäden repariert, die zur Zerstörung von Krebszellen vorgesehen sind. Ziel ist es, anhand von Enhancer-Methylierungen die Expression von MGMT vorherzusagen und dadurch die bestmögliche Behandlungsstrategie zu ermitteln.

Da Patienten mit Hirnmetastasen weniger effektiv auf die Therapie mit Temozolomid ansprechen als beispielsweise Patienten mit Glioblastom, ist ein tieferes Verständnis der zugrundeliegenden Prozesse erforderlich. Zu diesen Zweck wurden Proben von Melanom-Hirnmetastasen mit unterschiedlicher MGMT-Expression mittels Pyrosequenzierung analysiert. Dabei wurden gezielt Enhancerregionen des MGMT-Gens untersucht. Insgesamt wurden 92 verschiedene Cytosin-Phosphat-Guanin Dinukleotide analysiert, wobei sowohl intragenische als auch intergenische Enhancer berücksichtigt wurden.

Zwischen diesen beiden Genomregionen konnte ein signifikanter Unterschied festgestellt werden. Während die intergenischen Regionen eine gleichmäßige Verteilung der Methylierungsgrade aufwiesen, zeigten die intragenischen Enhancer deutlich höhere Methylierungsgrade bei MGMT-exprimierenden Proben im Vergleich zu nicht-exprimierenden Proben. Darüber hinaus konnte eine signifikant positive Korrelation zwischen der MGMT-Expression und der Methylierung intragenischer MGMT Enhancer beobachtet werden.

Diese Erkenntnis könnte gemeinsam mit dem MGMT-Promotormethylierungsstatus dazu beitragen, das Ansprechen auf Temozolomid genauer vorherzusagen und somit die Behandlungseffizienz zu steigern sowie unnötige Nebenwirkungen zu verhindern.

Zusätzlich wurden in dieser Arbeit zwei aus der Literatur bekannte Methoden zur Detektion von 5-Hydroxymethylcytosin verglichen. Dabei handelt es sich einerseits um die oxidative Bisulfit-Sequenzierung und andererseits um die chemisch-assistierte Pyridin-Boran-Sequenzierung. Die modifizierte Form von Cytosin entsteht durch Oxidation von 5-Methylcytosin und spielt eine bedeutsame Rolle in der Epigenetik, Genregulation und Krebsbiologie. Für den Methodenvergleich wurden beide Verfahren auf eine Reihe an Standards angewendet, die Cytosin, 5-Methylcytosin oder 5-Hydroxymethylcytosin enthielten. Dabei zeigte sich, dass die bisulfitfreie, chemisch-assistierte Pyridin-Boran-Sequenzierung die genauere und weniger aufwändige Methode darstellt. Einerseits ist kein zusätzlicher Analyseschritt wie bei der oxidativen Bisulfit-Sequenzierung erforderlich, andererseits muss keine spezifische Temperatur vorab für die Basenkonvertierung optimiert werden.

Acknowledgment

At this moment, I would like to express my genuine appreciation to everyone who was part of my journey through this study.

First of all, I would like to thank Univ.-Prof. Mag. Dr. Margit Cichna-Markl, who gave me the opportunity to work in her group and supervised me through my entire Master's thesis.

I would also like to thank Katharina Pühringer, who took her time to explain all necessary procedures and working steps. I benefited greatly from her knowledge and experience.

Furthermore, I would like to express my gratitude to the whole working group.

In addition, I would like to thank our cooperation partner, Mag.[a] Dr.[in] Priv.Doz.in Sabine Spiegl-Kreinecker, Department of Neurosurgery, Kepler University Hospital, Johannes Kepler University, Linz, for providing samples from melanoma patients.

Last but not least, sincere gratitude to my parents; without their support, my entire education would not have been possible.

Table of contents

1 Introduction

Modern medicine is capable of achieving miracles every day. Whether in detecting and treating genetic defects, performing precision and minimally invasive surgery using robotic assistance, or carrying out intrauterine procedures on unborn children. Diseases once considered incurable have become routine tasks in hospitals or can even be treated by simply taking medications every other day. However, one disease still haunts human civilisation in the 21st century: cancer. Although significant process has already been made in treatment options and therapeutic outcomes, a cancer diagnosis is not taken lightly by anyone. For this reason, countless efforts are being made to treat cancer more effectively, be it understanding why cancer develops, how it evades the immune system, or optimizing established treatments. The latter is an objective of this study.

The following section begins with an overview of gene expression, including the structure of deoxyribonucleic acid (DNA). It then provides a brief explanation of epigenetics and DNA methylation as core process. Finally, to support understanding of this study, a basic overview of cancer treatment and the role of O6-methylguanine-DNA-methyltransferase (MGMT) is presented.

1. 1 Deoxyribonucleic acid

DNA is undeniably crucial to our current understanding of human life and of most living creatures on Earth. It is the material basis of our genetic information. However, it took many years to reach this realization after its initial discovery in 1869. This finding, which led to a breakthrough in genetic research, was accomplished by Swiss physiological chemist Friedrich Miescher, during his analysis of pus cells. He was able to detect a so far unknown phosphorus-rich chemical, which he named “nuclein” due to its discovery in the cell nucleolus. Miescher even hypothesized that this nuclein serves as the material basis of heredity. [1–3]

The term “nuclein” was later changed to “nucleic acid” and eventually to “deoxyribonucleic acid”, or “DNA”.[4] Further investigation by Russian biochemist Phoebus Levene led to the proposal that DNA is composed of a sequence of nucleotides. This “polynucleotide” model suggested that each nucleotide contained one of four nitrogen-containing bases, a phosphate group and a sugar molecule. [5]

The Austrian biochemist Erwin Chargaff later expanded on Levene's work. Inspired by Oswald Avery's demonstration that genes are composed of DNA[6], Chargaff reached another groundbreaking conclusion. He concluded that nearly all DNA shares certain properties, despite variations in its composition. Particularly, the amount of each nitrogen-containing base was not random. The sum of adenine (A) typically approximates the sum of thymine (T), and the amount of guanine (G) is generally similar to the amount of cytosine (C). Simply put, the overall total of purines (adenine and guanine) and the overall amount of pyrimidines (cytosine and thymine) are usually equal. [7]

One question was still unsolved: How is genetic information encoded in DNA? How can the nucleic acid sequence be linked to the formation of the 20 proteinogenic amino acids and further the creation of proteins? This problem known as the “genetic code challenge” was addressed by a large number of scientists and, among others, solved by Marshall Nirenberg, Philipp Leder and Heinrich Matthaei. Their work indicated a triplet-based genetic code. Each set of three DNA or RNA bases corresponds to one amino acid.[8,9]

1.1.2 The structure of DNA

The discovery of DNA's three-dimensional structure took many years and involved the contributions of many researchers. In the end, James Watson and Francis Crick, with crucial insights into X-ray crystallography from Rosalind Franklin, were able to propose a double-helical model for the structure of DNA. Their model consisted of four main characteristics. First, the two strands of the double helix are connected by hydrogen bonds, with adenine always pairing with thymine and cytosine always pairing with guanine. Second, with the exception of Z-DNA, the double helix of regular DNA is right-hand oriented. Additionally, the two strands are antiparallel, meaning they are oriented in opposite directions. Finally, the bases are partially exposed and available for potential binding with other DNA-interacting molecules.[4,10] Figure 1 illustrates the three-dimensional double-helix model proposed by Watson and Crick. Additionally, the structure of RNA is provided.

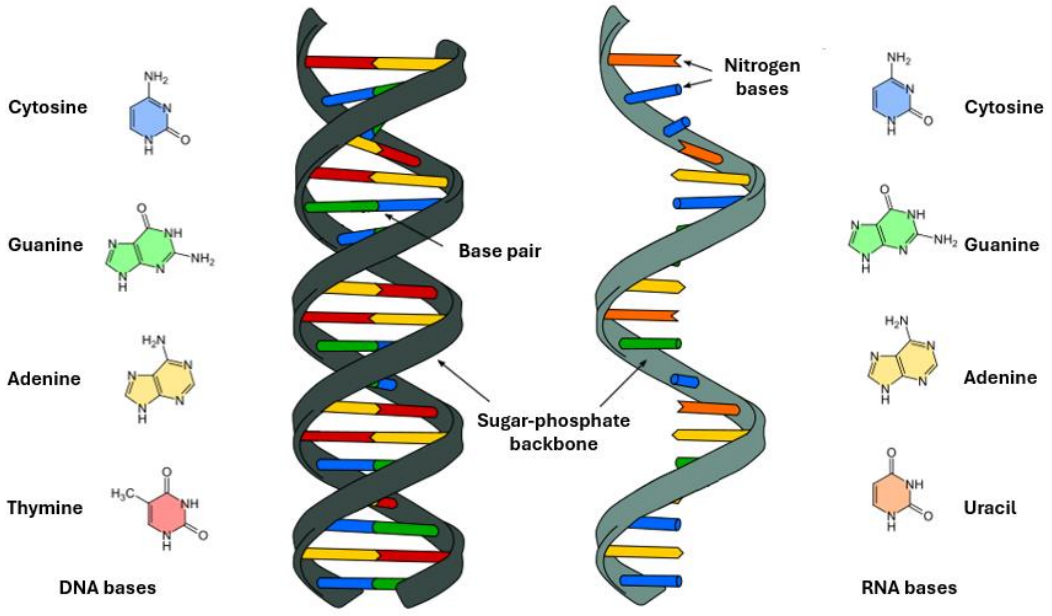

***Figure 1**: Double-helix model for the structure of DNA and single-stranded structure of RNA; modified from [11]*

1.1.3 Gene expression and its regulatory regions

The genetic information is stored in so-called genes. These genes encode protein molecules, which can be considered the "workhorses" of cells. All functions necessary for life are carried out by proteins. Enzymes that synthesize new cellular components or metabolise nutrients, as well as DNA polymerases and other enzymes involved in DNA replication, are all proteins. [12]

The expression of a gene is simply the production of its corresponding protein. This fundamental process consists of two major steps and is shown in Figure 2. First, the genetic information stored in DNA is transferred to a molecule known as messenger RNA (mRNA). This process, called transcription, is catalysed by an enzyme called RNA polymerase II, using DNA as a template for complementary base pairing. The resulting pre-mRNA is then processed into mature mRNA. This single-stranded nucleic acid serves as a template in the second step, known as translation. According to the genetic code, each group of three bases corresponds to a specific amino acid. The mRNA acts as a template to generate a chain of amino acids, which ultimately forms a protein.[12]

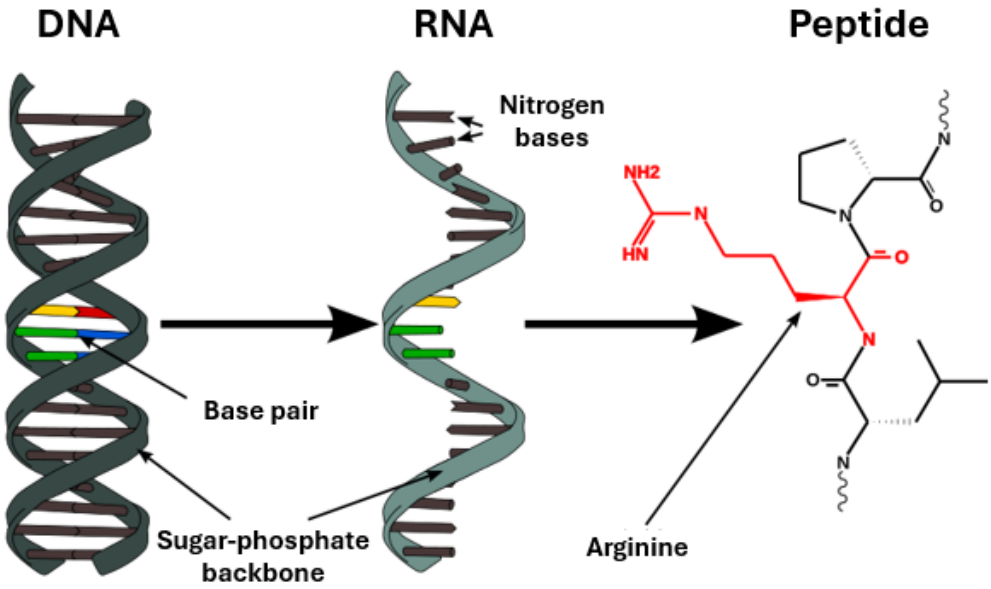

***Figure 2**: Genetic flow of information; from [13]*

An important point to consider is that not every location in the genome stores genetic information. The human genome contains three billion pairs of bases of which only 1.5 % code for proteins or different types of RNA like ribosomal RNA (rRNA) or transfer RNA (tRNA). These genes form structural reading units with similar composition.[14] The region responsible for initiating the transcription of a gene by the RNA-polymerase-II-machinery (for protein-coding regions) is termed the promoter. Within this, we can distinguish the core promoter and the proximal promoter. The core

promoter is the smallest segment necessary to initiate the transcription machinery. Typically, the core promoter encompasses the transcription start site plus about 35 nucleotides upstream and downstream. The proximal promoter is located directly upstream of the core region and spans approximately the regions from -50 to -200 in relation to the transcription start site. In this section, there are typically many recognition sites for a group of sequence-specific DNA-binding transcription factors.[15]

Enhancers are specific DNA elements that can be located at a considerable distance from the promoter and enhance transcription. The interactions between enhancers and their associated promoters are essential for this enhancement. In this process, it is not only important that the enhancer recognizes its promoter over a long distance, but also that it specifically activates only one of the many promoters in its immediate vicinity.[15] Surprisingly, studies have found that regulatory elements can exhibit both enhancer and promoter functions, and that the differentiation between these two DNA fragments does not have to be clear-cut.[16]

1.2 Epigenetics

The term "epigenetics" means outside conventional genetics. Today, it is commonly used to describe stable changes in the regulation of gene expression that occur and become established during development and cell proliferation.[17] This usage of the term has supplanted an earlier meaning, where "epigenetics" referred to the interpretation of the genotype during development into a specific phenotype.[18] Years of research have shown that DNA methylation, histone modifications, and RNA-based mechanisms are the primary methods of epigenetic control.[19]

1.2.1 DNA methylation

DNA methylation is regarded as an epigenetic mechanism in the mammalian genome, where a methyl group is added to the C5 position of cytosine, forming 5-methylcytosine (5-mC). This process regulates gene expression by either recruiting gene-repressing proteins or preventing transcription factors from binding to the DNA. During development, DNA methylation patterns change through a dynamic process of both de novo methylation and demethylation. This process ultimately leads to differentiated cells developing stable and distinct DNA methylation patterns that govern tissue-specific gene transcription.[20]

The methylation of bases in DNA is generally a suitable marker for a specific functional state of the DNA, as it is easy for the cell to maintain methylated DNA segments through replication. Although a newly synthesized DNA strand is initially unmethylated after replication, methylases can easily identify methylated bases in the complementary strand.[21]

5-Methylcytosine was first identified in 1925 by Johnson and Coghill when they isolated and crystalized nucleic acids from *Mycobacterium tuberculosis*.[22] Twenty-five years later

Wyatt also confirmed the presence of 5-mC in mammalian, plant, and insect DNA.[23] However, its biological significance was not immediately apparent for several decades. With the confirmation that nucleic acids carry genetic information and the revelation of the DNA double helix structure, interest in DNA methylation increased. Sinsheimer later noted that 5-mC is specifically located in the cytosine-phosphate-guanine (CpG) dinucleotide context, rather than being randomly distributed in DNA.[24]

CpG dinucleotides often occur in clusters forming short, GC rich DNA sequences. These so called CpG-islands are found in the immediate vicinity of approximately 70% of all human promoters. They can be located near the transcription start site, intragenic or intergenic. The methylation of CpG dinucleotides is referred to as an epigenetic mechanism for regulating gene activity.[25]

One common regulatory mechanism for gene activity is gene silencing. This can be accomplished through heavy methylation of its promoter. In many tested genes, methylated promoters are no longer accessible to DNase I. It is therefore assumed that the methylated sites are blocked by proteins that specifically recognize methylated DNA regions. These closed chromatin conformations also naturally prevent the promoter from being accessible to transcription factors.[21] In addition, enhancer methylation also plays an important role in gene regulation. Several studies support the influence of methylated enhancers on transcription of the associated gene.[26]

1.3 Cancer

Cancer represents a widespread and omnipresent problem across the global population. The International Agency for Research on Cancer (IARC) documented 18.7 million new cases and 9.7 million deaths in 2022 alone. With 2.5 million new cases, accounting for 12.4 % of the total, lung cancer was the most commonly occurring cancer worldwide. Second ranked female breast cancer (2.3 million cases, 11.6 %), followed by colorectal cancer (1.9 million cases, 9.6%). Mortality varies greatly among different types of cancer. Among them, lung cancer was the leading cause with 1.8 million deaths accounting for 18.7 % of total cancer deaths. Colorectal cancer (900 000 deaths, 9.3 %) and liver cancer (760 000 deaths, 7.8 %) came second and third. Cancer incidence is expected to rise in the coming years. It is predicted that 35 million new cancer cases will occur in 2050, marking nearly a doubling.[27]

Cancer is a disease characterized by dynamic changes in the genome. Among these changes in the genome, the formation of oncogenes, which have a dominant gain of function, and tumour suppressor genes, which experience a recessive loss of function, are of particular significance.[28] These invariable modifications at multiple sites in the genome occur through single point mutations or changes in the chromosome complement. During the transformation of normal human cells into malignant cancer cells, known as tumorigenesis, the cell undergoes a series of processes involving various molecular, biochemical, and cellular alterations. The hallmarks of cancer provide a framework for understanding the common traits of cancer cells.[29,30]

- Self- sufficiency in growth signals
- Insensitivity to anti-growth signals
- Evading apoptosis
- Limitless replicative potential
- Sustained angiogenesis
- Tissue invasion and metastasis
- Deregulating cellular energetics
- Genome instability and mutation
- Avoiding immune destruction
- Tumour-promoting inflammation

These hallmarks of cancer establish a framework for recurring features, but each tumour has its own unique characteristics. This is the reason why cancer treatment proves to be difficult.

1.3.1 Brain metastases

Brain metastases develop in the brain microvasculature through seeding of circulating cells from a primary tumour and are associated with advanced stages of cancer disease. This unique environment promotes tumour growth on the one hand and limits penetration of systematic therapeutics on the other hand. Since prognosis remains poor, brain metastases are a key contributor to cancer-related mortality.[31] Median survival of brain metastasis ranges from seven to 34 %.[32]

Approximately 20 % of all cancer patients eventually develop brain metastases, with lung cancer, breast cancer, and melanoma among the cancers most commonly associated with this complication. [31] Notably, seven to 16 % of brain metastases arise from melanoma alone. [32] Once melanoma becomes metastatic, brain metastases appear to be nearly inevitable, with up to 80 % of patients found to have brain metastases at autopsy. [33]

1.3.2 Cancer treatment

Even though there are many cancer treatment options available today, it remains a difficult challenge. The oldest and most straightforward method being surgery offers high chance of cure only when the cancer is non-metastatic and detected at a very early stage. When used as a monotherapy, surgery must be performed with extreme precision due to the high risk of local recurrence. Additionally, studies show that trauma caused by the operation can induce inflammation, which may promote the development of micro metastases. [34,35]

A different treatment strategy is radiotherapy, which is used in more than half of cancer patients and is considered one of the most effective treatments. This local therapy uses radiation beams to destroy tumours. [34]

Another way of treating cancer is by using cytostatics during chemotherapy. This type of medication aims to supress cell growth and cell division in cancer cells. One example of

such a cytostatic is the alkylating agent temozolomide (TMZ). TMZ causes DNA damage by the addition of methyl groups at the N7 and O6 positions of guanine and the N3 position of adenine residues. [36] However, response to TMZ critically depends on the expression of O6-methylguanine-DNA-methyltransferase, since it repairs alkylation lesions, preferentially methylation at position O6 of guanine. [37]

For completeness, it should also be mentioned that novel cancer treatments like monoclonal antibodies, chimeric antigen receptor T cells, or CRISPR/Cas9 are increasingly being used and improve the survival rate, quality of life, and prognosis of cancer patients.[34]

Despite significant advancements in cancer treatment, metastases still present a major challenge due to their biological heterogeneity and the difficulty of early detection. [38] Consequently, brain metastases are typically managed upon diagnosis using a multimodal therapeutic approach that includes chemotherapy, radiotherapy, surgery, and immunotherapy. [31] However, the effectiveness of systemic chemotherapy is often limited by the restrictive nature of the blood-brain barrier, which impedes the permeation of many agents. Historically, surgery and/or radiation for the treatment of melanoma brain metastases has resulted in a median overall survival of approximately four months from diagnosis. [33]

1.3.3 O6-methylguanine-DNA-methyltransferase

One way to maintain genomic stability and prevent cancer is through the DNA repair network. This process is achieved through a mismatch, recombination, and excision repair system. Additionally, mutagenic and cytotoxic adducts can be removed from DNA. These adducts may occur from endogenous mechanisms or exposure to environmental alkylating mutagens. Among them, O6-methylguanine (O6-mG) is assumed to be the most important in carcinogenesis and mutagenesis. During replication this methylated guanine base tends to pair with thymine resulting in a transition to adenine-thymine pairs. This mutagenic adduct of O6-mG can be repaired by the O6-methylguanine-DNA methyltransferase. Loss of this essential repair mechanism can lead to mutations and tumour induction.[39–41]

Epigenetic silencing of MGMT takes place in various human tumours and is frequently associated with hypermethylation at the promoter CpG islands. However, an increasing number of research indicates an association between MGMT promoter and enhancer methylation and MGMT protein expression. This relationship has been shown in glioblastoma.[42–44]

Nevertheless, MGMT also interferes with medical interventions. As previously discussed, alkylating agents are a common way to treat cancer. These chemotherapy-induced lesions trigger cytotoxicity and apoptosis. High activity of MGMT in cancer cells creates a resistance by diminishing the therapeutic effect of agents like TMZ.[40,45] However, resent studies have shown that response to TMZ was weak in brain metastasis. [46]

2 Aims

Melanoma brain metastases are a common and aggressive manifestation of melanoma, often treated with surgery, systemic therapy, radiotherapy, or combined of these approaches. Chemotherapeutic agents like temozolomide have also been used; however, their limited efficacy against brain metastases has led to a decline in their use.

The response to TMZ treatment generally varies among patients and is influenced by factors such as the expression of the DNA repair protein MGMT. Previous studies have shown that MGMT promoter methylation levels are inversely correlated with MGMT expression. This relationship serves as a predictive biomarker for TMZ responsiveness in glioblastoma patients. However, not all patients with hypermethylated MGMT promoters respond to TMZ, and some with unmethylated promoters do respond, raising questions about the reliability of promoter methylation as a sole predictor.

Given that enhancer regions also regulate gene expression, the aim of this thesis was to investigate whether CpG methylation in the MGMT enhancers correlates with MGMT expression and could serve as a more reliable marker for predicting the responsiveness of patients with brain metastases to TMZ. To achieve this, pyrosequencing methods targeting the MGMT enhancer region should be used on a stable cell line set of melanoma brain metastases, and the evaluated methylation levels should be tested for correlation with MGMT expression.

Furthermore, the thesis should validate and compare two established methods found in literature for detecting 5-hydroxymethylcytosine (5-hmC) to assess their suitability for future studies of DNA modifications. This involved oxidative bisulfite sequencing, where oxidation occurs before bisulfite sequencing, and, on the other hand, chemically assisted pyridine borane sequencing. The goal was to establish these methods within the research group.

3 Theoretical background

3.1 Preparation for DNA methylation analysis

This section presents the procedures required to perform DNA methylation analysis with single-base resolution. First, bisulfite sequencing (BS) will be discussed. This process enables the differentiation between methylated and unmethylated CpG sites and was used to analyse MGMT enhancers in brain metastases. Secondly, oxidative bisulfite sequencing (oxBS) and chemically assisted pyridine borane sequencing (CAPS) will be introduced. These methods were used to assess the detection of 5-hmC.

It is important to understand, that these methods alter the nucleotide sequence depending on the methylation level of cytosine. This difference in the base sequence can be detected with polymerase chain reaction (PCR) and subsequent pyrosequencing analysis. Table 1 summarises the base changes of these methods.[47]

***Table 1**: Base changes after conversion during BS, oxBS, and CAPS and PCR*

Original base	BS	oxBS	CAPS
C	T	T	C
5-mC	C	C	C
5-hmC	C	T	T

3.1.1 Bisulfite sequencing

Bisulfite sequencing is widely used in DNA methylation analyses and represents an essential component of many methods due to its low cost, reliability and scalability. Together with next generation sequencing (NGS) it provides a single-base resolution view of methylated CpG sites across different target sequences. The conversion is based on the selective chemical alteration of unmethylated cytosine into uracil. This is accomplished through three steps. First, during sulfonation, a sulfonyl group is introduced at the C3 position. This is followed by deamination and finally desulfonation. In contrast, methylated cytosines remain unmodified. [48,49] This reaction can be seen in Figure 3.

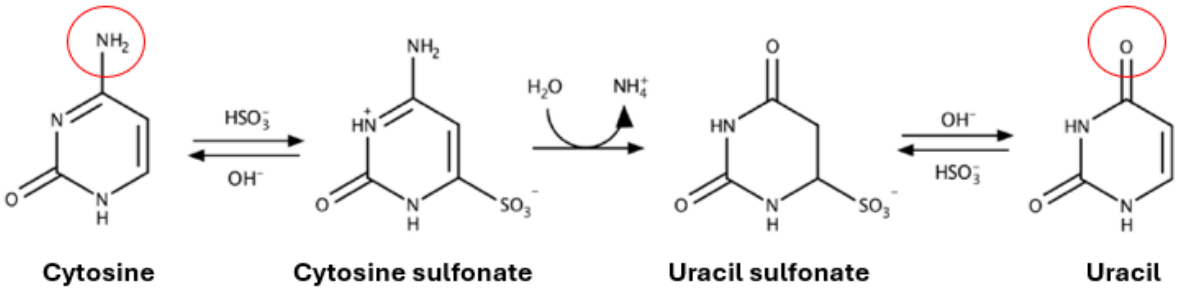

***Figure 3**: Bisulfite conversion, selective chemical alteration of unmethylated cytosine into uracil; modified from [48]*

During PCR amplification, the polymerase reads uracil as thymine. This process is shown in Figure 4. Consequently, the original methylation can be detected through sequencing. If a cytosine is detected at a previously selected position using pyrosequencing, a methylated cytosine in the original sequence is indicated. If, however a thymine is detected, this suggests that the site was not methylated in the original sequence.[48] This method can be used to evaluate the methylation status of a given CpG site.

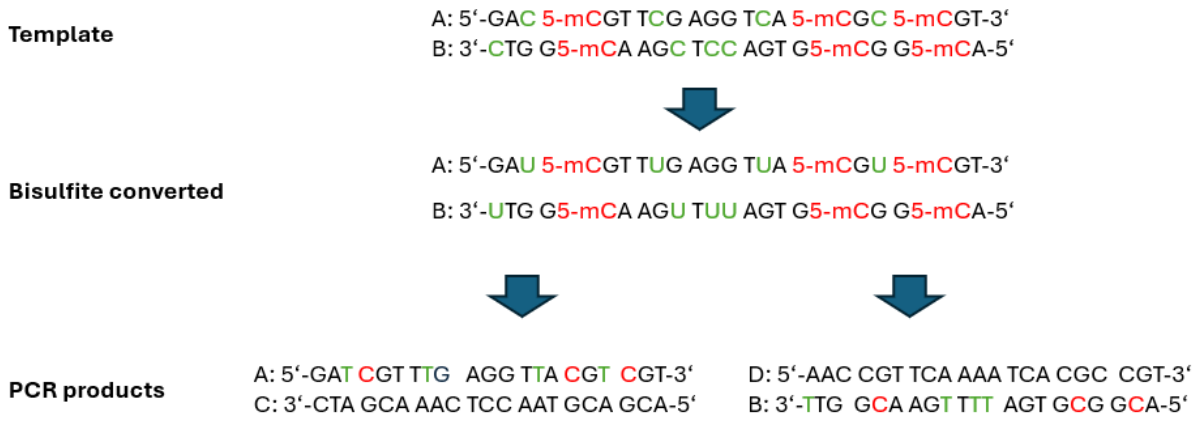

***Figure 4**: Sequence changes through bisulfite conversion and during PCR; modified from [48]*

3.1.2 Oxidative bisulfite sequencing

Modified cytosines like 5-mC and 5-hmC are predominant epigenetic markers and widespread in the genome. They are involved in gene regulation, cancer, and aging. Regular bisulfite sequencing, however, is not capable of distinguishing between those two methylated cytosine variants.[50] Therefore, oxidative bisulfite sequencing, which enables quantification at a single base resolution, can be applied. Prior to bisulfite treatment, selective chemical oxidation of 5-hmC is performed, with potassium ruthenate (K_2RuO_4). This results in the formation of 5-formylcytosine (5-fC), which later reacts with bisulfite and is converted to uracil. Potentially present carboxylcytosine is also converted to uracil.[51,52] The oxidation of 5-hmC is shown in Figure 5.

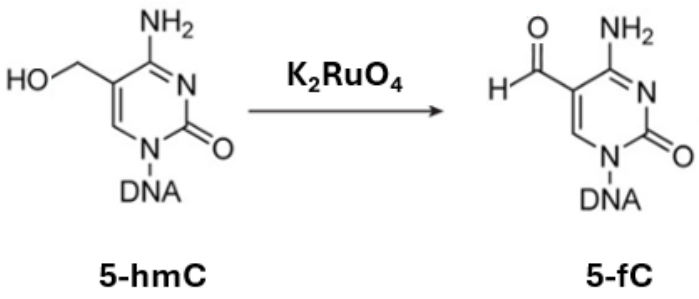

***Figure 5**: Oxidation of 5-hydroxymethylcytosine; modified from [53]*

As in regular bisulfite sequencing, uracil is read as thymine by the DNA polymerase during PCR. To calculate the 5-hmC level, regular bisulfite sequencing must be performed too. The difference in the methylation levels obtained from these two methods corresponds to the amount of 5-hmC. This is evident in Figure 6. Regular bisulfite sequencing detects both 5-mC and 5-hmC, and oxidative bisulfite sequencing only 5-mC. If both methods are applied to the same target sequence, the difference in detected methylation arises from the presence of 5-hmC. This process enables the determination of both 5-hmC and 5-mC, but introduces increased background noise, since two methods have to be applied. [52]

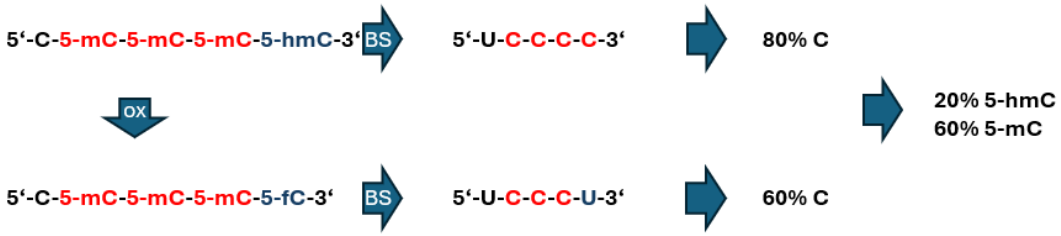

***Figure 6**: Schematic overview of oxidative bisulfite sequencing, ox = oxidation; modified from [52]*

3.1.3 Chemically assisted pyridine borane sequencing

To reduce background noise when detecting 5-hmC using oxidative bisulfite sequencing, an alternative approach can be applied: chemically assisted pyridine borane sequencing. This method allows for subtraction-free and specific genome sequencing of 5-hmC, and it does not require harsh bisulfite treatment. In this process specific chemical oxidation of 5-hmC to 5-fC is performed. For this reason, potassium ruthenate (K_2RuO_4), which is reported to be less DNA damaging and more oxidative than potassium perruthenate ($KRuO_4$), is applied. This oxidation, however, only works on single stranded DNA. The conversion rate from 5-hmC to 5-fC is reported to be 97.2 %. In the next step, borane reduction with 2-methylpyridine borane (pic-borane) is carried out to convert 5-fC to dihydrouracil (DHU).[47,54] This reaction can be seen in Figure 7.

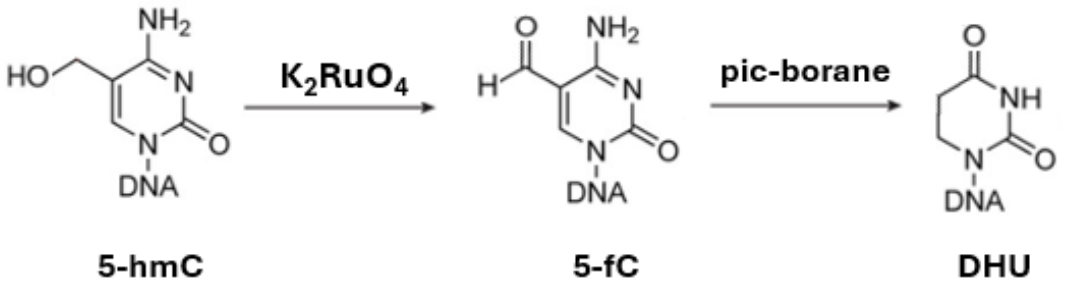

***Figure 7**: Chemical reactions performed during CAPS; modified from [54]*

After the successful and specific conversion of 5-hmC to DHU, PCR can be performed. During PCR, DHU is converted to thymine, which can be seen in Figure 8. This process enables the differentiation of 5-hmC and 5-mC, since 5-mC is not converted to thymine. Previously selected CpG sites containing thymine indicate the presence of 5-hmC in the original DNA sequence. The presence of cytosine indicates 5-mC or C in the original sequence.[47]

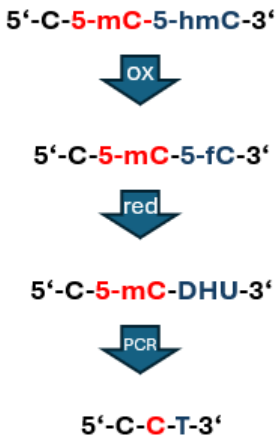

***Figure 8**: Sequence changes during CAPS, ox = oxidation, red = reduction; modified from [47]*

3.2 Polymerase chain reaction

The polymerase chain reaction (PCR) is a method to amplify DNA sequences and was invented by Kary Mullis in 1983.[55] The amplification proceeds in three distinct steps, which are carried out automatically. A repetition of these three steps is referred to as one cycle. The process starts with denaturation of double stranded DNA at 96 °C. This results in the formation of separate single strands, which then hybridise with primers (synthetic oligonucleotides) during the annealing step. It is important that the base sequence of the primers exactly matches the terminal regions of the DNA fragments to be amplified. The final step is known as elongation, during which a DNA polymerase incorporates individual deoxynucleotides complementary to the DNA template, starting from the 3’ end of the primer. This cycle can be repeated more than 30 times. After 30 cycles, theoretically, 2^{30} (1,073,741,824) copies are generated from a single DNA molecule. Because each new strand again serves as a template and synthesis always starts from the primers, only the DNA sequence between the primers is specifically amplified. [21] Figure 9 illustrates these three steps during the amplification.

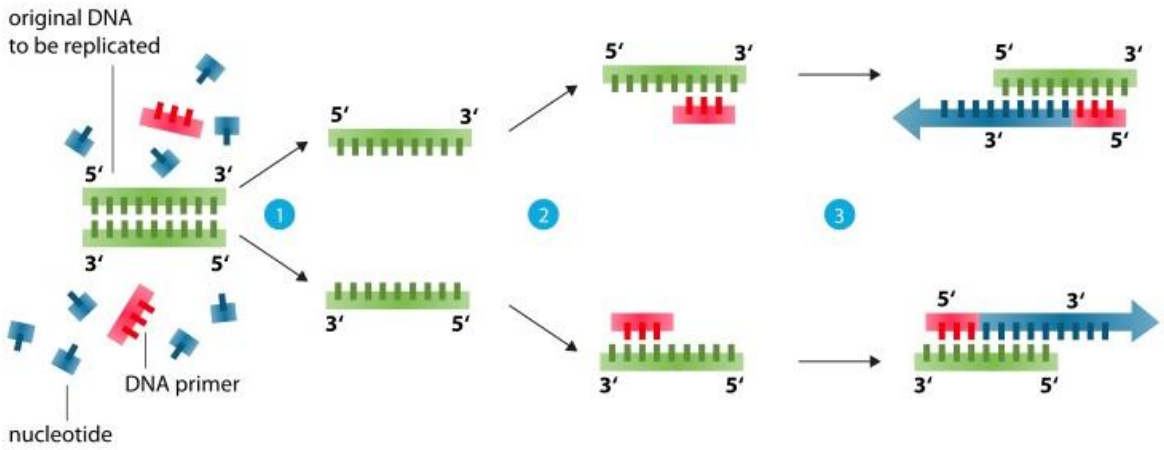

***Figure 9**: Polymerase chain reaction; modified from [56]*

PCR is based on the ability of a specific DNA polymerase from certain organisms, such as *Thermus aquaticus*, to withstand temperatures around 100 °C. A prerequisite is knowledge of the primer binding sites. However, the sequence between the primers can be unknown. The reaction mixture contains the DNA template, heat-stable DNA polymerase, two specific primers (forward and reverse), all four deoxynucleotide triphosphates, and an appropriate buffer. Additionally, a fluorescent dye can be added, that binds to double-stranded DNA in order to detect the generated product. This concept is known as real-time PCR. The key features of PCR include the ability to perform consecutive denaturation, hybridization, and elongation without interruption.[15]

A key quantitative parameter of real-time PCR is the cycle threshold value (Ct). It is defined as the number of PCR cycles required for the fluorescent signal to exceed a threshold level. The Ct value is inversely correlated with the amount of the target sequence. Lower Ct values indicate a higher initial concentration of the targeted DNA sequence and higher Ct values indicate a lower initial concentration prior to PCR.[57]

3.3 Pyrosequencing

Pyrosequencing (PSQ) is a DNA sequencing technology, which was primarily developed by Pal Nyren in the late 1980s. Its concept is based on a sequencing-by-synthesis approach, where the synthesis of a complementary DNA strand is observed in real-time. Due to the Watson-Crick base pairing rule, which states that nucleic base guanine always pairs cytosine and thymine with adenine, the sequence of the original template can be determined. The incorporation of a nucleotide releases pyrophosphate, which can be monitored via enzyme-coupled reactions generating bioluminescence. The discovery of this method represents a significant improvement and was at the time the only available commercial alternative to the Sanger method for DNA sequencing.[58] The development of high-throughput and more advanced sequencing methods known as “next generation sequencing methods” led to a tremendous increase in sequencing capabilities. PSQ has advantages, such as high accuracy, parallel processing, and ease of automation. In

addition, the need for labelled primers or nucleotides and gel-electrophoresis is eliminated. [59]

This technique detects inorganic pyrophosphate (PPi) in real time, released upon the successful incorporation of nucleotides during DNA synthesis. PPi is being converted into adenosine triphosphate (ATP) by the ATP sulfurylase. Following the detection of photons emitted by the luciferase enzyme, the signal is quantified. Unincorporated ATP and excess deoxynucleotides are degraded by the nucleotide-degrading enzyme apyrase. Photon emission serves as a key indicator of successful nucleotide incorporation. If nucleotides are added one at the time, the sequence of the complementary DNA strand can be determined.[60]

For this analysis, the DNA template is immobilised on a solid surface using the streptavidin-biotin interaction. For this reason, one of the primers used in PCR prior to sequencing must be biotinylated at its 5' terminus. The bound double stranded DNA is separated into the two single strands, and the pyrosequencing analysis can start by hybridization of a sequencing primer to the template. For each DNA template molecule one ATP molecule is generated per incorporated nucleotide. The generated photons witch a wavelength of 560 nm can easily be detected by a photodiode.[60]

Figure 10 illustrates all reactions that are ultimately relevant for light generation.

$$(DNA)_n + dXTP \xrightarrow{DNA\ Polymerase} (DNA)_{n+1} + PPi$$

$$PPi + APS \xrightarrow{ATP\ Sulfurylase} ATP + SO_4^{2-}$$

$$ATP + Luciferin + O_2 \xrightarrow{Luciferase} AMP + PPi + Oxyluciferin + CO_2 + Light$$

***Figure 10**: Chemical reactions involved in light generation during PSQ, AMP = adenosine monophosphate; from [61]*

In order to perform the analysis, four different enzymes (DNA polymerase, ATP sulfurylase, luciferase and apyrase) and two substrates (adenosine 5' phosphosulfate (APS) and luciferin) are necessary. Additionally, deoxyadenosine alpha-thio triphosphate (dATPαS), deoxyguanosine triphosphate (dGTP), deoxycytidine triphosphate (dCTP) and deoxythymidine triphosphate (dTTP) are essential for the pyrosequencing reaction. Since dATP would be recognised by the luciferase, the analogous dATPαS, which can be utilized by the DNA polymerase but is not recognized by luciferase, is needed.[61,62]

Apyrase is a key enzyme in the PSQ process. On the one hand, it degrades unincorporated deoxynucleoside triphosphates (dXTP). Emitted light can only be attributed to the incorporation of a new nucleotide and the generation of ATP by the ATP sulfurylase. On the other hand, apyrase breaks down excess ATP, which was not used by the luciferase.[63] Figure 11 shows the reactions of the enzyme apyrase.

$$ATP + dXTP \xrightarrow{Apyrase} ADP + dXDP + 2Pi$$

$$ADP + dXDP \xrightarrow{Apyrase} AMP + dXMP + 2Pi$$

***Figure 11**: Apyrase reactions during PSQ, Pi = inorganic phosphate group, ADP = adenosine diphosphate; from [61]*

For data analysis, it must be considered which DNA strand is used as the template for sequencing and immobilized on the solid phase via the biotin-streptavidin interaction. If the forward primer is biotinylated in PCR, the reverse strand is synthesized during pyrosequencing, and the methylation status is inferred from the dGTP/dATPaS ratio. However, if the reverse primer is biotinylated, the forward strand is synthesized during pyrosequencing, and the methylation status can be directly assessed from the dTTP/dCTP ratio. This approach is applicable when the methylation status of the sense strand is of interest.

3.4 Primer design

Precise primer design is a critical step in PCR, as it ensures specific amplification of the target DNA sequence. The synthetic oligonucleotides (primers) must be added in excess to the PCR reaction mixture. Otherwise, a low yield is to be expected. However, a high primer concentration can lead to mispairing, leading to unspecific PCR products. Furthermore, primer design should take a balanced G/C to A/T base pair ratio into account. Primer lengths should ideally be between 20 and 35 nucleotides long. The use of even longer oligonucleotides does not lead to an increase in specificity. It, however, leads to the formation of undesired secondary structures like hairpin loops as well as homo- and heterodimer formations of the primers. Another important parameter is the primer's melting temperature (Tm), which is defined as the temperature at which 50 % of the primer is bound to a complementary strand and 50 % is single stranded. This temperature defines the optimal annealing temperature, which is typically five degrees below the primer's melting temperature. Additionally, the annealing temperature should preferably be between 55 and 65 °C.[64,65]

For pyrosequencing, another primer referred to as the "sequencing primer" must be used. This oligonucleotide needs to be complementary to the biotin-labelled strand of the PCR product, and its length should be 16 to 24 nucleotides. Additionally, the sequencing primer should be unique to one position within the PCR product and should not contain any CpG sites.[65]

4 Materials and methods

4.1 Samples

The sample set used in this thesis was obtained from the Department of Neurosurgery at the Kepler University Hospital Linz. The sample set consisted of DNA extracts from in vitro-cultured primary cell lines, sampled and isolated from metastatic human tumours established between 2000 and 2016 from 20 melanoma patients (M01 – M20). Each sample was analysed twice in two separate PCR experiments. The resulting amplicons were analysed individually using PSQ.

In addition, a right hippocampal sample was provided by the Center for Anatomy and Cell Biology at the Medical University of Vienna. DNA was isolated using the DNeasy PowerMax Soil Kit[66], purified with Bio-Rad Micro Spin Columns, and ELGA water. This procedure was conducted by a previous member of the working group.

Clinical data for the melanoma samples are provided in Chapter 8.3 (Supplementary Table 18).

4.2 Bisulfite sequencing for DNA methylation analysis in melanoma brain metastases

Bisulfite sequencing of DNA from melanoma brain metastases was conducted in our lab using the Epitect Fast Bisulfite Conversion Kit (Qiagen)[67] according to the manufacturer's protocol[68], employing the low-concentration setup. This BS was carried out by Katharina Pühringer, MSc.

Figure 12 illustrates the workflow for analysing DNA methylation levels of MGMT enhancers in brain metastases. Bisulfite conversion is an essential step in sample preparation for subsequent PCR and PSQ analysis. In this case, we were interested in general DNA methylation without distinguishing between 5-hmC and 5-mC, thus, standard bisulfite conversion was sufficient.

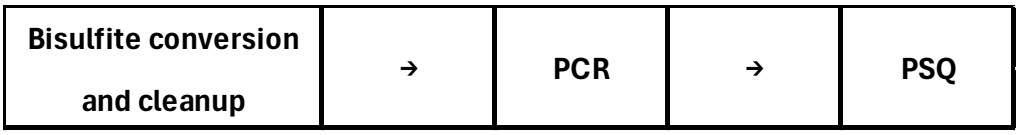

***Figure 12**: Workflow for DNA methylation analysis in brain metastases*

DNA extracts were thawed, vortexed, and combined with reagents in 200 µL tubes as specified in Table 2.

***Table 2**: Reaction setup of bisulfite conversion*

Components	High-concentration samples (1 ng - 2 µg) Volume [µL]	Low-concentration samples (1 ng - 500 ng) Volume [µL]
DNA	Variable*	Variable**
RNase-free water	Variable*	Variable**
Bisulfite solution	85	85
DNA protect buffer	35	15
Total volume	140	140

* DNA and RNase-free water should add up to 20 µL

** DNA and RNase-free water should add up to 40 µL

The tubes were thoroughly vortexed, and bisulfite conversion was carried out using the Bio-Rad iCycler Thermal Cycler, following a thermal program. A schematic thermal program is outlined in Table 3. The number of successive denaturation and incubation steps varied depending on the temperature program (see Table 4).

***Table 3**: Thermal cycler conditions for bisulfite conversion*

Step	Time [min]	Temperature [°C]
Denaturation #1	5	95
Incubation #1	Variable	60
Denaturation #2	5	95
Incubation #2	Variable	60
...	...	...
...	...	...
Hold	/	20

***Table 4**: Temperature programs and their parameters for bisulfite conversion*

Program no.	No. of incubations	Time [min]	Total incubation time [min]
1	2	30	20
2	4	60	40
3	4	160	140
4	6	320	290
5	6	460	430
6	6	600	570

Next, cleanup was started by briefly centrifuging the PCR tubes containing the bisulfite reactions. The complete bisulfite reaction mixtures were then transferred to clean 1.5 mL microcentrifuge tubes. To each sample, 310 µL of freshly prepared Buffer BL were added,

and the solutions were mixed by vortexing, followed by a brief centrifugation. Subsequently, 250 µL of ethanol (96 – 100 %) was added to each sample. The solutions were mixed thoroughly by pulse vortexing for 15 seconds (3 × 5 seconds) and centrifuged briefly again. The entire mixture from each tube was then transferred onto a MinElute DNA spin column.

The spin columns were centrifuged at 14,000 rcf for one minute, and the flow-through was discarded. The spin columns were returned to their collection tubes, and 500 µL of Buffer BW (wash buffer) were added to each column. The columns were centrifuged again at 14,000 rcf for one minute, and the flow-through was discarded. After placing the spin columns back into the collection tubes, 500 µL of Buffer BD (desulfonation buffer) were added, and the columns were incubated at room temperature for 15 minutes. Following the incubation, the spin columns were centrifuged at 14,000 rcf for one minute, and the flow-through was discarded.

The columns were washed twice by adding 500 µL of Buffer BW to each spin column, centrifuging at 14,000 rcf for one minute after each washing step, and discarding the flow-through. An additional washing step was performed using 250 µL of ethanol (96 – 100 %), followed by centrifugation at 14,000 rcf for one minute. To remove any residual liquid, the spin columns were transferred to new 2 mL collection tubes and centrifuged at 14,000 rcf for one minute.

Next, the spin columns were placed with open lids into clean 1.5 mL microcentrifuge tubes and incubated for five minutes at 60 °C on a heating block to ensure evaporation of any remaining liquid. Afterwards, the spin columns were transferred into clean 1.5 mL microcentrifuge tubes, and 15 µL of Buffer EB (elution buffer) were added directly to the centre of each spin column membrane. The columns were incubated at room temperature for one minute, followed by centrifugation at 12,000 rcf for one minute to elute the DNA. The converted DNA was stored at -20 °C.

The DNA concentration was quantified using the Qubit ssDNA Assay Kit (Thermo Fisher)[69]. The Qubit working solution was prepared by combining 1×n µL of Qubit reagent with 199×n µL of Qubit buffer, where n represents the total number of samples and standards. For calibration, 190 µL of the working solution was mixed with 10 µL of each of the two standards in Qubit tubes. The tubes were then vortexed and incubated at room temperature for one minute before measurements were performed using a Qubit 4 fluorometer (Thermo Fisher). For DNA concentration analysis, 198 µL of the working solution was mixed with 2 µL of the bisulfite-converted DNA extracts and again incubated at room temperature for one minute.

4.3 Primers

In this chapter, the primers used for each assay are introduced. Each assay was originally developed by previous members of the working group, including Simon Pflug, Philipp Czarda, and Katharina Pühringer. The selected primers were ordered from Sigma-Aldrich.

The development of each assay began with identifying the enhancer sequence on NCBI[70]. The identified sequence was imported into the PyroMark Q24 Advanced Software (version 3.0.1), where an in-silico bisulfite sequencing was performed. A target region was selected, and the software suggested forward primer, reverse primer, and sequencing primer for the assay.

The primers were then optimized by varying their length and position to improve their performance. The melting temperature of the primers was calculated using the OligoCalc web tool[71], which accounts for salt concentration. Secondary structures, such as hairpins or loops, were analysed using the RNAfold[72] program, while potential primer dimers were identified with the OligoAnalyzer[73] tool.

Furthermore, the BIsearch[74] tool was used to perform an in-silico PCR analysis. This step was crucial to verify the binding sites of the primers and to check whether the target regions contained single-nucleotide polymorphisms (SNPs). Additionally, the tool provided information on how many PCR products would be generated, ensuring the specificity and efficiency of the assay.

Table 5 lists the nine chosen enhancers of the MGMT gene, each of which was targeted with distinct assays to analyse CpG sites. The names of the enhancers were chosen by the working group in order of their occurrence in the genome.

***Table 5**: Analysed enhancers of the MGMT gene, location and CpG sites, * enh3 inter was suggested by Chen et al. [66] and is not listed in the Vista enhancer database, additionally the location of the promoter is listed, chr10 = chromosome 10*

Enhancer	Vista enhancer name	Location on chr10	CpGs
enh1 inter	hs542	128,165,799..128,166,830	8
enh2 inter	hs737	128,568,604..128,569,741	27
enh3 inter	*	128,906,630..128,909,942	46
enh4 inter	hs699	129,033,193..129,034,911	33
enh5 inter	hs562	129,308,258..129,310,478	32
promoter	/	129,466,685..129,467,446	98
enh6 intra	hs656	129,602,684..129,604,015	12
enh7 intra	hs696	129,605,804..129,607,046	26
enh8 intra	hs331	129,647,523..129,649,421	20
enh9 intra	hs589	129,716,557..129,717,922	21

The next section presents the sequences of the forward, reverse, and sequencing primers for each assay. Forward and reverse primers are used for PCR, while sequencing primers are used for PSQ.

enh1 inter

For this intergenic enhancer, only one assay was created to analyse CpGs 1 – 3. Primer sequences and their melting temperatures are shown in Table 6.

***Table 6**: Primer sequences and melting temperatures of Assay 1, analysing CpGs 1 – 3 on enh1 inter, [Btn] = biotin*

Primer	Sequence	T_m [°C]
Forward	5'-TGTTGGTTATTGTGAGTGATAGT-3‘	57.6
Reverse	5’-[Btn]-AAACTCCATCCACTAAAACCTA-3’	56.4
Sequencing	5’-ATTTTTTGTTATGTAAAGT-3’	42.3

enh2 inter

For this enhancer, five different assays were created to analyse CpGs 9, 12 – 19, 20 – 21, 22 – 25, and 26 – 27, respectively. Primer sequences and melting temperatures are shown in Table 7 – 11.

***Table 7**: Primer sequences and melting temperatures of Assay 2, analysing CpG 9 on enh2 inter, [Btn] = biotin*

Primer	Sequence	T_m [°C]
Forward	5'-[Btn]-GTAGGTAGGGTTTGTGTAGTT-3‘	57.5
Reverse	5’-TTAACTAATCCCAAATCTACATTCT-3’	57.6
Sequencing	5’-TCTACATTCTCTTCT-3’	37.8

***Table 8**: Primer sequences and melting temperatures of Assay 3, analysing CpGs 12 – 19 on enh2 inter, [Btn] = biotin*

Primer	Sequence	T_m [°C]
Forward	5'-[Btn]-GAGAATGTAGATTTGGGATTAGTTAA-3‘	60.1
Reverse	5’-ACCAATTAAACCCTAAATTATTTACATC-3’	59.9
Sequencing	5’-ATACAAAATATACCCTCC-3’	46.9

***Table 9**: Primer sequences and melting temperatures of Assay 4, analysing CpGs 20 – 21 on enh2 inter, [Btn] = biotin*

Primer	Sequence	T_m [°C]
Forward	5'-AGGGATTTGGAGGGTAGGTGAA-3‘	62.1
Reverse	5’-[Btn]-TCAACTATCTACTTAACACAAACCAC-3’	61.7
Sequencing	5’-AGTTGTGTTTGTTTAGG-3’	45

***Table 10**: Primer sequences and melting temperatures of Assay 5, analysing CpGs 22 – 25 on enh2 inter, [Btn] = biotin*

Primer	Sequence	T_m [°C]
Forward	5'-GTTGAGTGTGGTTTGTGTTAAGT-3‘	59.2
Reverse	5’-[Btn]-ACAACCTACCTCCTCTATACC-3’	59.5
Sequencing	5’-GTTAAGTAGATAGTTGA-3’	42.6

***Table 11**: Primer sequences and melting temperatures of Assay 6, analysing CpGs 26 – 27 on enh2 inter, [Btn] = biotin*

Primer	Sequence	T_m [°C]
Forward	5'-GGGTTTTGTGGAGGAATAATAAA-3‘	57.6
Reverse	5’-[Btn]-CTTTATACCTACAACATACTCCTA-3’	58.3
Sequencing	5’-GGGTTTTGTGGAGGAATAATAAA-3’	57.6

enh3 inter

For this enhancer, four different assays were designed to analyse CpGs 5 – 8, 11 – 18, 25 – 27, and 37 – 39, respectively. Tables 12 – 15 present the primer sequences and melting temperatures.

***Table 12**: Primer sequences and melting temperatures of Assay 7, analysing CpGs 5 – 8 on enh3 inter, [Btn] = biotin*

Primer	Sequence	T_m [°C]
Forward	5'-AGTTAGGAAATTAGAAATGGAATGTTT-3‘	59.2
Reverse	5’-[Btn]-CAAATCACACTCTAAATTCCCAATT-3’	59.2
Sequencing	5’-TGGTATTAGAGGTTA-3’	37.8

***Table 13**: Primer sequences and melting temperatures of Assay 8, analysing CpGs 11 – 18 on enh3 inter, [Btn] = biotin*

Primer	Sequence	T_m [°C]
Forward	5'-[Btn]-TTAAATAAGTGGTTTAGGTAGAGG-3‘	58.3
Reverse	5’-TACTAAACATTCCATTTCTAATTTCC-3’	58.4
Sequencing	5’-CCATTTCTAATTTCCTAACTC-3’	53.4

***Table 14**: Primer sequences and melting temperatures of Assay 9, analysing CpGs 25 – 27 on enh3 inter, [Btn] = biotin*

Primer	Sequence	T_m [°C]
Forward	5'-GTTGTAGGGTATATGAGTTTAGAT-3‘	58.3
Reverse	5’-[Btn]-TTCATAACTCAAATTAACACACACT-3’	57.6
Sequencing	5’-TTTTGTGTTGAATGG-3’	37.8

***Table 15**: Primer sequences and melting temperatures of Assay 10, analysing CpGs 37 – 39 on enh3 inter, [Btn] = biotin*

Primer	Sequence	T_m [°C]
Forward	5'-GAGGTTATTTGGAAAGTTGAGAT-3‘	57.6
Reverse	5’-[Btn]-CTAATAATCCAAACCCTCTATTC-3’	57.6
Sequencing	5’-TTTAGTGTTATGGGAG-3’	43.2

enh4 inter

For this enhancer, four different assays were created to analyse CpGs 11 – 12, 13 – 14, 15 – 22, and 23 – 24, respectively. Primer sequences and melting temperatures are listed in Tables 16 – 19.

***Table 16**: Primer sequences and melting temperatures of Assay 11, analysing CpGs 11 – 12 on enh4 inter, [Btn] = biotin*

Primer	Sequence	T_m [°C]
Forward	5'-AATTAAATTGTTAAGTAGGTATTAGAG-3‘	57.6
Reverse	5’-[Btn]-AAATATCAAACTCTCAAATCATCCT-3’	57.6
Sequencing	5’-TAGGTATTAGAGGTTG-3’	43.2

***Table 17**: Primer sequences and melting temperatures of Assay 12, analysing CpGs 13 – 14 on enh4 inter, [Btn] = biotin*

Primer	Sequence	T_m [°C]
Forward	5'-TTGGTTTGTGTGTTATTTATAGTAT-3‘	55.9
Reverse	5’-[Btn]-TCCTCAATATTCAAACTATCATAATA-3’	56.8
Sequencing	5’-GTTGAATTTAGTTTTTGTAA-3’	46.1

***Table 18**: Primer sequences and melting temperatures of Assay 13, analysing CpGs 15 – 22 on enh4 inter, [Btn] = biotin*

Primer	Sequence	T_m [°C]
Forward	5'-TGTGTTAGTTTTAGTGGTTTAGA-3‘	55.5
Reverse	5’-[Btn]-TAACACACAAACCAATCTCTC-3’	55.4
Sequencing	5’-TAGTTTTAGTGGTTTAGAAGT-3’	51.7

***Table 19**: Primer sequences and melting temperatures of Assay 14, analysing CpGs 23 – 24 on enh4 inter, [Btn] = biotin*

Primer	Sequence	T_m [°C]
Forward	5'-AGTTATTGGAGTTGGTATAATAGA-3‘	56.6
Reverse	5’-[Btn]-ATCTCTTATTCTAATTCAACCTTCA-3’	57.6
Sequencing	5’-ATTATGGAAAGATTAAT-3’	38

enh5 inter

For this enhancer, three different assays were developed to analyse CpGs 12 – 17, 20 – 22, and 23 – 27, respectively. Tables 20 – 22 show their primer sequences and melting temperatures.

***Table 20**: Primer sequences and melting temperatures of Assay 15, analysing CpGs 12 – 17 on enh5 inter, [Btn] = biotin*

Primer	Sequence	T_m [°C]
Forward	5'-TGTGGTAGTGGTATTTTTTAGTTAGTAGA-3‘	63.3
Reverse	5'-[Btn]-CCATTTTAATATACAACACTTTCCCTTTTT-3	62.6
Sequencing	5'-AATTATTTTTTATGATTGTTA-3'	44

***Table 21**: Primer sequences and melting temperatures of Assay 16, analysing CpGs 20 – 22 on enh5 inter, [Btn] = biotin*

Primer	Sequence	T_m [°C]
Forward	5'-TTTGTATATTGAAGAGGGAAGAAGAA-3‘	60.1
Reverse	5'-[Btn]-AAAAAAAATAATTACTCTAACAACCCTTT-3'	59.2
Sequencing	5'-ATTATTTTTTATATTTTAG-3'	37.8

***Table 22**: Primer sequences and melting temperatures of Assay 17, analysing CpGs 23 – 27 on enh5 inter, [Btn] = biotin*

Primer	Sequence	T_m [°C]
Forward	5'-ATTGTAAGGGAAAGGGTTGTTAGAGTAA-3'	64.4
Reverse	5'-[Btn]-AACTCCCCTACAAACTTTTCACCCTAC-3'	66.6
Sequencing	5'-AGGTTTTGTTTATTGTAATTTTATG-3'	54.3

Promoter

The promoter region was analysed with one assay at the CpG sites 72 – 83. Even though the promoter is not an enhancer it is listed here for the sake of completeness and to better understand the positions of the enhancers. Table 23 lists primer sequences and melting temperatures of this assay.

***Table 23**: Primer sequences and melting temperatures of Assay 18, analysing promotor CpGs 72 – 83, [Btn] = biotin*

Primer	Sequence	T_m [°C]
Forward	5'-GGATATGTTGGGATAGTT-3‘	49.3
Reverse	5'-[Btn]-CCCAAACACTCACCAAAT-3'	51.4
Sequencing	5'-GGATATGTTGGGATAGTT-3'	49.3

enh6 intra

For this enhancer, only one assay was designed to analyse CpGs 8 – 10. Primer sequences and melting temperatures are shown in Table 24.

***Table 24**: Primer sequences and melting temperatures of Assay 19, analysing CpGs 8 – 10 on enh6 intra, [Btn] = biotin*

Primer	Sequence	T_m [°C]
Forward	5'-TTAATGATTTTTAGTTGTTTGTTGT-3‘	54.3
Reverse	5’-[Btn]-TACTATTATTATACATATCCAAATAAA-3’	54.7
Sequencing	5’-AGATGATTAGTAAGTGAGA-3’	48.9

enh7 intra

For this enhancer, four different assays were created to analyse CpGs 1 – 3, 7 – 8, 9 – 13, and 19 – 22, respectively. Tables 25 – 28 summarize primer sequences and melting temperatures.

***Table 25**: Primer sequences and melting temperatures of Assay 20, analysing CpGs 1 – 3 on enh7 intra, [Btn] = biotin*

Primer	Sequence	T_m [°C]
Forward	5'-[Btn]-GGAATGTGTTATTTAATTGGTATGT-3‘	57.6
Reverse	5’-CAAATCCCACAACAAATCCTTAT-3’	57.6
Sequencing	5’-ATAACTCATATCCCT-3’	37.8

***Table 26**: Primer sequences and melting temperatures of Assay 21, analysing CpGs 7 – 8 on enh7 intra, [Btn] = biotin*

Primer	Sequence	T_m [°C]
Forward	5'-GAGGTTTGATATAAGTAATGATGG-3‘	58.3
Reverse	5’-[Btn]-CCTCCTAATCCCACAATACAA-3’	57.5
Sequencing	5’-TAAGTAATGATGGTATG-3’	42.6

***Table 27**: Primer sequences and melting temperatures of Assay 22, analysing CpGs 9 – 13 on enh7 intra, [Btn] = biotin*

Primer	Sequence	T_m [°C]
Forward	5'-AGGTTTGATATAAGTAATGATGGTAT-3‘	58.4
Reverse	5’-[Btn]-CCTATTCTCTCCCACTTCAATA-3’	58.4
Sequencing	5’-GTATTGTGGGATTAGGA-3’	47.5

***Table 28**: Primer sequences and melting temperatures of Assay 23, analysing CpGs 19 – 22 on enh7 intra, [Btn] = biotin*

Primer	Sequence	T_m [°C]
Forward	5'-[Btn]-GTGTATTGAAGTGGGAGAGAATA-3‘	59.2
Reverse	5’-CAATAACAATTTTACAAACACAAATAACTT-3’	59.8
Sequencing	5’-ATAACTTTTCATTCA-3’	32.4

enh8 intra

For this enhancer, three different assays were developed to analyse CpGs 2 – 4, 6 – 7, and 10 – 12, respectively. Primer sequences and melting temperatures are presented in Table 29 – 31.

***Table 29**: Primer sequences and melting temperatures of Assay 24, analysing CpGs 2 – 4 on enh8 intra, [Btn] = biotin*

Primer	Sequence	T_m [°C]
Forward	5'-GGGTTGTTAGAAAGTTGATGAAA-3‘	57.6
Reverse	5’-[Btn]-AAAAAAAACAATTCATCTCCCTTTAT-3’	56.8
Sequencing	5’-AGAAAGTTGATGAAATG-3’	42.6

***Table 30**: Primer sequences and melting temperatures of Assay 25, analysing CpGs 6 – 7 on enh8 intra, [Btn] = biotin*

Primer	Sequence	T_m [°C]
Forward	5'-ATTGAATTATGGGTTTATTTAAAATGGT-3‘	58.2
Reverse	5’-[Btn]-ACACTTTCCACCTTTTACTATCA-3’	57.6
Sequencing	5’-GAGGTTAAAATTTTTATAGATTGGA-3’	55.9

***Table 31**: Primer sequences and melting temperatures of Assay 26, analysing CpGs 10 – 12 on enh8 intra, [Btn] = biotin*

Primer	Sequence	T_m [°C]
Forward	5‘-GATTTTTTAAATTAGTGAAGAGTGGATATT-3‘	61
Reverse	5‘-[Btn]-AAATCCCACAACCACAAAAAAAAACAA-3‘	60.8
Sequencing	5‘-TTAAATTAGTGAAGAGTGGATATT-3‘	55

enh9 intra

For this enhancer, only one assay was created to analyse CpGs 6 – 11. Table 32 shows primer sequences and melting temperatures of this assay.

***Table 32**: Primer sequences and melting temperatures of Assay 27, analysing CpGs 6 – 11 on enh9 intra, [Btn] = biotin*

Primer	Sequence	T_m [°C]
Forward	5‘-TGGTTTAAGTTATTTAGGTTGAATGTTAAT-3	61
Reverse	5‘-[Btn]-CTACTCATTAAAAATACCATCACTCAAAT-3‘	62.1
Sequencing	5‘-ATTGAGTATATTTTATTAAGAA-3‘	47.4

4.4 Determination of 5-hydroxymethylcytosine

In this section, two different methods for determining 5-hydroxymethylcytosine are presented. To evaluate their effectiveness, varying temperature protocols were used. Additionally, standards were compared before applying the methods to genomic hippocampal samples. Sequences of these standards are listed in Table 33. These were diluted 1:15,000 from an initial concentration of 5 ng/µL and analysed using Assay 4 (Table 9).

***Table 33**: Sequence of oligonucleotide standards for 5-hmC determination*

Manufacturer	Methylation status	Sequence
Eurogentec	Unmethylated (C)	5'-AGGGATTTGGAGGGCAGGTGAAGCTGTGTTTGCCC AGGAAAGCGAGATCCTTAGCGAAGTCCC AGCTGAGTGTGGCCTGTGCCAAGCAGATAGCTGA-3‘
Eurogentec	Methylated (5-mC)	5‘-AGGGATTTGGAGGGCAGGTGAAGCTGTGTTTGCCC AGGAAAG(5-mC)GAGATCCTTAG(5-mC)GAAGTCCC AGCTGAGTGTGGCCTGTGCCAAGCAGATAGCTGA-3‘
Eurogentec	Hydroxymethylated (5-hmC)	5‘-AGGGATTTGGAGGGCAGGTGAAGCTGTGTTTGCCC AGGAAAG(5-hmC)GAGATCCTTAG(5-hmC)GAAGTCCC AGCTGAGTGTGGCCTGTGCCAAGCAGATAGCTGA-3‘

4.4.1 Oxidative bisulfite sequencing

The protocol for oxidative bisulfite sequencing had already been established in the working group. The approach involved the incorporation of a specialized oxidant as described by Liu et al.[54] Prior to conversion, genomic DNA had to be purified. For standards this process was not necessary.

Figure 13 illustrates the workflow of oxBS for the determination of 5-hmC. Here, oxidation is carried out prior to bisulfite sequencing and subsequent analysis using PCR and PSQ.

Oxidation	→	**Bisulfite conversion and cleanup**	→	**PCR**	→	**PSQ**

***Figure 13**: Workflow for 5-hydroxymethylcytosine determination using oxBS*

Genomic DNA was purified using Bio-Rad Micro Bio-Spin columns.[75] To prepare the column, it was inverted sharply several times to resuspend the settled gel and eliminate air bubbles. The tip was snapped off and the column was placed in a 2.0 mL microcentrifuge tube. Excess packing buffer was allowed to drain and discarded, and the column was placed back into the tube. For further preparation, the SSC buffer was replaced with Milli-Q water by spinning the column at 1,000 g for one minute in a 2.0 mL collection tube, discarding the eluate, and adding 500 µL of Milli-Q water. This process was repeated three more times. A final spin was performed for two minutes at 1,000 g,

ensuring the column did not dry out. Finally, the genomic DNA was added to the prepared column and centrifuged for four minutes at 1,000 g into a fresh tube.

The preparation of the oxidant began with the formulation of a 150 mM solution of potassium perruthenate ($KRuO_4$) in 0.5 M sodium hydroxide (NaOH) using ELGA water. The solution was incubated at 25°C for two days to produce potassium ruthenate (K_2RuO_4). During incubation, the solution was vortexed twice daily to eliminate bubbles, with a noticeable colour change to deep red indicating the formation of the desired product. The final oxidant solution was stored at -20 °C as a 10x stock for further use.

For the oxidation, 21.75 µL of pure unmethylated, methylated, or hydroxymethylated cytosine standards, or genomic hippocampus extract containing 100 ng DNA, were used. The DNA was denatured by adding 1.25 µL of 1 M NaOH and incubating it at 37 °C for 30 minutes. Meanwhile, the 10x oxidant was diluted 1:10 with ELGA water, and 2.88 µL of the diluted oxidant was added to the denatured DNA. The oxidation reaction was carried out at 37 °C and 850 rpm in a Thermo-Mixer for one hour. Subsequently, an additional 2.88 µL of the oxidant was added to the same reaction, followed by another incubation at 37 °C and 850 rpm in a Thermo-Mixer for one hour.

The following conversion was performed using the Epitect Fast Bisulfite Conversion Kit (Qiagen) [67] according to the manufacturer's protocol [68], employing the low-concentration setup. The oxidized DNA was diluted with RNase-free water to a final volume of 40 µL, and bisulfite solution along with DNA Protect Buffer was added (Table 34). The components were combined and thoroughly vortexed in a 200 µL tube.

***Table 34**: Reaction setup of oxidative bisulfite conversion*

Components	High-concentration samples (1 ng - 2 µg) Volume [µL]	Low-concentration samples (1 ng - 500 ng) Volume [µL]
Oxidized DNA	Variable *	Variable **
RNase-free water	Variable *	Variable **
Bisulfite solution	85	85
DNA protect buffer	35	15
Total volume	140	140

* DNA and RNase-free water should add up to 20 µL

** DNA and RNase-free water should add up to 40 µL

Oxidative bisulfite conversion was carried out using the Bio-Rad iCycler Thermal Cycler, following different thermal programs outlined in Table 35.

***Table 35**: Time programs for oxidative bisulfite conversion, one cycle consists of: denaturation at 95°C for 5 minutes followed by incubation at 60 °C for 10 minutes, 10-minute break between each incubation*

Program no.	No. of incubations	Time total [min]	Incubation time total [min]
1	2	30	20
2	4	60	40
3	4	160	140
4	6	320	290
5	6	460	430
6	6	600	570

Next, cleanup and determination of DNA concentration were performed. This procedure was analogous to the cleanup process following bisulfite conversion, as described in chapter 4.2. To determine 5-hmC levels, the results from oxidative bisulfite sequencing needed to be subtracted from those of standard bisulfite sequencing (Equation 1). Therefore, standard bisulfite sequencing was performed under the same conditions as oxBS. The protocol for the standard bisulfite sequencing is described in chapter 4.2.

$$\%(5\text{-}hmC) = \%(5\text{-}mC + 5\text{-}hmC)_{from\ BS} - \%(5\text{-}mC)_{from\ oxBS}$$

***Equation 1**: Calculation of 5-hmC levels for oxBS*

4.4.2 Chemically assisted pyridine borane sequencing

The bisulfite-free, chemically assisted pyridine borane sequencing method serves as an alternative to oxidative bisulfite sequencing and eliminates the need for standard bisulfite conversion prior to analysis. The protocol for this subtraction-free determination of 5-hmC was originally proposed by Liu et al. [54] and subsequently adapted by the working group. As in the previous protocol, standards containing unmethylated, methylated, and hydroxymethylated cytosines were used prior to analysing genomic DNA (Table 33). Figure 14 illustrates the workflow of CAPS. Note that DNA purification is required prior to the oxidation step.

Oxidation and cleanup	→	**Reduction and cleanup**	→	**PCR**	→	**PSQ**

***Figure 14**: Workflow for 5-hydroxymethylcytosine determination using CAPS*

This protocol also required the synthesis of potassium ruthenate, which is described in chapter 4.4.1. Likewise, 21.75 µL of a sample containing 100 ng of hippocampus DNA or standards were used in each reaction. Genomic DNA had to be purified using a Bio-Rad micro-column, as described in chapter 4.4.1.

The reaction was started by denaturing the DNA with 1.25 µL of 1 M NaOH, followed by incubation for 30 minutes at 37 °C. The oxidant K_2RuO_4 was diluted 1:10 with ELGA water, and 2.88 µL were added to the denatured DNA. After incubation for one hour at 37 °C and 850 rpm in a Thermo-Mixer, 2.88 µL of the oxidant were added again, followed by another incubation for one hour. The solution should remain orange for the whole duration of the oxidation. Any shift to green, brown, or black implies a reaction of the oxidant with contaminants and indicates that the oxidation has likely failed.

Prior to the next step, 3 µL of a 1000 ng/µL Qiagen Carrier-RNA solution were added to each sample as background. The oxidized DNA was then purified using Micro Bio-Spin columns (Bio-Rad). Prior to adding the samples, the columns were centrifuged at 1,000 rcf for two minutes to eliminate the packing buffer. Following this, the DNA samples were loaded onto the columns, and the mixtures were centrifuged at 1,000 rcf for an additional four minutes to complete the purification process.

The purified, oxidized DNA was introduced into a reaction mixture consisting of 0.6 M MES (4-morpholineethanesulfonic acid, Sigma Aldrich, dissolved in ELGA water) and 0.2 M pic-borane (2-methylpyridine borane complex, Thermo Fisher, freshly prepared in absolute ethanol). The mixture was incubated at 37 °C with continuous shaking at 850 rpm for two hours to promote the reduction process.

For the cleanup process, seven volumes of Oligo Binding Buffer were added to the sample and transferred into IC spin columns (Zymo Research)[76]. The columns were centrifuged at 12,000 rcf for 30 seconds, and the flow-through was discarded. The columns were then washed twice with 200 µL of Wash Buffer under the same centrifugation conditions. Finally, the DNA was eluted by adding 15 µL of pre-warmed DNA Elution Buffer (65 °C) to the column, incubating for one minute, and centrifuging for 30 seconds. The concentration of the obtained DNA was measured using the Qubit ssDNA Assay kit from Thermo Fisher[69] (see section 4.2.) The treated DNA was stored at -20 °C.

4.5 Polymerase chain reaction results

All amplifications were performed using the PyroMark PCR Kit from Qiagen.[77] The reactions were conducted using either the QuantStudio 5 Thermocycler (Thermo Fisher) or the Rotor-Gene Q Thermocycler (Qiagen). For DNA methylation level analysis of melanoma brain metastases two independent measurements were performed. Each was performed on a different thermocycler to increase time efficiency and assess robustness. PCR conditions for each assay had already been optimized by the working group to ensure reliable results (Table 37 and Supplementary Table 1).

For each amplification, a total volume of 20 µL was used, but the volume of DNA extract varied, due to the limited availability of sample material. For DNA methylation level analysis of melanoma brain metastases 1 µL of a 2.5 ng/µL extract and 19 µL master mix were used. For the determination of 5-hydroxymethylcytosine 2 µL of a 2.5 ng/µL extract and 18 µL master mix were used. Table 36a and 36b depict the utilized components of

each PCR run. Primer concentrations are depended on the used assay (Supplementary Table 1).

***Table 36a**: PCR reaction setup for enhancer methylation analysis (Primer conc. in Supplementary Table 1)*

Components	Volume [µL] Primer concentration*	
	0.2 µM	0.4 µM
Rnase-free water	5.2	4.4
2x PyroMark PCR Master Mix	10	10
10x CoralLoad Concentrate	2	2
20x EvaGreen Dye	1	1
Primer forward 10 µM	0.4	0.8
Primer reverse 10 µM	0.4	0.8
Mastermix per well	19	19
DNA-extract 2.5 ng/µl	1	1

***Table 36b:** PCR reaction setup for 5-hmC determination (Primer conc. in Supplementary Table 1)*

Components	Volume [µL] Primer concentration*	
	0.2 µM	0.4 µM
Rnase-free water	4.2	3.4
2x PyroMark PCR Master Mix	10	10
10x CoralLoad Concentrate	2	2
20x EvaGreen Dye	1	1
Primer forward 10 µM	0.4	0.8
Primer reverse 10 µM	0.4	0.8
Mastermix per well	18	18
DNA-extract 2.5 ng/µl	2	2

*Primer concentration depended on the used assay

Table 37 illustrates the thermal cycling program used for the amplifications with both thermocyclers. Additionally, each assay included two no-template controls (NTCs), where the DNA extract was replaced with RNase-free water to check for contamination. The amplification products were stored at -20 °C until PSQ analysis.

***Table 37**: Thermal cycling program, * annealing temperature (T_a) depended on the specific assay (for more information see Supplementary Table 1), HRM = High-Resolution Melting*

	Step	Time	Temperature [°C]	Repeat
Hold 1	Denaturation, polymerase activation	15 min	95	
Cycling 1	Denaturation	30 s	94	50 cycles
	Annealing	30 s	T_a (variable)*	
	Elongation	30 s	68	
Hold 2	Final elongation	10 min	68	
Hold 3	Denaturation	1 min	95	
Hold 4	Strand pairing	1 min	40	
HRM		-	65 - 85	0.1°C/step (RotorGene) 0.05°C/step (QuantStudio)

4.6 Pyrosequencing results

The PyroMark Q48 Autoprep and Q48 Advanced Reagents from Qiagen[78] were used for pyrosequencing of all PCR products. Lyophilized enzyme and substrate were dissolved in annealing buffer, and primers were diluted to 4 µM using ELGA water. All necessary reagents, including nucleotides, primers, binding buffer, denaturation solution, enzyme solution, and substrate solution, were loaded into the system. Additionally, 3 µL of magnetic streptavidin-coated Sepharose beads (Qiagen)[78] were added to each well of the Q48 disc. Before starting the system, 10 µL of amplicons were pipetted into each well. The system then automatically added 2 µL of primer along with the other reagents for analysis.

4.7 Data analysis

Raw PCR data from both Rotor-Gene Q Series Software (Qiagen) and QuantStudio Design & Analysis Software (Thermo Fisher) were exported to Microsoft Excel to generate an overview of the results.

Raw PSQ data were exported from PyroMark Q48 Autoprep Software (Qiagen) to Microsoft Excel to calculate mean values.

Since the LLOQ (lower limit of quantification) of PSQ is known to be 5 %, raw data had to be adjusted prior to statistical evaluation and graphical illustration. Results that were below 5 % (<LLOQ) were replaced with 2.5 % and results above 95 % were replaced with 97.5 % (<ULOQ (upper limit of quantification)).

Statistical analysis was performed using SPSS Statistics (IBM) for Kaplan-Meier plots, Spearman's rho, and Mann-Whitney U tests. Additionally, the Mann-Whitney U test calculator from Statistics Kingdom was used.

5 Results and discussion

One aim of this thesis was to investigate whether CpG methylation in MGMT enhancers correlates with MGMT expression. Pyrosequencing assays targeting MGMT enhancer regions were applied to a set of melanoma brain metastases (see chapter 4.1). The evaluated methylation levels were tested for correlation with MGMT expression, results are shown in the following chapter.

Secondly, two established methods from the literature for detecting 5-hydroxymethylcytosine were assessed for future studies of DNA modifications. Oxidative bisulfite sequencing and chemically assisted pyridine borane sequencing were applied to a set of standards and a hippocampal sample (see chapter 4.4). The evaluation of these methods is also presented in this section.

5.1 DNA methylation analysis

MGMT enhancer methylation levels in melanoma brain metastasis samples were determined for nine enhancers in total. Five enhancers (enh1 inter, enh2 inter, enh3 inter, enh4 inter, enh5 inter) are located upstream and not within the MGMT gene and therefore intergenic. The other four enhancers (enh6 intra, enh7 intra, enh8 intra, enh9 intra) are located within the gene and therefore intragenic. Detailed information on all assays is given in chapter 4.3. For all methylation data presented below, the mean values were from two independent measurement runs per sample were calculated.

The first analysis of CpGs in the promoter region were determined by Katharina Pühringer, MSc. The second analysis was carried out in this master thesis. In the following section, promoter results will be presented first, followed by the MGMT enhancer methylation levels.

The correlation between MGMT expression and methylation levels in the MGMT promoter and enhancer regions will be discussed.

5.1.1 Promoter methylation

Promoter methylation levels were analysed for twelve CpG sites (No. 72 – 82). Primer sequences are given in chapter 4.3. Raw MGMT promoter methylation data is available in chapter 8.2 (Supplementary Table 11 – 12).

Figure 15 shows the distribution of methylation levels across twelve analysed CpG sites in the MGMT promoter in melanoma brain metastasis samples. A significant difference ($p \leq 0.001$) can be observed between samples that express MGMT and those that do not. MGMT-expressing samples showed much lower methylation levels across the promoter region, with seven out of nine samples exhibiting methylation levels below the LLOQ of the method used. In contrast, non-expressing samples showed distinctly elevated methylation levels.

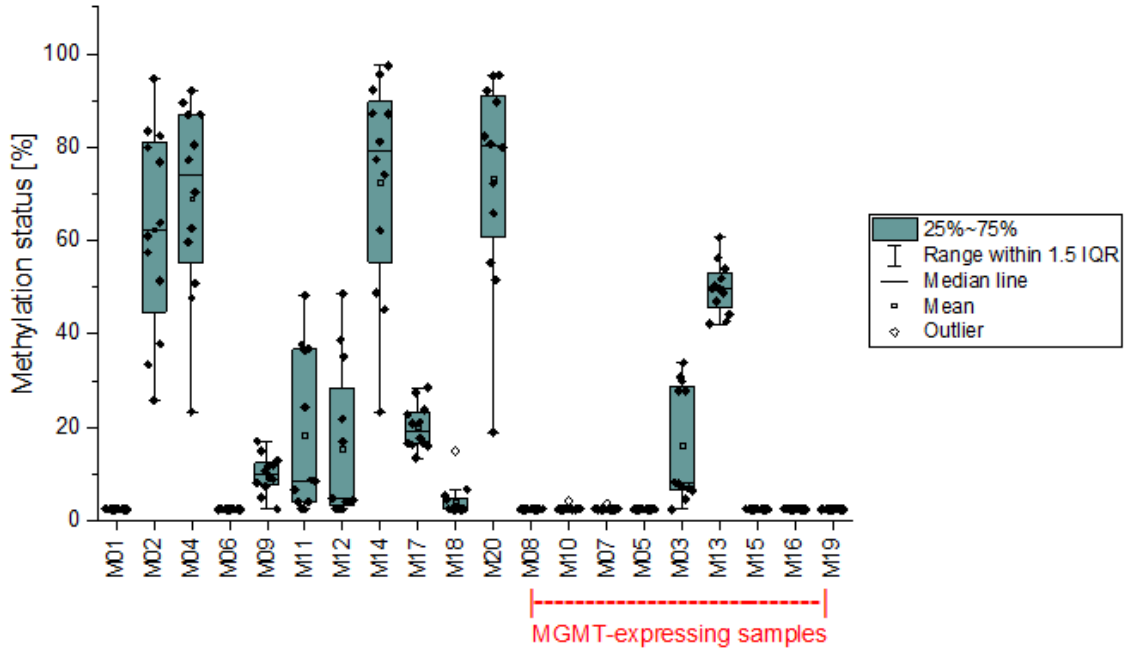

***Figure 15**: Distribution of methylation levels across twelve CpG sites in the MGMT promoter in melanoma brain metastasis samples determined by PSQ. MGMT-expressing samples are ordered by increasing expression, with M16 and M19 showing the highest expression levels (see chapter 8.3, Supplementary Table 18); IQR = interquartile range*

However, there were two samples in each group, which did not align with these established findings. Samples M03 and M13, both of which express MGMT, showed clear methylation across the twelve analysed CpG sites. Therefore, promoter methylation alone, cannot reliably predict the absence of MGMT expression. Conversely, samples M01 and M06, which do not express MGMT, display methylation levels below the LLOQ. These findings suggest an alternative mechanism of gene silencing that does not involve promoter methylation alone. For this reason, analysing methylation levels across enhancer regions might provide further insight into the regulatory mechanisms controlling MGMT expression.

Figure 16 compares the distribution of MGMT promoter methylation across twelve CpG sites between MGMT-expressing and non-expressing samples. Across all CpG sites, MGMT-expressing samples (red) showed a significantly lower methylation level. The majority of MGMT-expressing samples even showed a methylation level below LLOQ. For non-expressing samples (grey) a considerable methylation level was detected.

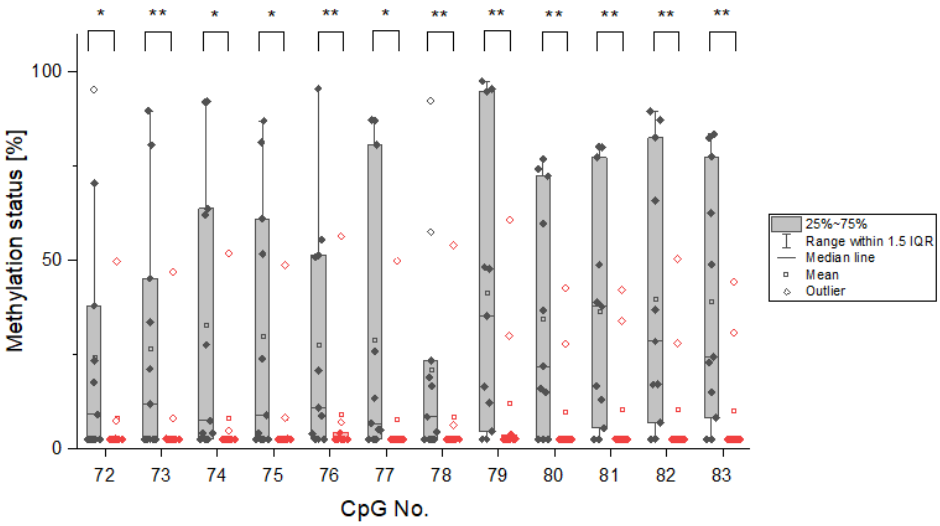

***Figure 16**: Comparison of MGMT promoter methylation distribution across twelve CpG sites in MGMT-expressing and non-expressing melanoma brain metastasis samples determined by PSQ; Grey: non MGMT-expressing samples, red: MGMT-expressing samples, IQR = interquartile range, *p≤0.05, **p≤0.01*

The scatterplot in Figure 17 illustrates the association between methylation of the twelve MGMT promoter CpG sites and MGMT expression in melanoma brain metastasis samples. As shown in Figures 15 and 16, non MGMT-expressing samples exhibited high methylation levels across the twelve analysed CpG sites, whereas seven out of nine MGMT-expressing samples were completely unmethylated at all twelve sites. Samples M03 and M13, which belong to the MGMT-expressing group, showed methylation in the promoter region. Both samples exhibited a MGMT protein expression level of 0.2 (see chapter 8.3 Supplementary Table 18).

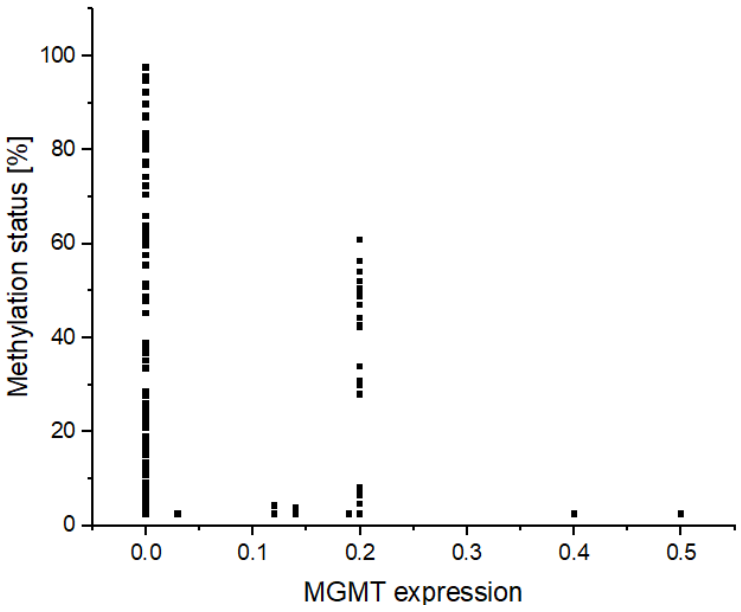

***Figure 17**: Association between methylation levels of the twelve MGMT promoter CpG sites and MGMT expression in the 20 analysed melanoma brain metastasis samples*

Correlation between MGMT promoter methylation for all twelve analysed CpG sites and MGMT expression was assessed using Spearman-Rho correlation coefficients, as shown in Table 38. All correlations were inverse, indicating that higher MGMT promoter methylation was associated with lower MGMT expression. However, only six CpG sites showed a statistically significant correlation with p-values below 0.05.

***Table 38**: MGMT promoter: Correlation between methylation levels at specific CpG sites and MGMT expression; *p≤0.05*

CpG	Spearman Rho	p-value
72	-0.318	0.172
73	-0.318	0.172
74	-0.459	0.042*
75	-0.408	0.074
76	-0.402	0.079
77	-0.522	0.018*
78	-0.371	0.108
79	-0.483	0.031*
80	-0.441	0.052
81	-0.510	0.021*
82	-0,510	0.210*
83	-0.510	0.210*

5.1.2 Enhancer methylation

In the following section, the results of methylation analysis across nine different enhancers in melanoma brain metastasis samples are presented. The enhancers are arranged according to their order in the genome (enh1 inter, enh2 inter, enh3 inter, enh4 inter, enh5 inter, [promoter] enh6 intra, enh7 intra, enh8 intra, enh9 intra). Primer sequences are provided in chapter 4.3. The samples were independently analysed twice and mean values were calculated. Raw MGMT enhancer methylation data is available in chapter 8.2 (Supplementary Table 2 – 10, 13 – 17).

Due to the use of previously established assays, CpG coverage varied between enhancers and was not extended within this master thesis.

<u>enh1 inter (Assay 1)</u>

MGMT methylation levels were analysed for three CpG sites (No. 1 – 3) on enh1 inter. Figure 18 illustrates the distribution of methylation levels across these three sites. A statistically significant difference (p≤0.001) between MGMT-expressing and non-expressing samples was observed.

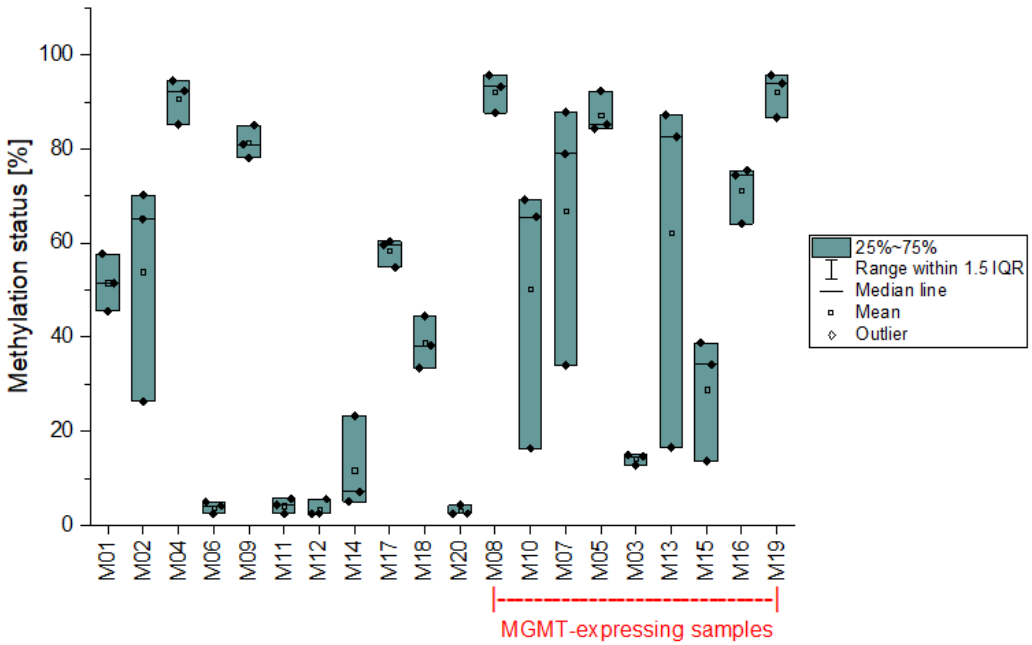

***Figure 18**: Distribution of methylation levels across three CpG sites in enh1 inter in melanoma brain metastasis samples determined by PSQ. MGMT-expressing samples are ordered by increasing expression, with M16 and M19 showing the highest expression levels (see chapter 8.3, Supplementary Table 18); IQR = interquartile range*

Figure 19 compares the MGMT enhancer methylation distribution between MGMT-expressing samples and non-expressing samples. Two out of the three CpG sites showed a statistically significant difference between the two groups. Both Figures 18 and 19 indicate a higher methylation level across CpG sites in enh1 inter in MGMT-expressing samples.

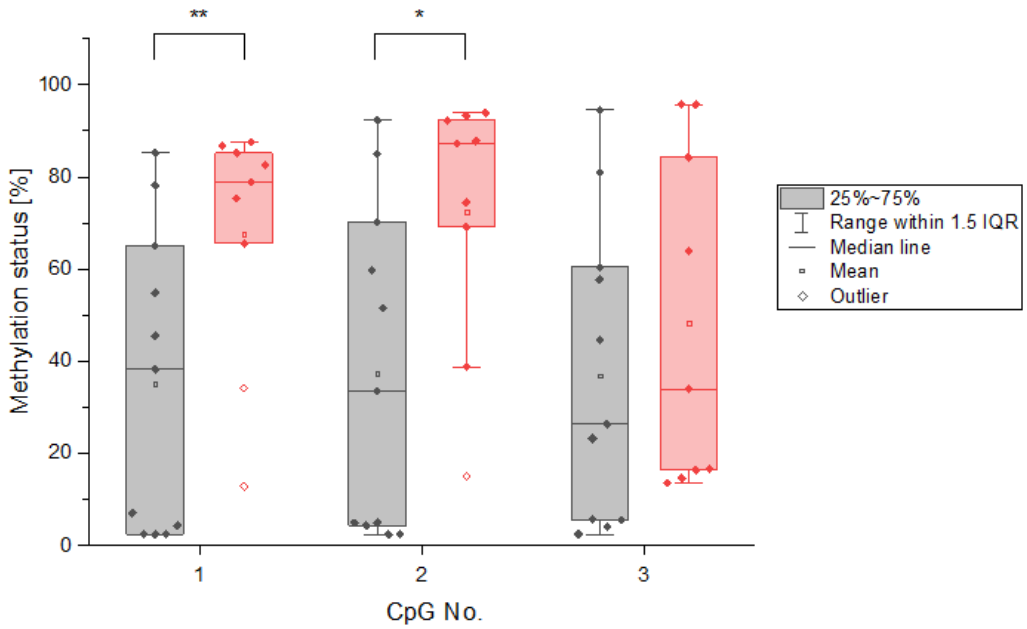

***Figure 19**: Comparison of methylation distribution in enh1 inter across three CpG sites in MGMT-expressing and non-expressing melanoma brain metastasis samples determined by PSQ, Grey: non MGMT-expressing samples, red: MGMT-expressing samples, IQR = interquartile range, *p≤0.05, **p≤0.01*

Table 39 and Figure 20 present the association between MGMT expression and methylation status across the analysed enhancer CpG sites. A statistical trend was observed. It appears as though samples with higher methylation levels exhibited higher MGMT expression. This relationship was further supported by Spearman's Rho values. Two out of the three analysed CpG sites showed a statistically significant correlation, with p-values below 0.05.

***Table 39**: enh1 inter: Correlation between methylation levels at specific CpG sites and MGMT expression; *p≤0.05*

CpG	Spearman Rho	p-value
1	0.460	0.041*
2	0.467	0.034*
3	0.222	0.347

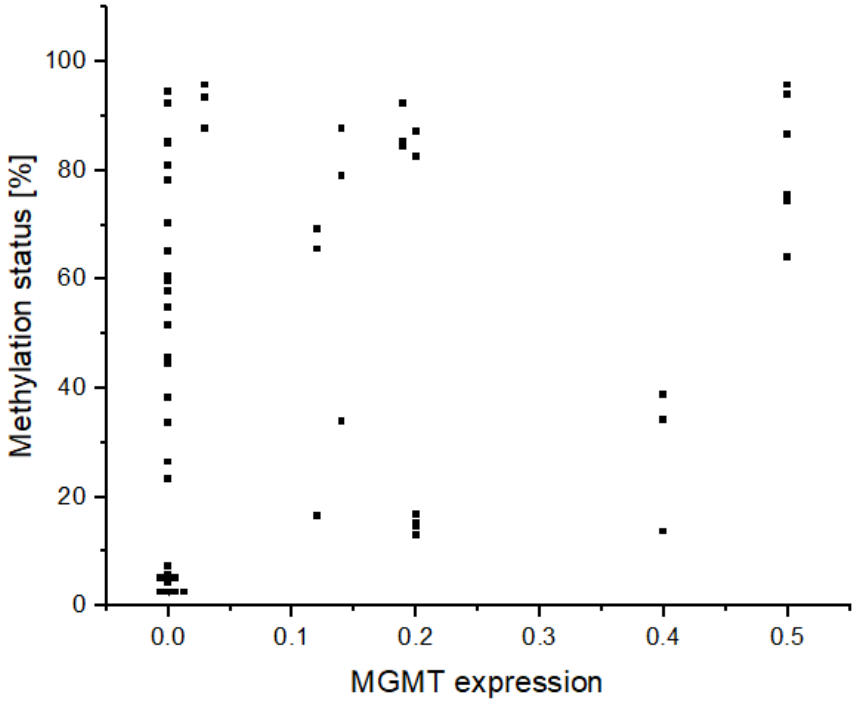

***Figure 20**: Association between methylation levels of the three CpG sites in enh1 inter and MGMT expression in the 20 analysed melanoma brain metastasis samples*

<u>enh2 inter (Assay 2 – 6)</u>

The enhancer enh2 inter was targeted by five different assays to analyse 17 CpG sites located within the enhancer (No. 9, 12 – 27). Additionally, two CpG sites immediately downstream (27+1, 27+2) were targeted by one of the assays. Figure 21 shows the distribution of methylation levels across these CpG sites. No clear trend can be observed in this plot. Methylation levels were generally low for both the MGMT-expressing and non-expressing groups. Only one sample from of each group (M01 and M16) displayed consistently high methylation across all analysed CpG sites.

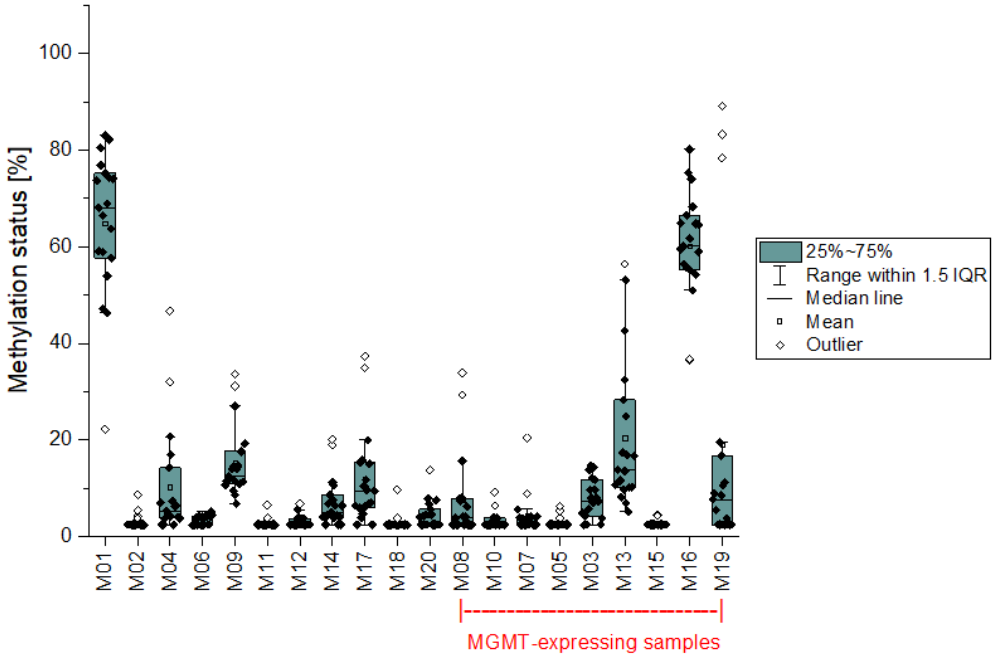

***Figure 21**: Distribution of methylation levels across 17 (+2) CpG sites in enh2 inter in melanoma brain metastasis samples determined by PSQ. MGMT-expressing samples are ordered by increasing expression, with M16 and M19 showing the highest expression levels (see chapter 8.3, Supplementary Table 18); IQR = interquartile range*

Figure 22 illustrates the methylation distribution of enh2 inter across the analysed CpG sites in MGMT-expressing and non-expressing melanoma brain metastasis samples. Similar to Figure 21, no clear trend or major differences between the two groups were observed. Overall, methylation levels were low across all samples.

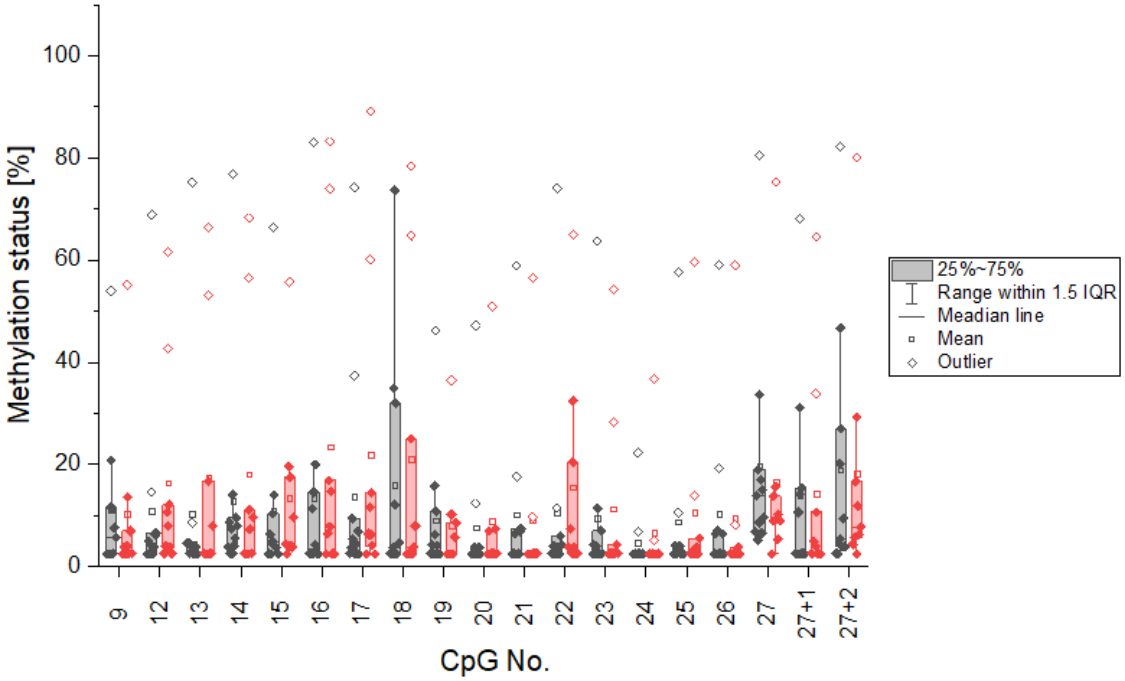

***Figure 22**: Comparison of methylation distribution in enh2 inter across 17 (+2) CpG sites in MGMT-expressing and non-expressing melanoma brain metastasis samples determined by PSQ; Grey: non MGMT-expressing samples, red: MGMT-expressing samples, IQR = interquartile range*

Figure 23 and Table 40 present the results of the correlation analysis. No statistically significant p-values were obtained for this enhancer analysis. Therefore, neither a positive nor a negative correlation between CpG methylation and MGMT expression could be identified for enh2 inter.

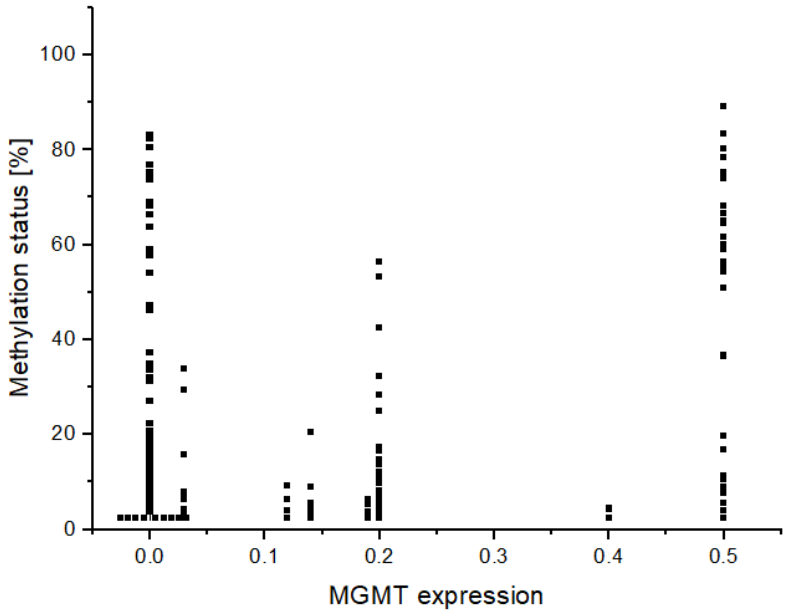

***Figure 23**: Association between methylation levels of the 17 (+2) CpG sites in enh2 inter and MGMT expression in the 20 analysed melanoma brain metastasis samples*

***Table 40**: enh2 inter: Correlation between methylation levels at specific CpG sites and MGMT expression*

CpG	Spearman Rho	p-value
9	-0.003	0.991
12	0.246	0.295
13	0.209	0.377
14	0.110	0.664
15	0.332	0.153
16	0.324	0.164
17	0.302	0.195
18	0.148	0.533
19	0.087	0.715
20	0.116	0.626
21	-0.093	0.697
22	0.219	0.354
23	0.015	0.949
24	0.152	0.522
25	0.139	0.560
26	-0.024	0.921
27	-0.150	0.528
+1	0.015	0.949
+2	0.154	0.516

enh3 inter (Assay 7 – 10)

The enhancer enh3 inter showed a similar pattern to enh2 inter. This enhancer, targeted by four different assays covering 18 specific CpG sites (No. 5 – 8, 11 – 18, 25 – 27, 37 – 39), exhibited varying methylation levels across all 20 samples. The methylation distribution shown in Figure 24 also indicates no difference between MGMT-expressing and non-expressing samples.

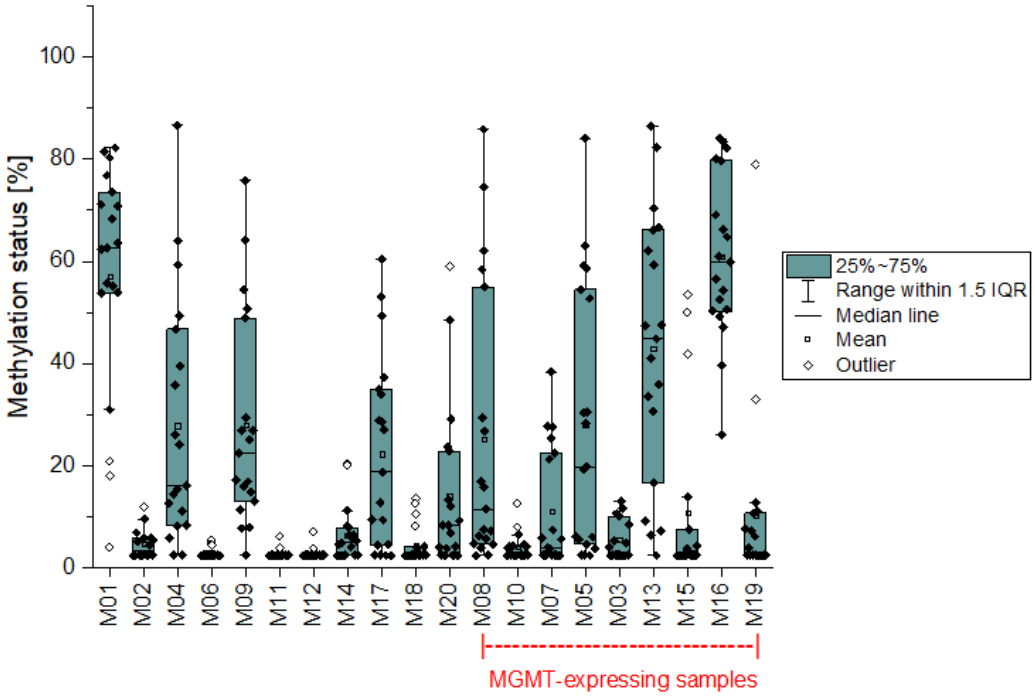

***Figure 24**: Distribution of methylation levels across 18 CpG sites in enh3 inter in melanoma brain metastasis samples determined by PSQ. MGMT-expressing samples are ordered by increasing expression, with M16 and M19 showing the highest expression levels (see chapter 8.3, Supplementary Table 18); IQR = interquartile range*

Similar findings are shown in Figure 25, which depicts the methylation distribution of enh3 inter in MGMT-expressing and non-expressing samples. No clear trend is observed, as both groups exhibited varying methylation levels across the 18 different CpG sites. A localised low methylation region at CpGs 25 – 27 in both groups was found. Nearly all samples showed methylation levels below the LLOQ.

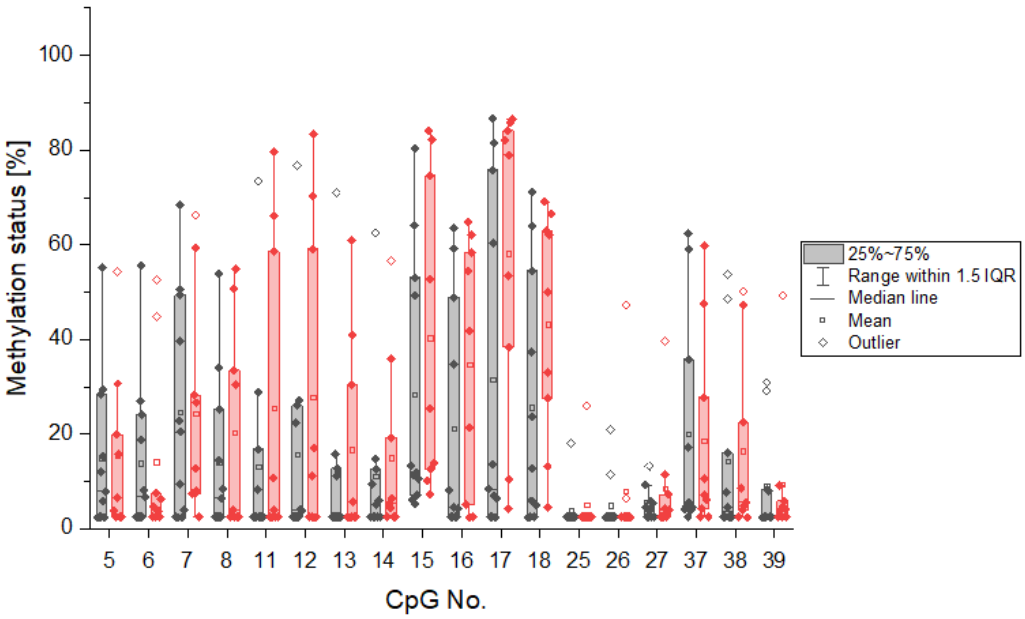

***Figure 25**: Comparison of methylation distribution in enh3 inter across 18 CpG sites in MGMT-expressing and non-expressing melanoma brain metastasis samples determined by PSQ; Grey: non MGMT-expressing samples, red: MGMT-expressing samples, IQR = interquartile range*

Figure 26 illustrates the association between methylation levels of enh3 inter and MGMT expression. No clear trend can be identified.

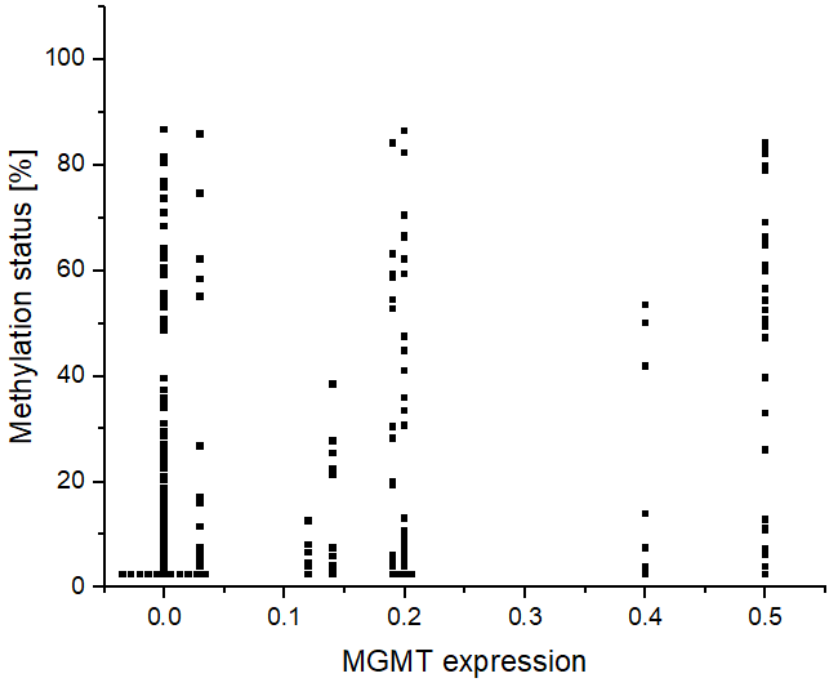

***Figure 26**: Association between methylation levels of the 18 CpG sites in enh3 inter and MGMT expression in the 20 analysed melanoma brain metastasis samples*

Table 41 presents the results of the correlation analysis between MGMT enhancer methylation and MGMT expression. As with enh2 inter, no statistically significant p-values were obtained. Therefore, no statistical correlation between CpG methylation and MGMT expression could be identified for enh3 inter.

***Table 41**: enh3 inter: Correlation between methylation levels at specific CpG sites and MGMT expression*

CpG	Spearman Rho	p-value
5	0.023	0.924
6	0.037	0.877
7	0.089	0.709
8	0.028	0.908
11	0.276	0.239
12	0.163	0.492
13	0.117	0.623
14	0.103	0.664
15	0.247	0.294
16	0.259	0.270
17	0.403	0.078
18	0.381	0.097
25	0.164	0.491
26	0.152	0.522
27	0.030	0.899
37	-0.005	0.985
38	0.156	0.524
39	0.131	0.592

<u>enh4 inter (Assay 11 – 14)</u>

enh4 inter was targeted by four assays, which analysed 14 CpG sites in total (No. 11 – 24). Figure 27 illustrates the distribution of methylation levels across these CpG sites in the 20 samples. A significant trend ($p \leq 0.001$) could be identified between MGMT-expressing and non-expressing samples. Samples expressing MGMT tended to exhibit higher methylation levels. The non-expressing group includes three samples with methylation levels below than the LLOQ and four samples with a mean methylation of approximately 5 %. Nevertheless, four samples (M01, M04, M09 and M17) in this group showed substantially higher methylation levels, resulting in a heterogeneous distribution. In contrast, all MGMT-expressing samples displayed medium to high methylation levels.

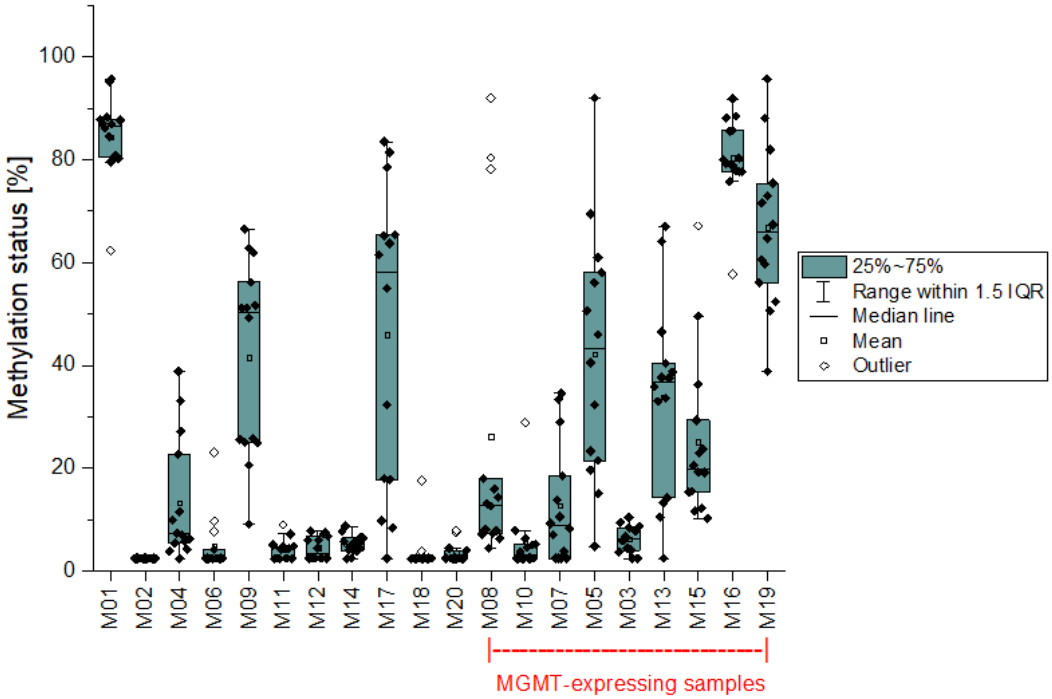

***Figure 27**: Distribution of methylation levels across 14 CpG sites in enh4 inter in melanoma brain metastasis samples determined by PSQ. MGMT-expressing samples are ordered by increasing expression, with M16 and M19 showing the highest expression levels (see chapter 8.3, Supplementary Table 18); IQR = interquartile range*

Figure 28 shows the methylation distribution across all 14 CpG sites in the MGMT enhancer for MGMT-expressing and non-expressing samples. For each CpG mean methylation of all samples are higher in the MGMT-expressing group.

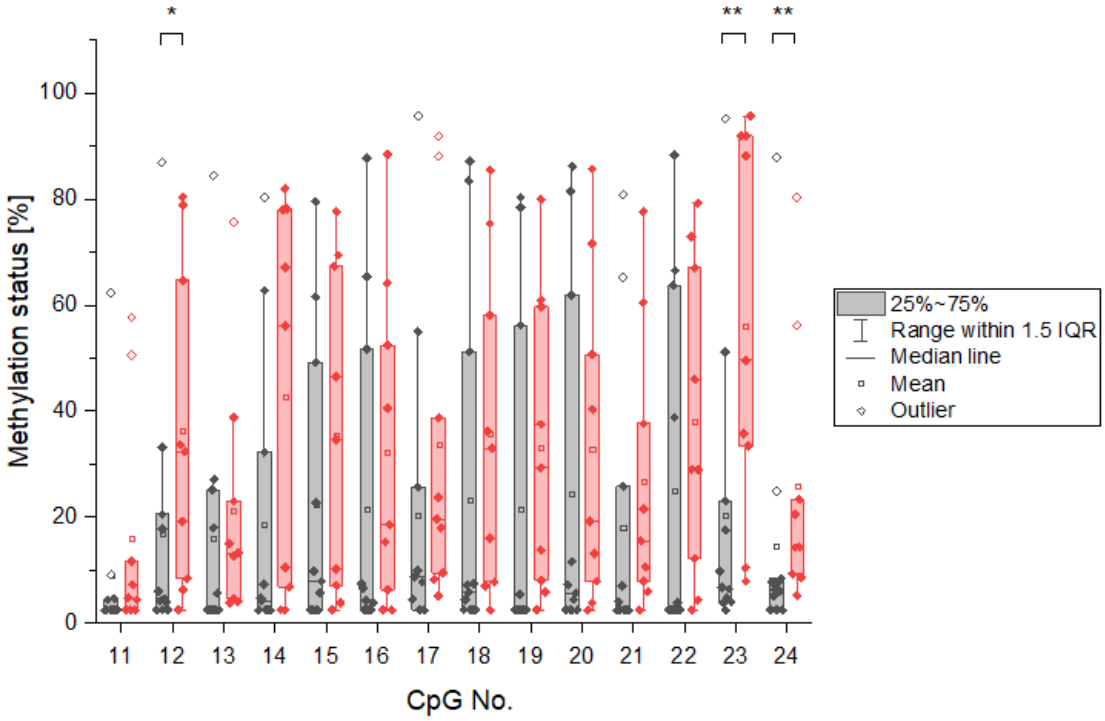

***Figure 28**: Comparison of methylation distribution in enh4 inter across 14 CpG sites in MGMT-expressing and non-expressing melanoma brain metastasis samples determined by PSQ; Grey: non MGMT-expressing samples, red: MGMT-expressing samples, IQR = interquartile range, *p≤0.05, **p≤0.01*

Figure 29 illustrates the association between enh4 inter methylation levels and MGMT expression in the samples. It is evident that samples lacking expression exhibited a broad range of methylation levels. Moreover, samples with higher expression levels also exhibited higher methylation levels. This positive correlation is further supported by Spearman's Rho calculations, as shown in Table 42.

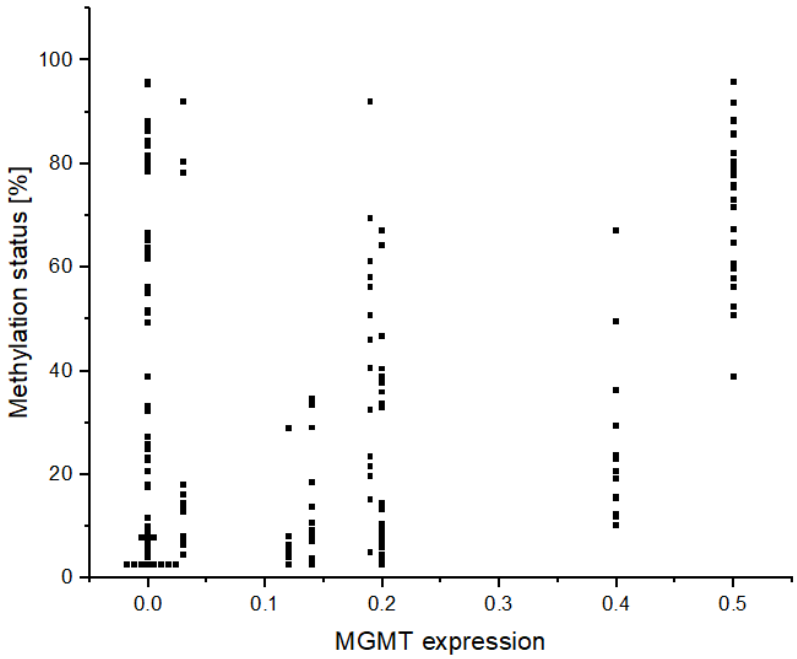

***Figure 29**: Association between methylation levels of the 14 CpG sites in enh4 inter and MGMT expression in the 20 analysed melanoma brain metastasis samples*

Spearman's Rho values indicate a positive correlation between MGMT expression and methylation levels in enh4 inter. However, this correlation was statistically significant at only six of the 14 sites.

***Table 42**: enh4 inter: Correlation between methylation levels at specific CpG sites and MGMT expression; *p≤0.05, **p≤0.01*

CpG	Spearman Rho	p-value
11	0.405	0.076
12	0.442	0.051
13	0.412	0.071
14	0.457	0.043*
15	0.362	0.117
16	0.349	0.132
17	0.455	0.044*
18	0.435	0.055
19	0.480	0.032*
20	0.369	0.110
21	0.464	0.039*
22	0.417	0.067
23	0.575	0.008**
24	0.570	0.009**

enh5 inter (Assay 15 – 17)

Enhancer enh5 inter was targeted by three different assays to assess methylation levels at 14 CpG sites (No. 12 – 17, 20 – 27). Additionally, one CpG site (27+1) located immediately downstream was analysed as well. Figure 30 displays the methylation distribution for all 20 samples. For this enhancer, no clear trend in methylation levels between MGMT-expressing and non-expressing samples was observed.

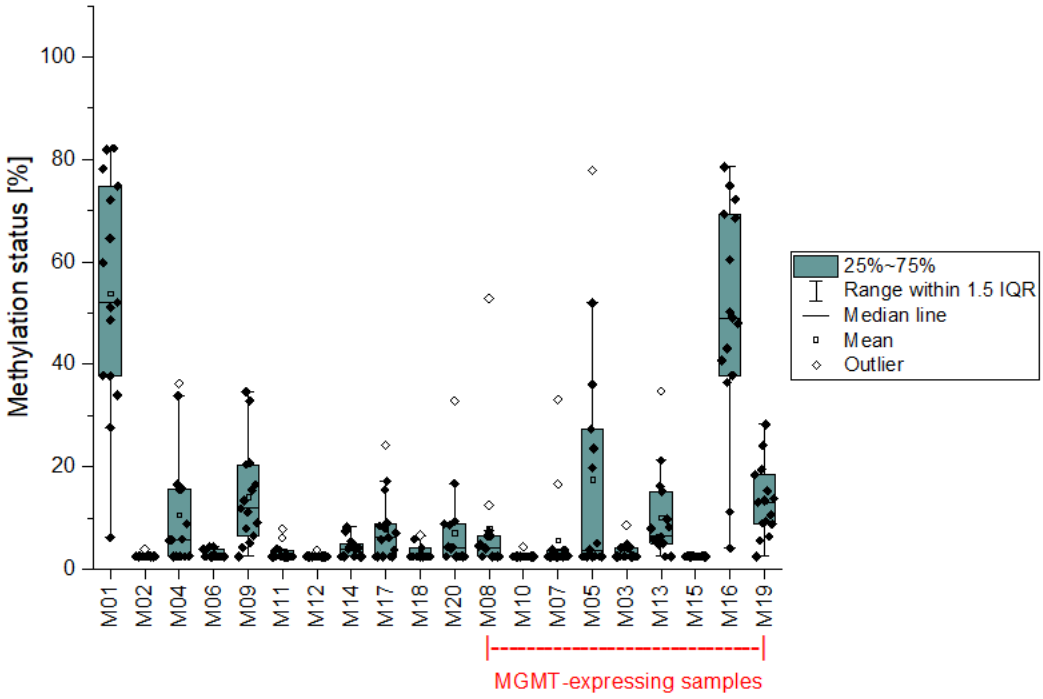

***Figure 30**: Distribution of methylation levels across 14 (+1) CpG sites in enh5 inter in melanoma brain metastasis samples determined by PSQ. MGMT-expressing samples are ordered by increasing expression, with M16 and M19 showing the highest expression levels (see chapter 8.3, Supplementary Table 18); IQR = interquartile range*

In Figure 31 methylation levels are compared between MGMT-expressing and non-expressing samples. Compared to other intergenic enhancers, enh6 inter exhibited relatively low methylation levels in both sample groups. Aside from a few outliers, only a small number of samples showed methylation levels above 30 %. The vast majority of samples had methylation levels below 10 %. Apart from low methylation, no other trends or notable features were observed.

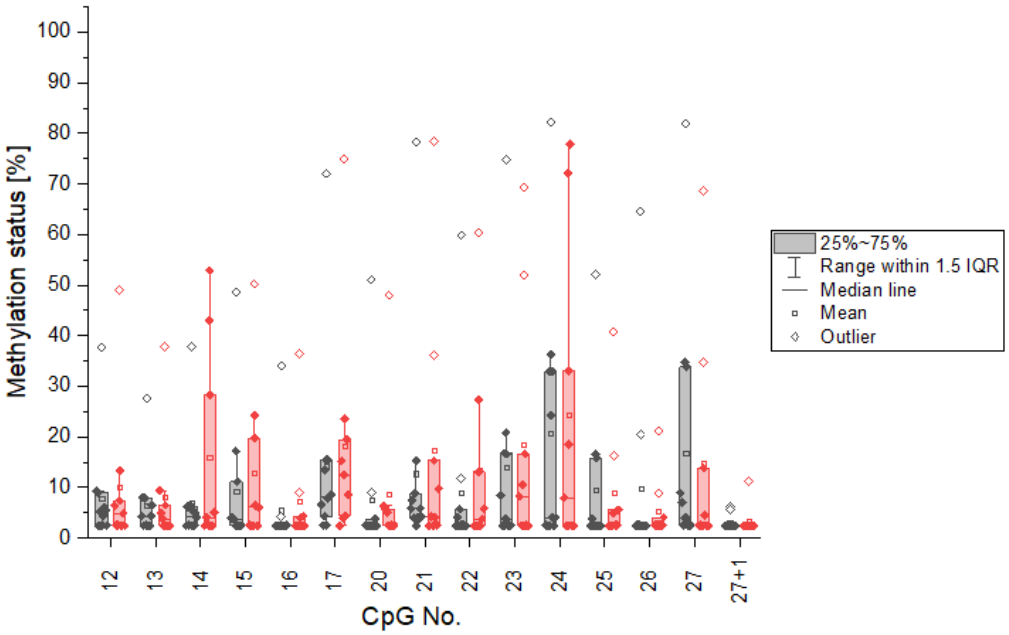

***Figure 31**: Comparison of methylation distribution in enh5 inter across 14 (+1) CpG sites in MGMT-expressing and non-expressing melanoma brain metastasis samples determined by PSQ; Grey: non MGMT-expressing samples, red: MGMT-expressing samples, IQR = interquartile range*

Figure 32 illustrates the associations between enh5 inter methylation levels and MGMT expression. It can be observed that samples with no, medium, or high MGMT expression exhibited varying methylation levels ranging from zero to about 80 %. Therefore, no trend could be identified.

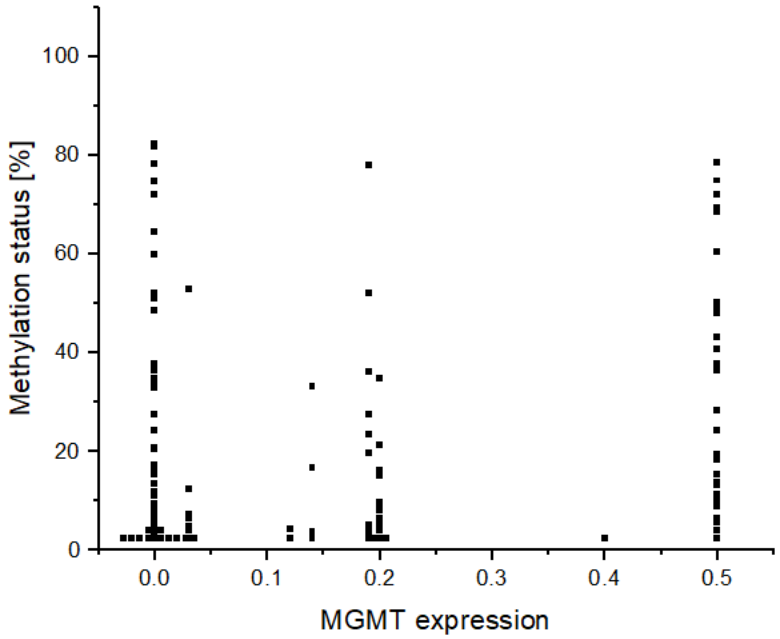

***Figure 32**: Association between methylation levels of the 14 (+1) CpG sites in enh5 inter and MGMT expression in the 20 analysed melanoma brain metastasis samples*

Correlation analysis between CpG methylation and MGMT expression for enh5 inter using Spearman's Rho values is presented in Table 43. As with enh2 inter and enh3 inter, no statistically significant p-values were found.

***Table 43**: enh5 inter: Correlation between methylation levels at specific CpG sites and MGMT expression*

CpG	Spearman Rho	p-value
12	0.123	0.607
13	0.124	0.601
14	0.143	0.549
15	0.223	0.345
16	0.355	0.125
17	0.229	0.332
20	0.287	0.220
21	0.109	0.647
22	0.330	0.155
23	0.107	0.653
24	0.058	0.807
25	0.146	0.538
26	0.260	0.269
27	0.013	0.957
27+1	0.036	0.881

The analysis of five intergenic MGMT enhancers regarding CpG methylation yielded divergent results. For two enhancers (enh1 inter and enh4 inter), a statistically significant positive correlation between enhancer methylation and MGMT expression was observed for some CpG sites. The other three enhancers did not show a statistically significant correlation.

The next section presents the correlation analysis between MGMT expression and MGMT enhancer methylation of four different intragenic enhancers. Since these enhancers are located in the MGMT gene, it should be examined whether the methylation level differs from that in intergenic enhancers. Again all 20 samples were independently analysed twice, and the mean values of the methylation levels were presented.

enh6 intra (Assay 19)

For enh6 intra, located in the MGMT gene, one assay was used to assess methylation at three CpG sites (No. 8 – 10). Figure 33 shows the distribution of methylation levels across the three CpG sites for the sample set consisting of 20 melanoma brain metastasis samples.

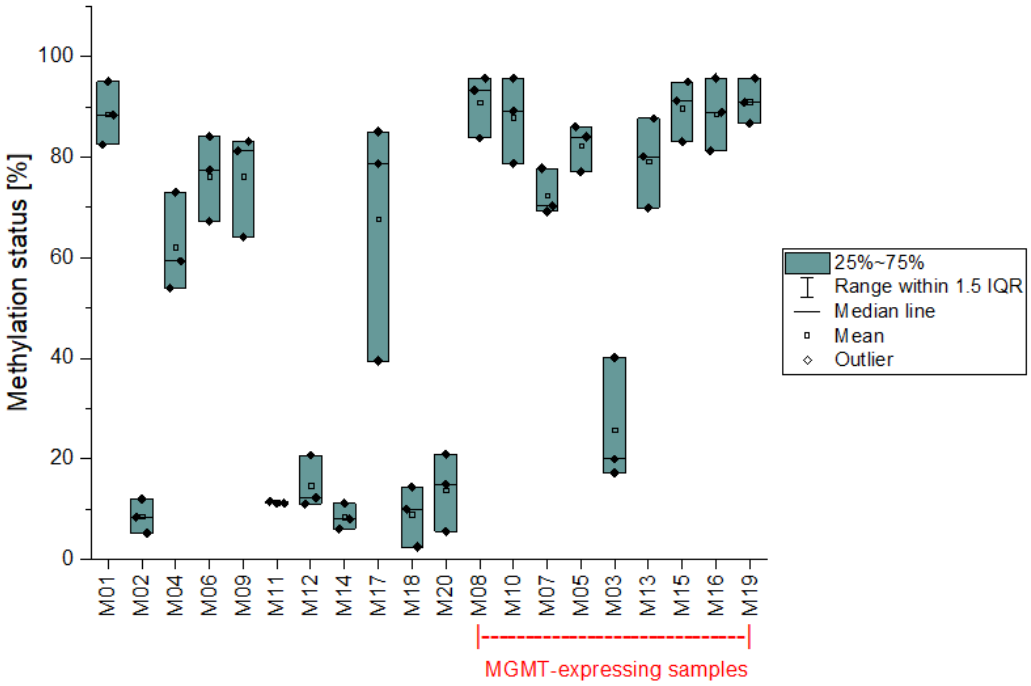

***Figure 33**: Distribution of methylation levels across three CpG sites in enh6 intra in melanoma brain metastasis samples determined by PSQ. MGMT-expressing samples are ordered by increasing expression, with M16 and M19 showing the highest expression levels (see chapter 8.3, Supplementary Table 18); IQR = interquartile range*

A statistically significant difference ($p \leq 0.001$) between the two groups was observed. All but one MGMT-expressing sample (M03) exhibited methylation levels of 70 – 95 % at the analysed CpG sites. Sample M03 showed methylation levels of 20 – 40 %. This sample was also one of the two samples from the MGMT-expressing group that showed deviations in the methylation analysis of the promoter CpG sites (Chapter 5.1.1). Sample M13, which also showed deviations in the promoter methylation levels, was, however, inconspicuous regarding enh6 intra methylation. The non-expressing samples showed varying levels ranging from about 10 % to 90 %.

Figure 34 shows the enhancer methylation in MGMT-expressing and non-expressing samples for all three CpG sites.

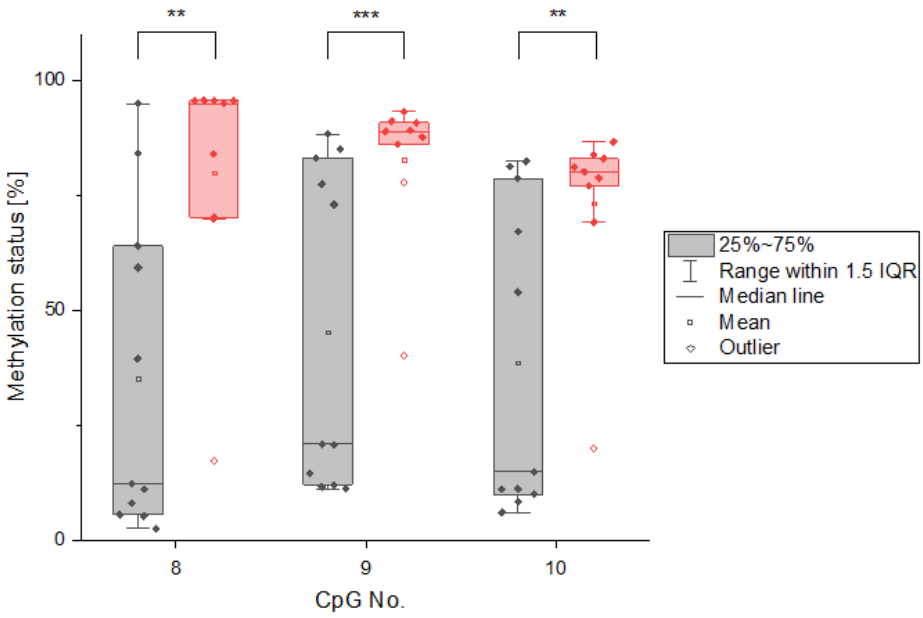

Figure 34: *Comparison of methylation distribution in enh6 intra across three CpG sites in MGMT-expressing and non-expressing melanoma brain metastasis samples determined by PSQ; Grey: non MGMT-expressing samples, red: MGMT-expressing samples, IQR = interquartile range, **p≤0.01, ***p≤0.001*

It is evident that MGMT-expressing samples showed a significantly higher and more homogenous methylation distribution than non-expressing samples in Figure 34. This trend is also visible in Figure 35. Regarding enh6 intra, MGMT expression increased with the degree of enh6 intra methylation.

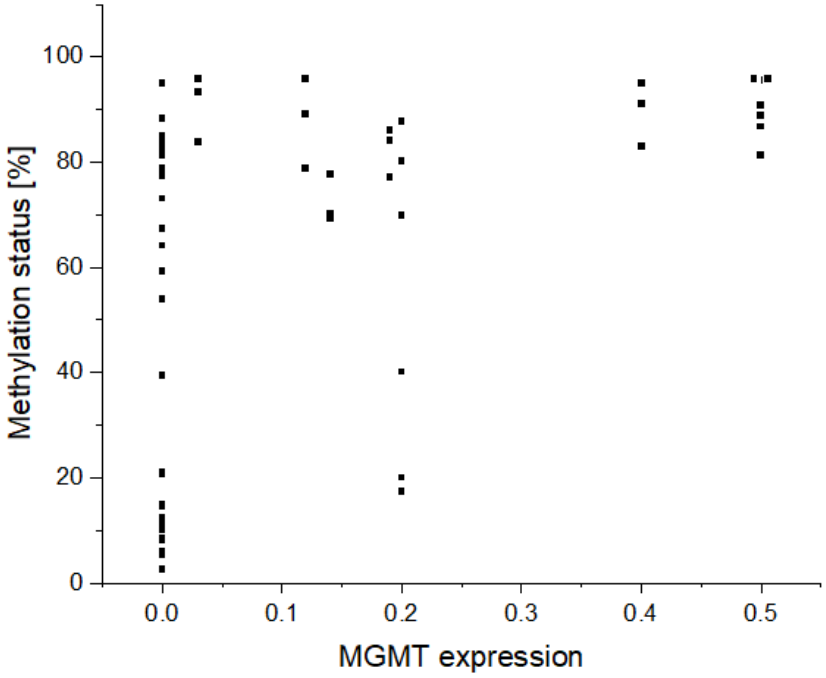

Figure 35*: Association between methylation levels of the three CpG sites in enh6 intra and MGMT expression in the 20 analysed melanoma brain metastasis samples*

Correlation analysis between MGMT enhancer methylation in enh6 intra and MGMT expression is shown in Table 44. A strong positive correlation is indicated by Spearman's Rho values. Additionally, statistically significant p-values below 0.01 were detected for all CpG sites.

***Table 44**: enh6 intra: Correlation between methylation levels at specific CpG sites and MGMT expression; **p≤0.01*

CpG	Spearman Rho	p-value
8	0.623	0.003**
9	0.657	0.002**
10	0.573	0.008**

enh7 intra (Assay 20 – 23)

The enhancer enh7 intra was analysed using four assays targeting eleven CpG sites (No. 7 – 13, 19 – 22). The methylation distribution across all 20 samples is shown in Figure 36. This enhancer also displayed significantly higher methylation levels in MGMT-expressing samples (p≤0.001). Only sample M03 deviates from this trend, with a mean methylation level of about 10 %. All other expressing sample showed average levels of at least 70 %. In MGMT non-expressing samples, methylation levels varied considerably. Four samples (M01, M04, M06 and M09) showed levels around 70 % or higher, while the remaining seven non-expressing samples exhibited clearly lower methylation levels.

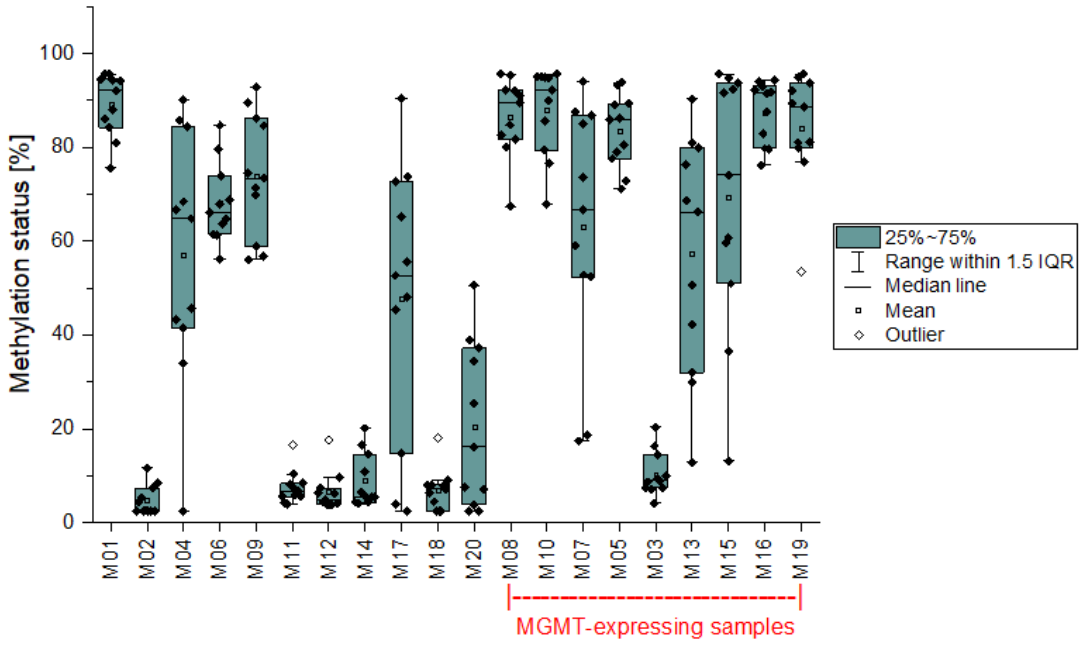

***Figure 36**: Distribution of methylation levels across eleven CpG sites in enh7 intra in melanoma brain metastasis samples determined by PSQ. MGMT-expressing samples are ordered by increasing expression, with M16 and M19 showing the highest expression levels (see chapter 8.3, Supplementary Table 18); IQR = interquartile range*

Figure 37 illustrates methylation levels for MGMT non-expressing and expressing samples across eleven CpG sites. Once again, a clear trend is observable. For each CpG site, MGMT-expressing samples exhibited higher mean methylation levels than non-expressing samples.

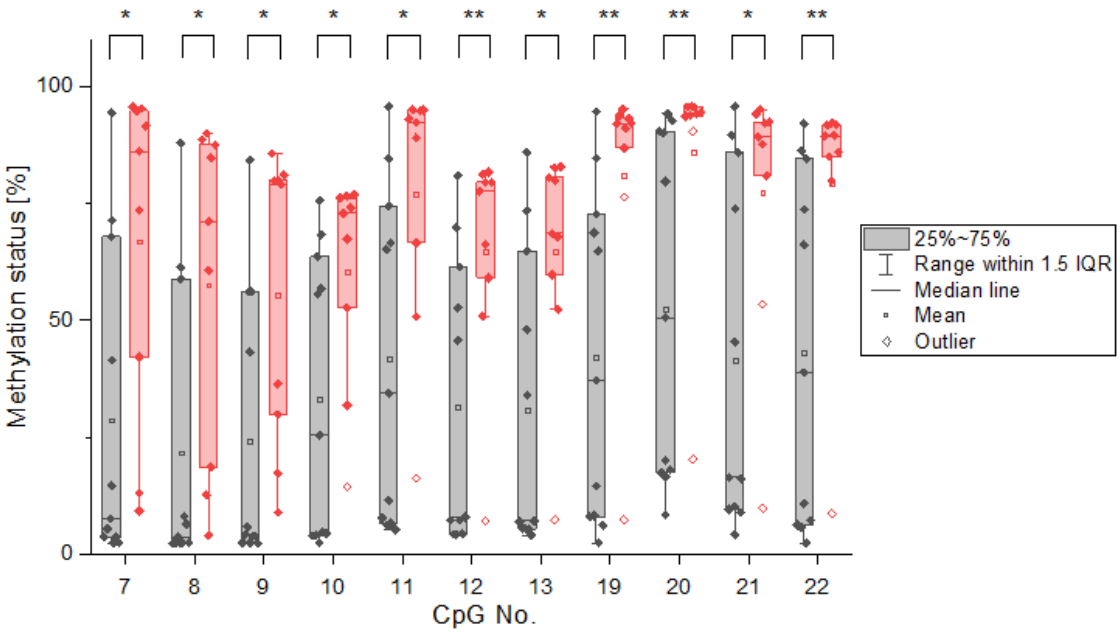

***Figure 37**: Comparison of methylation distribution in enh7 intra across eleven CpG sites in MGMT-expressing and non-expressing melanoma brain metastasis samples determined by PSQ; Grey: non MGMT-expressing samples, red: MGMT-expressing samples, IQR = interquartile range, *p≤0.05, **p≤0.01*

This trend is further supported by a Spearman Rho correlation analysis. The results of this test are presented in Table 45. A positive correlation between MGMT expression and methylation at enh7 intra was observed, with ten out of eleven CpG sites showing statistically significant correlations (p-values <0.05). Figure 38 also illustrates this trend.

***Table 45**: enh7 intra: Correlation between methylation levels at specific CpG sites and MGMT expression; *p≤0.05, **p≤0.01*

CpG	Spearman Rho	p-value
7	0.516	0.020*
8	0.555	0.011*
9	0.469	0.037*
10	0.535	0.015*
11	0.484	0.030*
12	0.465	0.039*
13	0.514	0.020*
19	0.523	0.018*
20	0.589	0.006**
21	0.395	0.084
22	0.512	0.21*

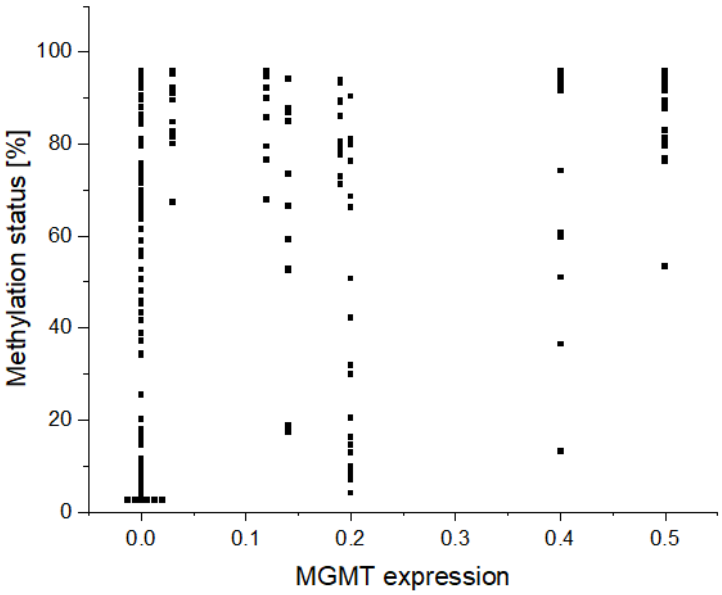

***Figure 38**: Association between methylation levels of the eleven CpG sites in enh7 intra and MGMT expression in the 20 analysed melanoma brain metastasis samples*

enh8 intra (Assay 24 – 26)

The next analysed enhancer was assessed using three assays targeting eight different CpG sites (No. 2 – 4, 6, 7, 10 – 12). The methylation distribution in Figure 39 again shows similarities to other intragenic enhancers. The difference between MGMT-expressing and non-expressing was statistically significant ($p \leq 0.001$). The MGMT-expressing sample M03 once again displayed the lowest methylation levels within this group. Apart from this sample, all remaining expressing samples exhibited high methylation levels. As before, MGMT non-expressing samples showed varying levels.

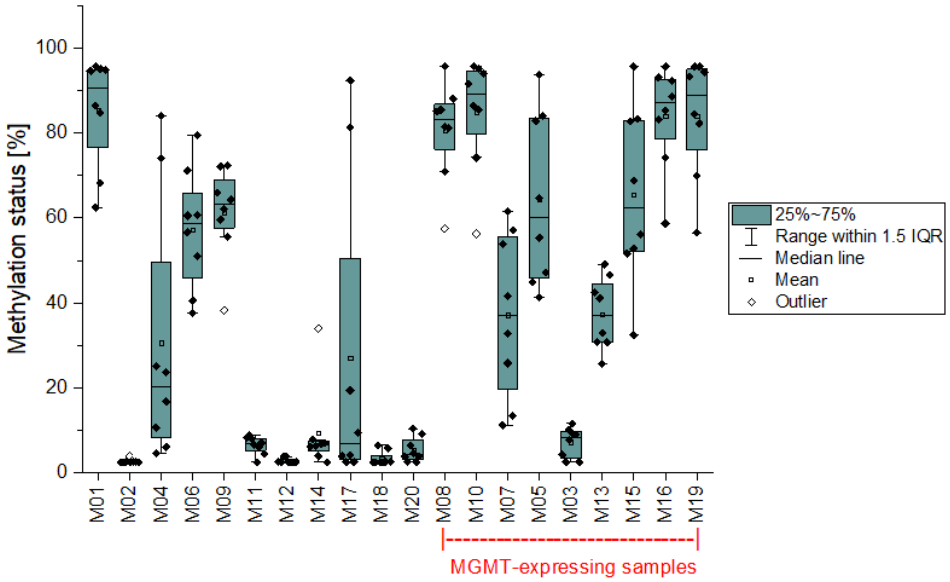

***Figure 39**: Distribution of methylation levels across eight CpG sites in enh8 intra in melanoma brain metastasis samples determined by PSQ. MGMT-expressing samples are ordered by increasing expression, with M16 and M19 showing the highest expression levels (see chapter 8.3, Supplementary Table 18); IQR = interquartile range*

Figure 40 compares the methylation distribution of enh8 intra across eight CpG sites in MGMT-expressing and non-expressing samples. Similar to enh6 intra and enh7 intra, expressing samples exhibited higher mean methylation levels than non-expressing samples at each CpG site.

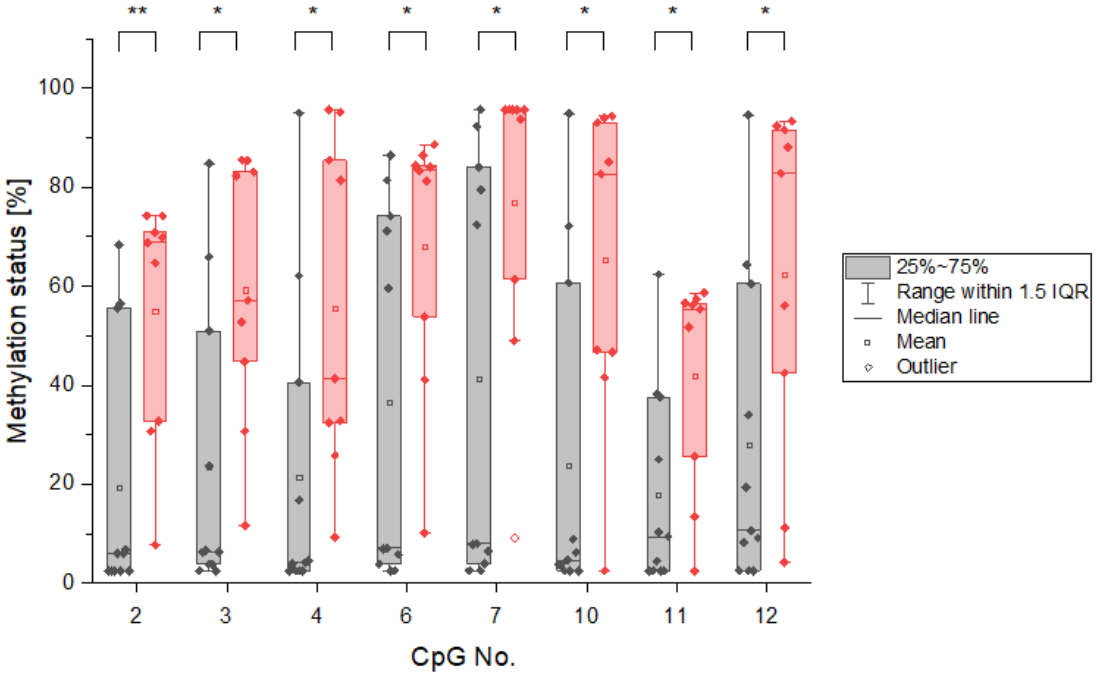

***Figure 40**: Comparison of methylation distribution in enh8 intra across eight CpG sites in MGMT-expressing and non-expressing melanoma brain metastasis samples determined by PSQ; Grey: non MGMT-expressing samples, red: MGMT-expressing samples, IQR = interquartile range, *p≤0.05, **p≤0.01*

This trend is again reflected in the association between methylation levels in enh8 intra and MGMT expression, as shown in Figure 41. The methylation status was positively correlated with MGMT expression. This is also evident in Table 46. The correlation applies to all CpG sites, each of which showed statistically significant p-values.

***Table 46**: enh8 intra: Correlation between methylation levels at specific CpG sites and MGMT expression; *p≤0.05, **p≤0.01*

CpG	Spearman Rho	p-value
2	0.661	0.002**
3	0.510	0.022*
4	0.548	0.012*
6	0.514	0.020*
7	0.535	0.015*
10	0.451	0.046*
11	0.470	0.037*
12	0.446	0.049*

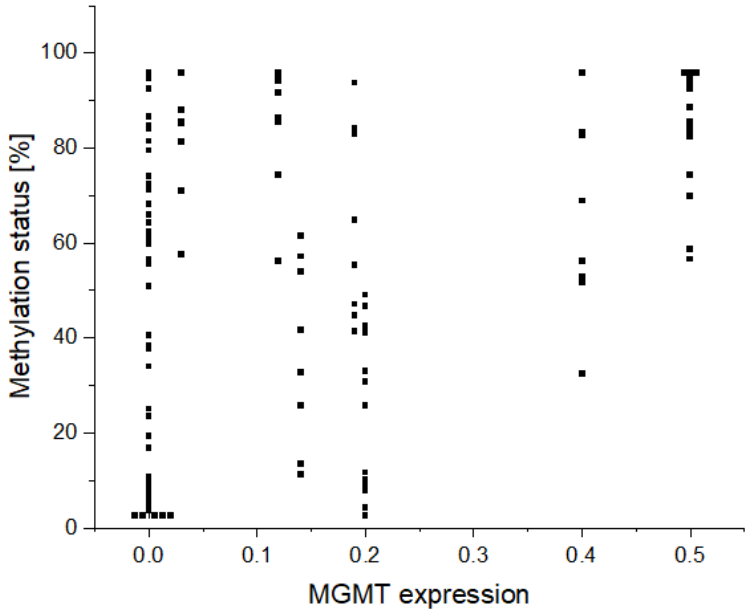

***Figure 41**: Association between methylation levels of the eight CpG sites in enh8 intra and MGMT expression in the 20 analysed melanoma brain metastasis samples*

enh9 intra (Assay 27)

The enhancer enh9 intra was analysed at six CpG sites (No. 6 – 11) using a single assay. The methylation distribution across all 20 samples is shown in Figure 42. Sample M03, with a mean methylation of approximately 30 %, was once again an outlier within the MGMT-expressing sample group. All other expressing samples showed higher methylation levels. Once again, a statistically significant difference between the two groups was observed (≤0.001).

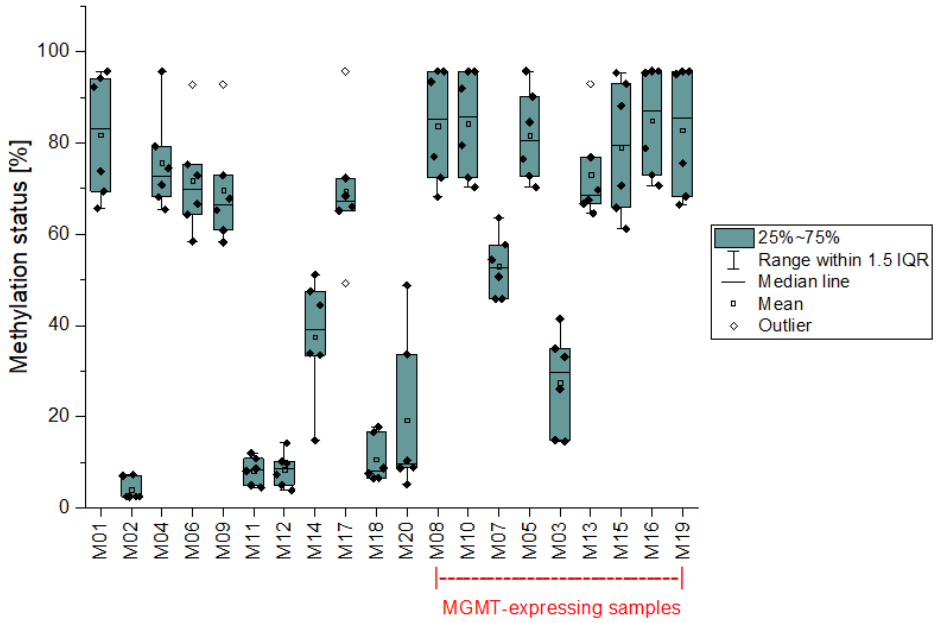

***Figure 42**: Distribution of methylation levels across six CpG sites in enh9 intra in melanoma brain metastasis samples determined by PSQ. MGMT-expressing samples are ordered by increasing expression, with M16 and M19 showing the highest expression levels (see chapter 8.3, Supplementary Table 18); IQR = interquartile range*

Figure 43 shows the comparison of methylation distribution in enh9 intra across six CpG sites between MGMT non-expressing (grey) and expressing (red) samples. The previously observed trend in intragenic enhancers was again identified. MGMT-expressing samples exhibited significantly higher methylation levels across CpG sites.

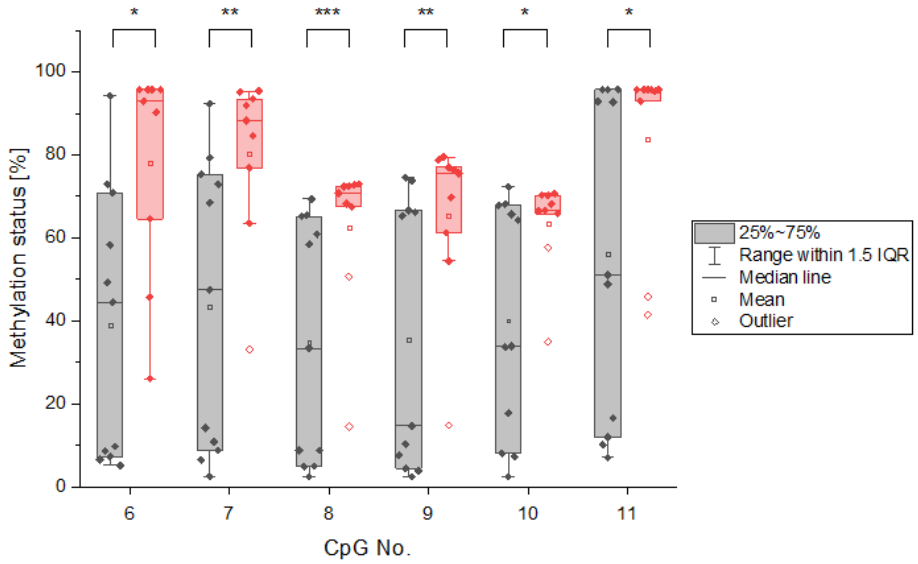

***Figure 43**: Comparison of methylation distribution in enh9 intra across six CpG sites in MGMT-expressing and non-expressing melanoma brain metastasis samples determined by PSQ; Grey: non MGMT-expressing samples, red: MGMT-expressing samples, IQR = interquartile range, *p≤0.05, **p≤0.01, ***p≤0.001*

This statistical trend was once again validated using Spearman Rho analysis. The results in Table 47 indicate a positive correlation between enh9 intra methylation and MGMT expression. Four out of six CpG sites exhibited statistically significant correlations with p-values below 0.05.

***Table 47**: enh9 intra: Correlation between methylation levels at specific CpG sites and MGMT expression; *p≤0.05, **p≤0.01*

CpG	Spearman Rho	p-value
6	0.568	0.009**
7	0.594	0.006**
8	0.605	0.005**
9	0.512	0.021*
10	0.423	0.063
11	0.380	0.098

Figure 44 also shows the association between MGMT expression and enh9 intra methylation. Samples with higher expression exhibit higher methylation levels.

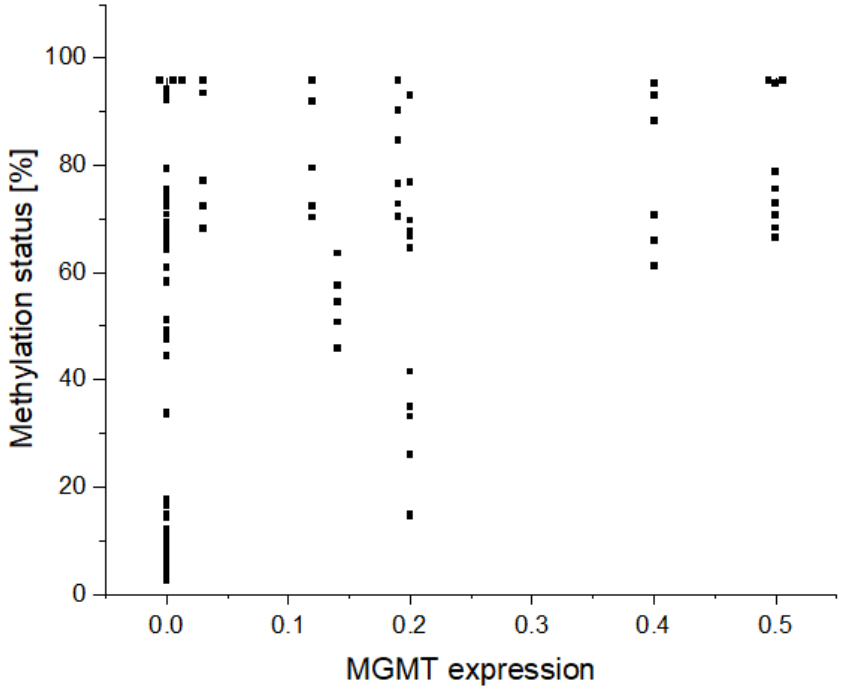

***Figure 44**: Association between methylation levels of the six CpG sites in enh9 intra and MGMT expression in the 20 analysed melanoma brain metastasis samples*

The presented results of methylation analysis of MGMT enhancers and the associated correlation with MGMT expression reveal a significant difference between intergenic and intragenic enhancers. Among all analysed intergenic enhancer CpG sites, only eight out of 66 showed a significant positive correlation. By contrast, 25 out of the 28 CpG sites located within intragenic enhancers exhibited a significant positive correlation.

The following figure (Figure 45) highlights the difference in methylation levels between MGMT-expressing and non-expressing samples for both intergenic and intragenic enhancers. This illustration reveals a significantly greater difference between MGMT expressing and non-expressing samples in intragenic enhancers compared to intergenic ones ($p \leq 0.001$).

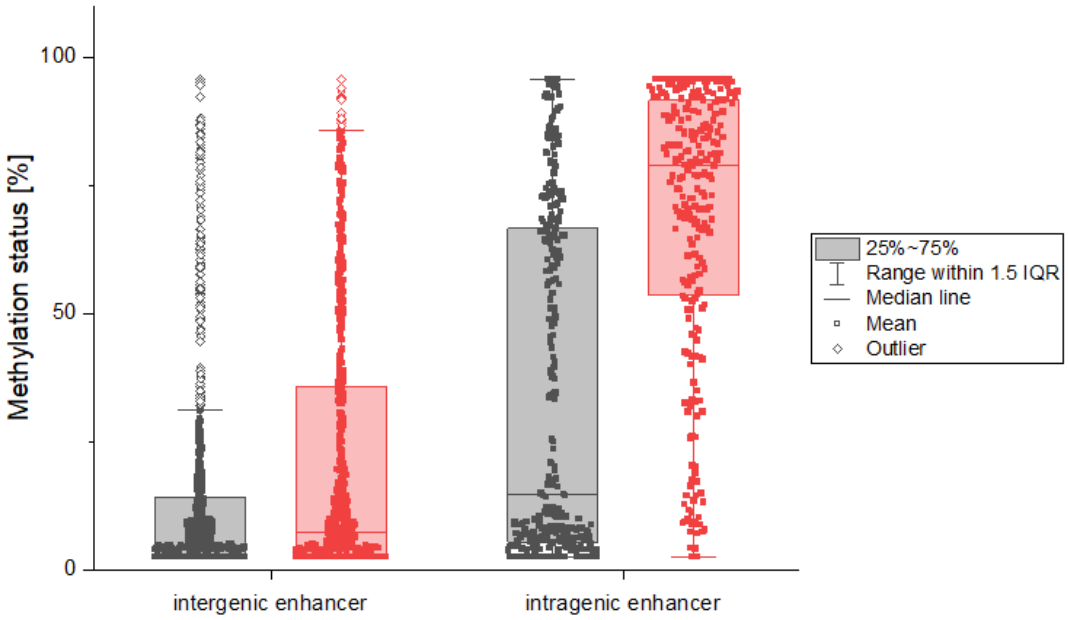

***Figure 45**: Comparison of MGMT enhancer methylation distribution across all analysed CpG sites in MGMT-expressing and non-expressing melanoma brain metastasis samples determined by PSQ; Grey: non MGMT-expressing samples, red: MGMT-expressing samples, IQR = interquartile range*

At this point, several open questions will be addressed. The aim of this section was to investigate whether MGMT enhancer methylation correlates with MGMT expression in melanoma brain metastasis samples. The evaluation was based primarily on MGMT protein expression. Nonetheless, MGMT mRNA expression was also determined by our research partners at the Kepler Klinikum in Linz. A comparison of MGMT protein expression and MGMT mRNA expression for each sample is shown in Table 48. The samples are ordered by increasing protein expression.

***Table 48**: MGMT protein expression and mRNA expression for all 20 melanoma brain metastasis samples*

Sample	MGMT prot.exp.	MGMT mRNA exp.
M01	0	4.20
M02	0	0.00
M04	0	0.90
M06	0	4.00
M09	0	1.50
M11	0	0.00
M12	0	0.34
M14	0	1.70
M17	0	0.00
M18	0	0.00
M20	0	0.70
M08	0.03	1.03
M10	0.12	1.80
M07	0.14	0.66
M05	0.19	0.38
M03	0.2	0.00
M13	0.2	0.90
M15	0.4	1.70
M16	0.5	3.50
M19	0.5	1.00

It is known that the relationship between protein concentration and mRNA concentration does not have to be linear, but some irregularities stand out. For example, the two samples with by far the highest MGMT mRNA expression (M01 and M06) lacked protein expression. However, the sample with the third highest mRNA expression (M16) also showed the highest protein expression. Moreover, samples M01 and M06 lacked MGMT promoter methylation and exhibited high CpG intragenic enhancer methylation, similar to the MGMT-expressing sample group. Additionally, sample M03 showed average protein expression compared to other MGMT-expressing samples. However, no mRNA expression was detected. Notably, seven out of nine MGMT-expressing samples did not show promoter methylation, with M03 being one of the samples with higher methylation levels. Furthermore, sample M03 exhibited the lowest MGMT intragenic CpG methylation levels among all MGMT-expressing samples.

These observations could be due to a variety of factors. One possible explanation is the heterogeneity of the metastatic brain tissue samples, which may contain varying proportions of tumour cells, glial cells, immune cells, and other cell types. Such variability might influence both methylation patterns and expression data. In addition, post-transcriptional and post-translational regulatory mechanisms, mRNA degradation, or differences in mRNA translation efficiency could contribute to the observed discrepancies. Furthermore, potential technical variability or different sensitivities of the detection methods cannot be entirely ruled out.

5.2 Determination of 5-hydroxymethylcytosine

This section presents the results of comparing oxBS and CAPS for the detection of 5-hmC. To facilitate understanding of the analysis, Table 49 again illustrates the sequence changes in sample DNA after treatment with the respective methods. As shown, oxBS specifically converts 5-mC to cytosine. To calculate the 5-hmC content in a sample using oxBS, standard BS must first be performed, and the resulting values subtracted. In contrast, CAPS allows direct determination of 5-hmC content by subtracting the measured cytosine value from 100. These principles are described in more detail in Chapters 3.1.2 and 3.1.3.

***Table 49**: Base changes after conversion during BS, oxBS, and CAPS and PCR*

Original base	BS	oxBS	CAPS
C	T	T	C
5-mC	C	C	C
5-hmC	C	T	T

Initially, both methods – oxBS (Chapter 4.4.1) and CAPS (Chapter 4.4.2) – were tested using standards (Table 33) to assess their accuracy. Following this method validation, a hippocampal sample (HC) was analysed. Although the methylation level of this hippocampal sample was unknown, the assay was nonetheless performed to test its applicability to a genomic sample. All samples were measured in triplicate.

The data presented in this chapter are the methylation levels of the individual CpG sites. Since the methylation status of the three standards is known, an expected value is also specified for the analysis of the standards. Mean bias was calculated using this expected value.

5.2.1 Oxidative bisulfite sequencing

The results of regular bisulfite sequencing using standards are presented in Table 50. For this validation only two temperature programs (TPs) were selected (Further information on the temperature programs can be found in Table 3 and Table 4). Both temperature settings produced acceptable results for the standard containing only unmethylated cytosine. For standards containing 5-mC or 5-hmC, only temperature program TP1 (two cycles of 5 min denaturation at 95°C and 10 min incubation at 60°C) yielded accurate results. TP6, on the other hand, did not produce reliable results. This may be due to the formation of cytosine-5-methylenesulfonate during sulfonation, which has been reported to stall DNA polymerase during PCR and can lead to underrepresentation of 5-hmC content.[79]

***Table 50**: Cytosine content [%] determined by bisulfite sequencing using different standards (Table 33) and temperature programs (TP); detailed information on the temperature programs in chapter 4.2 Table 3 and Table 4*

	TP1		TP6	
Standard	**CpG1**	**CpG2**	**CpG1**	**CpG2**
C	2.35	2.51	1.90	1.41
C	2.10	2.23	1.63	1.61
C	/	/	1.75	1.39
Expected Value	0	0	0	0
Mean Error	+2.2	+2.4	+1.8	+1.5
5-mC	96.85	96.72	77.88	78.26
5-mC	96.53	96.36	77.85	77.61
5-mC	/	/	77.90	77.62
Expected Value	100	100	100	100
Mean Error	-3.3	-3.5	-22.1	-22.2
5-hmC	96.73	95.58	79.10	78.91
5-hmC	96.29	95.61	79.59	78.84
5-hmC	/	/	79.04	79.17
Expected Value	100	100	100	100
Mean Error	-3.5	-4.4	-20.8	-21.0

Table 51 shows the results of oxidative bisulfite sequencing with the different standards. Temperature programs are further detailed in chapter 4.4.1, Table 35. For the sample containing only unmethylated cytosine, the programs TP2, TP3, and TP4 worked best. However, the other programs also performed acceptable, considering the mean error.

***Table 51**: Cytosine content [%] determined by oxidative bisulfite sequencing using different standards (Table 33) and temperature programs (TP); detailed information on the programs in chapter 4.4.1 Table 35*

	TP1		TP2		TP3		TP4		TP5		TP6	
Standard	**CpG1**	**CpG2**	**CpG1**	**CpG2**	**CpG1**	**CpG2**	**CpG1**	**CpG2**	**CpG1**	**CpG2**	**CpG1**	**CpG2**
C	3.01	2.64	0.33	0.41	0.57	0.67	0.43	0.41	1.54	1.34	0.95	0.90
C	2.17	2.05	0.68	0.46	0.73	0.76	0.51	0.46	1.23	1.36	0.88	0.84
C	2.06	1.79	0.60	0.57	0.87	0.96	0.41	0.45	0.71	0.95	0.72	0.74
Expected Value	0	0	0	0	0	0	0	0	0	0	0	0
Mean Error	+2.4	+2.2	+0.5	+0.5	+0.7	+0.8	+0.5	+0.4	+1.2	+1.2	+0.9	+0.8
5-mC	96.63	96.03	94.50	94.07	91.50	91.57	84.35	84.02	80.93	81.15	80.22	79.96
5-mC	96.61	96.03	94.24	93.62	91.11	91.24	83.96	83.78	76.80	86.29	80.01	79.96
5-mC	96.27	95.94	94.82	94.13	90.72	90.69	85.09	85.05	82.42	82.15	80.77	80.12
Expected Value	100	100	100	100	100	100	100	100	100	100	100	100
Mean Error	-3.5	-4.0	-5.5	-6.1	-8.9	-8.8	-15.5	-15.7	-20.0	-16.8	-19.7	-20.0
5-hmC	29.07	28.78	13.90	13.26	7.67	8.09	3.47	3.27	1.51	1.27	2.10	2.19
5-hmC	30.77	29.86	13.03	12.38	7.82	8.25	2.73	2.69	2.11	2.45	2.72	1.96
5-hmC	28.41	26.55	19.73	18.57	7.71	7.04	3.53	3.22	3.09	3.31	2.89	2.10
Expected Value	0	0	0	0	0	0	0	0	0	0	0	0
Mean Error	+29.4	+28.4	+15.6	+14.7	+7.7	+7.8	+3.2	+3.1	+2.2	+2.3	+2.6	+2.1

The standard containing 5-mC at both CpG sites should yield a value of 100 %. Notably, with longer temperature programs, the determined value decreased. This effect could be caused by inappropriate conversion of 5-mC to thymine. This process was described by Genereux et al. and occurs if treatment duration with bisulfite exceeds the time to complete conversion for the majority of unmethylated cytosines.[80] The programs TP1, TP2, and TP3 provided acceptable results.

For the standard containing 5-hmC at both CpG sites, using oxBS a level of 0 % was expected. However, these results were only approximately observed with temperature programs 4, 5 and 6. Shorter programs, on the other hand, showed a substantially higher mean bias. TP1 and TP2 did not deliver adequate results. Considering all three standards, the program TP3 provided the best results.

Table 52 presents the results obtained by the 5-hmC analysis for the triplicate determination of the hippocampal sample (further information on the hippocampal sample in Chapter 4.4.1 and 4.4.2). As stated in Chapter 4.4.1, values from oxBS must be subtracted from those obtained via regular BS. Results in Table 50 and 51 indicate that temperature program 3 (four cycles of 5 min denaturation at 95°C and 35 min incubation at 60°C) yielded the most plausible results when both BS and oxBS are required. For BS, the shortest temperature program produced the better results regarding 5-hmC, with values decreasing as the program lengthened (Table 50). Conversely, for oxBS, the longest temperature program performed best, with 5-hmc content increasing as the program shortened (Table 51). Therefore, when both methods are applied to the same sample set, temperature program 3 is recommended. This results in 5-hmC contents of 25.5 % and 20.2 % for CpG sites 1 and 2, respectively.

***Table 52**: 5-hmC content [%] obtained by oxBS for hippocampal samples using different temperature programs (TPs); % 5-hmC content calculated using means*

	TP1		TP2		TP3		TP4		TP5		TP6	
	CpG1	**CpG2**	**CpG1**	**CpG2**	**CpG1**	**CpG2**	**CpG1**	**CpG2**	**CpG1**	**CpG2**	**CpG1**	**CpG2**
BS	74.31	52.38	71.69	50.05	68.39	47.47	64.85	46.80	57.06	30.90	59.58	39.41
BS	73.53	51.14	71.22	49.09	68.17	47.75	64.29	46.42	64.19	44.01	57.06	39.37
BS	52.96	41.79	72.27	51.45	68.46	49.54	68.37	48.19	60.06	43.23	60.54	41.44
oxBS	50.65	34.01	41.87	29.31	43.86	29.78	38.73	24.07	42.20	23.58	40.19	21.49
oxBS	48.82	34.97	43.56	28.24	41.53	27.16	38.02	23.25	37.52	24.98	40.35	23.08
oxBS	50.51	33.99	44.93	28.53	42.98	27.18	36.92	24.03	40.97	23.88	40.56	21.34
%5-hmC	16.9	14.1	28.3	21.5	25.6	20.2	27.9	23.4	20.2	15.2	18.7	18.1

5.2.2 Chemically assisted pyridine borane sequencing

This section addresses to the 5-hmC analysis using CAPS. First, the method was also validated using the three different standards (Table 33). The results are listed in Table 53. Using this method, standards containing either cytosine or 5-mC at both CpG sites are expected to each yield results of 100%. The 5-hmC standard on the other hand, should generate values of 0 %.

***Table 53**: Cytosine content [%] obtained from CAPS*

	Measured cytosine content		Calculated 5-hmC content	
Standard	**CpG1**	**CpG2**	**CpG1**	**CpG2**
C	98.62	96.55		
C	97.44	96.09		
C	98.88	96.8		
Expected Value	100	100		
Mean Error	-1.7	-3.5		
5-mC	97.62	96.35		
5-mC	98.19	96.17		
5-mC	95.78	94.94		
Expected Value	100	100		
Mean Error	-2.8	-4.2		
5-hmC	2.34	3.77	97.66	96.23
5-hmC	4.42	5.24	95.58	94.76
5-hmC	4.59	6.38	95.41	93.62
Expected Value	0	0	100	100
Mean Error	+3.8	+5.1	-3.8	-5.1

Table 54 presents the measured cytosine content and calculated 5-hmC content for the hippocampal sample, measured in triplicate using CAPS. CpG1 showed mean 5-hmC content of approximately 13 %, while CpG 2 exhibited a mean of around 12%.

***Table 54**: 5-hmC content [%] obtained by CAPS for hippocampal samples*

	Measured cytosin content		Calculated 5-hmC content	
Sample	**CpG1**	**CpG2**	**CpG1**	**CpG2**
HC	86.39	88.13	13.61	11.87
HC	87.36	87.92	12.64	12.08
HC	87.40	88.46	12.60	11.54
Mean	87.1	88.2	13.0	11.8

5.2.3 Comparison of methods for determination of 5-hmC

The comparison of the two presented methods is primarily based on the conversion rate for the analysed standards. Since oxidative bisulfite sequencing requires preceding regular bisulfite sequencing, the accuracy of this second step must be evaluated too. As shown in the previous chapter, the bias of bisulfite sequencing decreased with longer temperature programs. Temperature program 1 (two cycles of 5 min denaturation at 95°C and 10 min incubation at 60°C) achieved a conversion rate of approximately 96 %, while the same method using TP6 (six cycles of 5 min denaturation at 95°C and 95 min incubation at 60°C) yielded only about 79 %. In the case of oxidative bisulfite sequencing, the duration of the conversion had a similar effect. However, shorter programs resulted in lower conversion rates, increasing from about 71.1 % for TP1 to approximately 98 % for the longest program, TP6. Regarding oxBS, the method presented in this thesis using the temperature programs TP3 – 6 yielded better results than some of those reported in the literature. Booth et al., for example, described a 5-hmC to uracil conversion rate of 92 % using oxBS. [81] CAPS, on the other hand, exhibited a 5-hmC conversion rate of nearly 96 %. This, however, exceeds the reported conversion rate of 5-hmC to thymine of 83.1 % using CAPS by Liu et al. [54]

Considering that two separate reactions are required to determine 5-hmC content using oxidative bisulfite sequencing, the method involves greater inaccuracy and time investment compared to CAPS, which requires only a single reaction. Moreover, the conversion rate of CAPS is sufficient to provide meaningful and informative insights. Therefore, the use of CAPS should be prioritized when evaluating 5-hmC content.

Regarding the analysed hippocampal sample, CAPS yielded a mean methylation level of 13 % for CpG1 and 11.8 % for CpG2. If all temperature programs are considered, oxBS produced a mean methylation level of 22.9 % for CpG1 and 18.8 % for CpG2.

6 Conclusion

One of the aims of this thesis was to investigate whether CpG methylation in MGMT enhancers correlates with MGMT expression in melanoma brain metastases. This correlation was already confirmed in glioblastoma by our research group. In glioblastoma, promoter methylation is a biomarker for the responsiveness of patients to chemotherapeutics like TMZ, since MGMT can inhibit its effectiveness. However, sometimes these predictions using promoter methylation alone are not sufficient. Better understanding of MGMT expression is necessary. Since the microenvironments of glioblastoma and brain metastases are similar, it can be assumed that certain parallels may emerge.

Therefore, a sample set of melanoma brain metastases was analysed using pyrosequencing methods targeting the MGMT enhancer regions. The methylation levels were statistically evaluated for correlation with MGMT expression. On the one hand, five intergenic enhancers, which are located upstream of the gene, were analysed. On the other hand, four intragenic enhancers, which are located in the MGMT gene, were examined as well.

Regarding intergenic enhancers, no clear trend could be observed between samples with high MGMT expression and samples with low or none MGMT expression. Methylation levels were distributed evenly between the two groups. Only six analysed enhancer CpG sites exhibited a statistically significant positive correlation between methylation and MGMT expression. The other 58 CpG sites did not show a significant correlation. Therefore, this study concludes no general correlation between intergenic enhancer methylation and MGMT expression.

A different picture emerged for intragenic enhancers. A significantly higher methylation pattern of intragenic enhancer CpG sites was observed in MGMT-expressing samples compared to non-expressing ones. Twenty-five out of 28 enhancer CpG sites exhibited a significant positive correlation. In comparison to promoter methylation as a currently used marker for MGMT expression in glioblastoma, this study suggests a more reliable prognosis using intragenic enhancer methylation for melanoma brain metastasis. Only six out of twelve promoter CpG sites showed a statistically significant negative correlation with MGMT expression.

Still, not all questions are answered. Irregularities regarding protein expression and mRNA expression could influence the outcome of this study, since all correlation analyses were based on MGMT protein expression. Additionally, it should be mentioned that only a few CpG sites were investigated in this study. For the MGMT promoter, twelve out of 98 CpG sites were analysed.

This study is intended to serve as a basis for further research on the correlation between MGMT enhancer methylation and MGMT expression in brain metastases. Ideally, a

comprehensive analysis of all intragenic MGMT enhancer CpG sites should be conducted, to the extent possible. Furthermore, the methylation status of silencers may also provide additional insight into the underlying biological processes. Correlation analysis of promoter, enhancer, and silencer methylation together with MGMT expression could severely improve the prediction of responsiveness of patients to TMZ and could therefore lead to better personalised medicine and eliminate possible side effects for patients, who do not respond to the medication anyway.

The second aim of this thesis was the validation and comparison of two methods described in literature for detecting 5-hydroxymethylcytosine. The methods are oxidative bisulfite sequencing and chemically assisted pyridine borane sequencing. Both methods specifically modify the base sequence in order to differentiate 5-hmC from cytosine or 5-mC. For oxBS, there needs to be an additional step to achieve this goal. Since oxBS cannot differentiate 5-hmC directly, regular bisulfite sequencing must be applied as well. The evaluation of both BS and oxBS then yields the 5-hmC content.

Six different temperature programs for regular BS and oxBS were tested. The bias for 5-hmC did increase with longer programs for BS. This could be explained by the formation of a by-product derived from 5-hmC that interferes with PCR. For oxBS however, the bias did decrease with longer programs. The best condition for BS yielded a 96 % conversion rate for the used standard. Regarding oxBS, the longest program was able to achieve the best result of 98 % conversion rate. The analysis of 5-hmC using CAPS does not include a second step and therefore no accumulated error rate. With a conversion rate of nearly 96 %, CAPS proved to be the more accurate and time saving method.

7 References

(1) Hall, K.; Sankaran, N. DNA Translated: Friedrich Miescher's Discovery of Nuclein in Its Original Context. *The British Journal for the History of Science* **2021**, *54* (1), 99–107. https://doi.org/10.1017/S000708742000062X.

(2) Miescher, F. Ueber Die Chemische Zusammensetzung Der Eiterzellen. *Hoppe-Seyler's medizinisch-chemische Untersuchungen* **1871**, No. 4, 441–460.

(3) Lamm, E.; Harman, O.; Veigl, S. J. Before Watson and Crick in 1953 Came Friedrich Miescher in 1869. *Genetics* **2020**, *215* (2), 291–296. https://doi.org/10.1534/genetics.120.303195.

(4) Pray, L. Discovery of DNA Structure and Function: Watson and Crick. 1(1):100. *Nature Education* **2008**, *1* (1), 100.

(5) Levene, P. A. Structure of Yeast Nucleic Acid. *Journal of Biological Chemistry* **1920**, *43* (2), 379–382. https://doi.org/10.1016/S0021-9258(18)86289-5.

(6) Avery, O. T.; MacLeod, C. M.; McCarty, M. Studies on the Chemical Nature of the Substance Inducing Transformation of Pneumococcal Types. *Journal of Experimental Medicine* **1944**, *79* (2), 137–158. https://doi.org/10.1084/jem.79.2.137.

(7) Chargaff, E. Chemical Specificity of Nucleic Acids and Mechanism of Their Enzymatic Degradation. *Experientia* **1950**, *6* (6), 201–209. https://doi.org/10.1007/BF02173653.

(8) Nirenberg, M. W.; Matthaei, J. H. The Dependence of Cell-Free Protein Synthesis in *E. Coli* upon Naturally Occurring or Synthetic Polyribonucleotides. *Proceedings of the National Academy of Sciences* **1961**, *47* (10), 1588–1602. https://doi.org/10.1073/pnas.47.10.1588.

(9) Nirenberg, M.; Leder, P. RNA Codewords and Protein Synthesis: The Effect of Trinucleotides upon the Binding of sRNA to Ribosomes. *Science* **1964**, *145* (3639), 1399–1407. https://doi.org/10.1126/science.145.3639.1399.

(10) Watson, J. D.; Crick, F. H. C. Molecular Structure of Nucleic Acids: A Structure for Deoxyribose Nucleic Acid. *Nature* **1953**, *171* (4356), 737–738. https://doi.org/10.1038/171737a0.

(11) Difference DNA RNA-DE. https://commons.wikimedia.org/wiki/File:Difference_DNA_RNA-DE.svg (accessed 2025-06-18).

(12) Clancy, S.; Brown, W. Translation: DNA to mRNA to Protein. *Nature Education* **2008**, *1* (1), 101.

(13) DNA-RNA-Peptide ABCC11 MT. https://commons.wikimedia.org/wiki/File:DNA-RNA-Peptide_ABCC11_MT.svg (accessed 2025-06-18).

(14) Anaya, J.-M.; Shoenfeld, Y.; Rojas-Villarraga, A.; Levy, R. A.; Cervera, R. *Autoimmunity: From Bench to Bedside*, First edition, p 3–4; CREA texts collection; Center for Autoimmune Diseases Research, School of Medicine and Health Sciences, El Rosario University: Bogota, Colombia, 2013.

(15) Graw, J.; Hennig, W. *Genetik*, 5. Aufl. 2010, pp 89–90, 289–291, 293, 604; Springer-Lehrbuch; Springer Berlin Heidelberg: Berlin, Heidelberg, 2010. https://doi.org/10.1007/978-3-642-04999-6.

(16) Andersson, R.; Sandelin, A. Determinants of Enhancer and Promoter Activities of Regulatory Elements. *Nature Reviews Genetics* **2020**, *21* (2), 71–87. https://doi.org/10.1038/s41576-019-0173-8.

(17) Jaenisch, R.; Bird, A. Epigenetic Regulation of Gene Expression: How the Genome Integrates Intrinsic and Environmental Signals. *Nature Genetics* **2003**, *33* (S3), 245–254. https://doi.org/10.1038/ng1089.
(18) Haldane, J. B. S. Organisers and Genes. *Nature* **1940**, *146* (3700), 413–413. https://doi.org/10.1038/146413a0.
(19) Zhang, Y.; Sun, Z.; Jia, J.; Du, T.; et al. Overview of Histone Modification. In *Histone Mutations and Cancer*; Fang, D., Han, J., Eds.; Advances in Experimental Medicine and Biology; Springer Singapore: Singapore, 2021; Vol. 1283, pp 1–16. https://doi.org/10.1007/978-981-15-8104-5_1.
(20) Moore, L. D.; Le, T.; Fan, G. DNA Methylation and Its Basic Function. *Neuropsychopharmacol* **2013**, *38* (1), 23–38. https://doi.org/10.1038/npp.2012.112.
(21) Mortimer, C. E.; Müller, U.; Beck, J. *Chemie: das Basiswissen der Chemie*, 12. Auflage, pp 581–582; Georg Thieme Verlag: Stuttgart New York, 2015.
(22) Johnson, T. B.; Coghill, R. D. Research on Pyrimidines. C111. The Discovery of 5-Methyl-Cytosine in Tuberculinic Acid, the Nucleic Acid of the Tubercle Bacillus. *Journal of the American Chemical Society* **1925**, *47* (11), 2838–2844. https://doi.org/10.1021/ja01688a030.
(23) Wyatt, G. R. Occurrence of 5-Methyl-Cytosine in Nucleic Acids. *Nature* **1950**, *166* (4214), 237–238. https://doi.org/10.1038/166237b0.
(24) Mattei, A. L.; Bailly, N.; Meissner, A. DNA Methylation: A Historical Perspective. *Trends in Genetics* **2022**, *38* (7), 676–707. https://doi.org/10.1016/j.tig.2022.03.010.
(25) Nordheim, A., Knippers, R., Eds.; *Molekulare Genetik*, 10th ed.; Georg Thieme Verlag: Stuttgart, 2015; p b-002-101354. https://doi.org/10.1055/b-002-101354.
(26) Angeloni, A.; Bogdanovic, O. Enhancer DNA Methylation: Implications for Gene Regulation. *Essays in Biochemistry* **2019**, *63* (6), 707–715. https://doi.org/10.1042/EBC20190030.
(27) Global cancer burden growing, amidst mounting need for services. https://www.who.int/news/item/01-02-2024-global-cancer-burden-growing--amidst-mounting-need-for-services (accessed 2025-06-18).
(28) Weinberg, R. A. How Cancer Arises. *Scientific American* **1996**, *275* (3), 62–70. https://doi.org/10.1038/scientificamerican0996-62.
(29) Hanahan, D.; Weinberg, R. A. The Hallmarks of Cancer. *Cell* **2000**, *100* (1), 57–70. https://doi.org/10.1016/S0092-8674(00)81683-9.
(30) Hanahan, D.; Weinberg, R. A. Hallmarks of Cancer: The Next Generation. *Cell* **2011**, *144* (5), 646–674. https://doi.org/10.1016/j.cell.2011.02.013.
(31) Achrol, A. S.; Rennert, R. C.; Anders, C.; Soffietti, R.; Ahluwalia, M. S.; Nayak, L.; et al. Brain Metastases. *Nature Reviews Disease Primers* **2019**, *5* (1), 5. https://doi.org/10.1038/s41572-018-0055-y.
(32) Powell, A. M.; Watson, L.; Luzietti, L.; Prekovic, S.; Young, L. S.; Varešlija, D. The Epigenetic Landscape of Brain Metastasis. *Oncogene* **2025**, *44* (27), 2227–2239. https://doi.org/10.1038/s41388-025-03315-1.
(33) Fischer, G. M.; Jalali, A.; Kircher, D. A.; Lee, W.-C.; McQuade, J. L.; Haydu, L. E.; et al. Molecular Profiling Reveals Unique Immune and Metabolic Features of Melanoma Brain Metastases. *Cancer Discovery* **2019**, *9* (5), 628–645. https://doi.org/10.1158/2159-8290.CD-18-1489.

(34) Qu, Z. Investigating Conventional and Novel Methods for Treatment of Cancer. In *Proceedings of the 12th International Conference on Bioscience, Biochemistry and Bioinformatics*; ACM: Tokyo Japan, 2023; pp 103–111. https://doi.org/10.1145/3586139.3586154.
(35) Tohme, S.; Simmons, R. L.; Tsung, A. Surgery for Cancer: A Trigger for Metastases. *Cancer Research* **2017**, *77* (7), 1548–1552. https://doi.org/10.1158/0008-5472.CAN-16-1536.
(36) Lee, S. Y. Temozolomide Resistance in Glioblastoma Multiforme. *Genes & Diseases* **2016**, *3* (3), 198–210. https://doi.org/10.1016/j.gendis.2016.04.007.
(37) Soll, J. M.; Sobol, R. W.; Mosammaparast, N. Regulation of DNA Alkylation Damage Repair: Lessons and Therapeutic Opportunities. *Trends in Biochemical Sciences* **2017**, *42* (3), 206–218. https://doi.org/10.1016/j.tibs.2016.10.001.
(38) Parker, A. L.; Benguigui, M.; Fornetti, J.; Goddard, E.; Lucotti, S.; Insua-Rodríguez, J.; Wiegmans, A. P.; et al. Current Challenges in Metastasis Research and Future Innovation for Clinical Translation. *Clinical & Experimental Metastasis* **2022**, *39* (2), 263–277. https://doi.org/10.1007/s10585-021-10144-5.
(39) Iwakuma, T. High Incidence of Nitrosamine-Induced Tumorigenesis in Mice Lacking DNA Repair Methyltransferase. *Carcinogenesis* **1997**, *18* (8), 1631–1635. https://doi.org/10.1093/carcin/18.8.1631.
(40) Gerson, S. L. MGMT: Its Role in Cancer Aetiology and Cancer Therapeutics. *Nature Reviews Cancer* **2004**, *4* (4), 296–307. https://doi.org/10.1038/nrc1319.
(41) Soejima, H.; Zhao, W.; Mukai, T. Epigenetic Silencing of the *MGMT* Gene in Cancer. *Biochemistry and Cell Biology* **2005**, *83* (4), 429–437. https://doi.org/10.1139/o05-140.
(42) Zappe, K.; Pühringer, K.; Pflug, S.; Berger, D.; Böhm, A.; Spiegl-Kreinecker, S.; Cichna-Markl, M. Association between MGMT Enhancer Methylation and MGMT Promoter Methylation, MGMT Protein Expression, and Overall Survival in Glioblastoma. *Cells* **2023**, *12* (12), 1639. https://doi.org/10.3390/cells12121639.
(43) Pühringer, K.; Czarda, P.; Iluca, S.; Zappe, K.; Weis, S.; Spiegl-Kreinecker, S.; Cichna-Markl, M. Association of Intergenic and Intragenic MGMT Enhancer Methylation with MGMT Promoter Methylation, MGMT Protein Expression and Clinical and Demographic Parameters in Glioblastoma. *International Journal of Molecular Sciences* **2025**, *26* (7), 3390. https://doi.org/10.3390/ijms26073390.
(44) Zappe, K.; Pühringer, K.; Pflug, S.; Berger, D.; Weis, S.; Spiegl-Kreinecker, S.; Cichna-Markl, M. Association of MGMT Promoter and Enhancer Methylation with Genetic Variants, Clinical Parameters, and Demographic Characteristics in Glioblastoma. *Cancers* **2023**, *15* (24), 5777. https://doi.org/10.3390/cancers15245777.
(45) Hassel, J. C.; Sucker, A.; Edler, L.; Kurzen, H.; Moll, I.; Stresemann, C.; et al. MGMT Gene Promoter Methylation Correlates with Tolerance of Temozolomide Treatment in Melanoma but Not with Clinical Outcome. *British Journal of Cancer* **2010**, *103* (6), 820–826. https://doi.org/10.1038/sj.bjc.6605796.
(46) Ma, W.; Li, N.; An, Y.; Zhou, C.; Bo, C.; Zhang, G. Effects of Temozolomide and Radiotherapy on Brain Metastatic Tumor: A Systematic Review and Meta-Analysis. *World Neurosurgery* **2016**, *92*, 197–205. https://doi.org/10.1016/j.wneu.2016.04.011.
(47) Liu, Y.; Siejka-Zielińska, P.; Velikova, G.; Bi, Y.; Yuan, F.; Tomkova, M.; Bai, C.; Chen, L.; Schuster-Böckler, B.; Song, C.-X. Bisulfite-Free Direct Detection of 5-

Methylcytosine and 5-Hydroxymethylcytosine at Base Resolution. *Nature Biotechnology* **2019**, *37* (4), 424–429. https://doi.org/10.1038/s41587-019-0041-2.
(48) R. Corbin, K.; M. Rodriguez Lopez, C. Library Preparation for Whole Genome Bisulfite Sequencing of Plant Genomes. In *DNA Methylation Mechanism*; Budak, M., Yıldız, M., Eds.; IntechOpen, 2020. https://doi.org/10.5772/intechopen.90716.
(49) Frommer, M.; McDonald, L. E.; Millar, D. S.; Collis, C. M.; Watt, F.; Grigg, G. W.; et al. A Genomic Sequencing Protocol That Yields a Positive Display of 5-Methylcytosine Residues in Individual DNA Strands. *Proceedings of the National Academy of Sciences* **1992**, *89* (5), 1827–1831. https://doi.org/10.1073/pnas.89.5.1827.
(50) Wanunu, M.; Cohen-Karni, D.; Johnson, R. R.; Fields, L.; Benner, J.; Peterman, N.; et al. Discrimination of Methylcytosine from Hydroxymethylcytosine in DNA Molecules. *Journal of the American Chemical Society* **2011**, *133* (3), 486–492. https://doi.org/10.1021/ja107836t.
(51) Booth, M. J.; Branco, M. R.; Ficz, G.; Oxley, D.; Krueger, F.; Reik, W. Quantitative Sequencing of 5-Methylcytosine and 5-Hydroxymethylcytosine at Single-Base Resolution. *Science* **2012**, *336* (6083), 934–937. https://doi.org/10.1126/science.1220671.
(52) De Borre, M.; Branco, M. R. Oxidative Bisulfite Sequencing: An Experimental and Computational Protocol. In *DNA Modifications*; Ruzov, A., Gering, M., Eds.; Methods in Molecular Biology; Springer US: New York, NY, 2021; Vol. 2198, pp 333–348. https://doi.org/10.1007/978-1-0716-0876-0_26.
(53) Xu, H.; Chen, J.; Cheng, J.; Kong, L.; Chen, X.; Inoue, M.; et al. Modular Oxidation of Cytosine Modifications and Their Application in Direct and Quantitative Sequencing of 5-Hydroxymethylcytosine. *Journal of the American Chemical Society* **2023**, *145* (13), 7095–7100. https://doi.org/10.1021/jacs.3c01663.
(54) Liu, Y.; Hu, Z.; Cheng, J.; Siejka-Zielińska, P.; Chen, J.; Inoue, M.; et al. Subtraction-Free and Bisulfite-Free Specific Sequencing of 5-Methylcytosine and Its Oxidized Derivatives at Base Resolution. *Nature Communications* **2021**, *12* (1), 618. https://doi.org/10.1038/s41467-021-20920-2.
(55) Mullis, K. B.; Faloona, F. A. Specific Synthesis of DNA in Vitro via a Polymerase-Catalyzed Chain Reaction. In *Methods in Enzymology*; Elsevier, 1987; Vol. 155, pp 335–350. https://doi.org/10.1016/0076-6879(87)55023-6.
(56) Polymerase chain reaction. https://commons.wikimedia.org/wiki/File:Polymerase_chain_reaction.svg (accessed 2025-06-18).
(57) Bonacorsi, S.; Visseaux, B.; Bouzid, D.; Pareja, J.; Rao, S. N.; Manissero, D.; et al. Systematic Review on the Correlation of Quantitative PCR Cycle Threshold Values of Gastrointestinal Pathogens With Patient Clinical Presentation and Outcomes. *Frontiers in Medicine* **2021**, *8*, 711809. https://doi.org/10.3389/fmed.2021.711809.
(58) Nyrén, P. The History of Pyrosequencing®. In *Pyrosequencing Protocols*; Humana Press: New Jersey, 2006; Vol. 373, pp 1–14. https://doi.org/10.1385/1-59745-377-3:1.
(59) Fakruddin; Mazumdar, R. M.; Chowdhury, A.; Hossain, N.; Mahajan, S.; Islam, S. Pyrosequencing-A Next Generation Sequencing Technology. *World Applied Sciences Journal 24* (12), 1558–1571. https://doi.org/10.5829/idosi.wasj.2013.24.12.2972.

(60) Elahi, E.; Ronaghi, M. Pyrosequencing: A Tool for DNA Sequencing Analysis. In *Bacterial Artificial Chromosomes*; Humana Press: New Jersey, 2004; Vol. 255, pp 211–220. https://doi.org/10.1385/1-59259-752-1:211.
(61) Ronaghi, M.; Uhlén, M.; Nyrén, P. A Sequencing Method Based on Real-Time Pyrophosphate. *Science* **1998**, *281* (5375), 363–365. https://doi.org/10.1126/science.281.5375.363.
(62) Ronaghi, M.; Karamohamed, S.; Pettersson, B.; Uhlén, M.; Nyrén, P. Real-Time DNA Sequencing Using Detection of Pyrophosphate Release. *Analytical Biochemistry* **1996**, *242* (1), 84–89. https://doi.org/10.1006/abio.1996.0432.
(63) Rizzi, E. The Pyrosequencing Protocol for Bacterial Genomes. In *Bacterial Pangenomics*; Mengoni, A., Galardini, M., Fondi, M., Eds.; Methods in Molecular Biology; Springer New York: New York, NY, 2015; Vol. 1231, pp 49–75. https://doi.org/10.1007/978-1-4939-1720-4_4.
(64) Müller, H.-J.; Prange, D. R. *PCR - Polymerase-Kettenreaktion*, 2. Aufl. 2016, pp 6–8; SpringerLink Bücher; Springer Spektrum: Berlin Heidelberg, 2016. https://doi.org/10.1007/978-3-662-48236-0.
(65) Mikeska, T.; Felsberg, J.; Hewitt, C. A.; Dobrovic, A. Analysing DNA Methylation Using Bisulphite Pyrosequencing. In *Epigenetics Protocols*; Tollefsbol, T. O., Ed.; Methods in Molecular Biology; Humana Press: Totowa, NJ, 2011; Vol. 791, pp 33–53. https://doi.org/10.1007/978-1-61779-316-5_4.
(66) DNeasy PowerMax Soil Kit. https://www.qiagen.com/us/products/discovery-and-translational-research/dna-rna-purification/dna-purification/microbial-dna/dneasy-powermax-soil-kit (accessed 2025-01-06).
(67) Qiagen – EpiTect Fast Bisulfite Conversion Kit. https://www.qiagen.com/us/products/discovery-and-translational-research/epigenetics/dna-methylation/bisulfite-conversion-assays/epitect-fast-bisulfite-conversion-kit (accessed 2024-12-22).
(68) Qiagen – EpiTect Fast Bisulfite Conversion Handbook. https://www.qiagen.com/us/resources/resourcedetail?id=ab2427dc-3da9-412c-8c37-7e78d397b6ac&lang=en (accessed 2024-12-22).
(69) Thermo Fischer – Qubit ssDNA Assay kit. https://www.thermofisher.com/document-connect/document-connect.html?url=https://assets.thermofisher.com/TFS-Assets%2FLSG%2Fmanuals%2FQubit_ssDNA_Assay_UG.pdf (accessed 2024-12-22).
(70) National Library of Medicine – National Center for Biotechnology Information. https://www.ncbi.nlm.nih.gov (accessed 2024-12-23).
(71) Oligo Calc: Oligonucleotide Properties Calculator. biotools.nubic.northwestern.edu/OligoCalc.html (accessed 2024-12-23).
(72) RNAfold *Webserver*. rna.tbi.univie.ac.at/cgi-bin/RNAWebSuite/RNAfold.cgi (accessed 2024-12-23).
(73) Oligo Analyzer. https://eu.idtdna.com/pages/tools/oligoanalyzer?returnurl=%2Fcalc%2Fanalyzer (accessed 2024-12-23).
(74) Primer Design and Search Too*l*. bisearch.enzim.hu/?m=genompsearch (accessed 2024-12-23).
(75) Bio-Rad Micro Bio-Spin columns. https://www.bio-rad.com/de-at/sku/7326204-micro-bio-spin-chromatography-columns?ID=7326204 (accessed 2025-01-07).

(76) *Z*ymo-Spin IC Columns. https://zymoresearch.eu/products/zymo-spin-ic-columns?srsltid=AfmBOooDSXmcF7JXjTi7iwXXNJrYmoR4_KYYh8n9Yc1cKYqHw_Mr2Xx (accessed 2025-01-07).
(77) *P*yroMark PCR kit Qiag*en*. https://www.qiagen.com/de-at/products/discovery-and-translational-research/pcr-qpcr-dpcr/pcr-enzymes-and-kits/end-point-pcr/qiagen-multiplex-pcr-kit?catno=206143 (accessed 2025-01-07).
(78) *P*yroMark Q48 Autop*rep*. https://www.qiagen.com/de-us/products/discovery-and-translational-research/pyrosequencing/pyromark-q48-autoprep-and-accessories?catno=9002471 (accessed 2025-01-08).
(79) Huang, Y.; Pastor, W. A.; Shen, Y.; Tahiliani, M.; Liu, D. R.; Rao, A. The Behaviour of 5-Hydroxymethylcytosine in Bisulfite Sequencing. *PLoS ONE* **2010**, *5* (1), e8888. https://doi.org/10.1371/journal.pone.0008888.
(80) Genereux, D. P.; Johnson, W. C.; Burden, A. F.; Stoger, R.; Laird, C. D. Errors in the Bisulfite Conversion of DNA: Modulating Inappropriate- and Failed-Conversion Frequencies. *Nucleic Acids Research* **2008**, *36* (22), e150–e150. https://doi.org/10.1093/nar/gkn691.
(81) Booth, M. J.; Ost, T. W. B.; Beraldi, D.; Bell, N. M.; Branco, M. R.; Reik, W. Oxidative Bisulfite Sequencing of 5-Methylcytosine and 5-Hydroxymethylcytosine. *Nature Protocols* **2013**, *8* (10), 1841–1851. https://doi.org/10.1038/nprot.2013.115.

8 Appendix

8.1 Annealing temperatures for each PCR run

Supplementary Table 1: Primer concentration and annealing temperatures for each PCR reaction

Assay	Enhancer	Primer conc. [µM]	Ta [°C] PCR #1	Ta [°C] PCR #2
Assay 1	enh1 inter	0.4	53.5	53.5
Assay 2	enh2 inter	0.4	55.7	56.5
Assay 3	enh2 inter	0.4	56.5	56.3
Assay 4	enh2 inter	0.4	60.7	60.7
Assay 5	enh2 inter	0.4	58.1	58.1
Assay 6	enh2 inter	0.4	56.6	56.6
Assay 7	enh3 inter	0.4	59	59
Assay 8	enh3 inter	0.4	58	58
Assay 9	enh3 inter	0.4	58	58
Assay 10	enh3 inter	0.4	58	58.1
Assay 11	enh4 inter	0.4	56.6	56.6
Assay 12	enh4 inter	0.4	54.6	55.3
Assay 13	enh4 inter	0.4	52.6	52
Assay 14	enh4 inter	0.4	55.6	55.3
Assay 15	enh5 inter	0.4	59.6	59.6
Assay 16	enh5 inter	0.4	56.2	56.3
Assay 17	enh5 inter	0.2	61.4	61.4
Assay 18	Promoter	0.4	56	55.9
Assay 19	enh6 intra	0.4	51.3	52
Assay 20	enh7 intra	0.2	53.5	53.5
Assay 21	enh7 intra	0.2	56.5	56.6
Assay 22	enh7 intra	0.2	56.5	56.5
Assay 23	enh7 intra	0.4	55	54.6
Assay 24	enh8 intra	0.2	55	55.9
Assay 25	enh8 intra	0.4	56.5	56.6
Assay 26	enh8 intra	0.4	59.8	59.8
Assay 27	enh9 intra	0.4	58	58.1

8.2 Raw methylation data for MGMT enhancers determined using PSQ

Supplementary Table 2: enh1 inter methylation levels [%] in melanoma metastasis samples determined by PSQ

	CpG1		CpG2		CpG3	
Sample	PCR #1	PCR #2	PCR #1	PCR #2	PCR #1	PCR #2
M01	46.45	44.70	50.88	52.02	58.32	57.11
M02	65.74	64.49	70.88	69.53	25.88	26.91
M03	11.60	14.12	14.51	15.58	18.60	10.75
M04	85.07	85.39	92.71	91.87	93.31	>ULOQ
M05	86.69	83.70	93.91	90.61	82.22	86.46
M06	<LLOQ	<LLOQ	<LLOQ	7.52	<LLOQ	5.75
M07	81.18	76.78	90.97	84.63	34.83	33.10
M08	87.34	87.95	94.16	92.41	>ULOQ	>ULOQ
M09	77.29	78.93	86.38	83.67	78.42	83.52
M10	63.08	68.00	68.18	70.11	12.97	19.77
M11	<LLOQ	<LLOQ	<LLOQ	6.11	<LLOQ	8.88
M12	<LLOQ	<LLOQ	<LLOQ	<LLOQ	<LLOQ	8.60
M13	82.22	82.85	89.11	85.33	13.72	19.61
M14	6.76	7.50	<LLOQ	7.50	23.43	23.09
M15	37.29	31.15	41.49	36.09	15.33	11.92
M16	73.31	77.44	75.74	73.16	68.80	59.20
M17	55.30	54.42	59.22	60.19	58.68	62.14
M18	38.21	38.23	33.01	34.09	41.88	47.31
M19	86.50	86.94	92.99	94.84	>ULOQ	>ULOQ
M20	<LLOQ	6.11	<LLOQ	<LLOQ	<LLOQ	<LLOQ

Supplementary Table 3 and 4: enh2 inter methylation levels [%] in melanoma metastasis samples determined by PSQ

	CpG9		CpG12		CpG13		CpG14		Cp15		CpG16		CpG17		CpG18		CpG19		CpG20	
Sample	PCR #1	PCR #2	PCR #1	PCR #2	PCR #1	PCR #2	PCR #1	PCR #2	PCR #1	PCR #2	PCR #1	PCR #2	PCR #1	PCR #2	PCR #1	PCR #2	PCR #1	PCR #2	PCR #1	PCR #2
M01	53.18	54.74	65.73	72.02	71.85	78.53	71.95	81.74	63.31	69.53	80.88	85.13	73.60	74.81	74.53	72.84	44.85	47.69	46.97	47.45
M02	<LLOQ	<LLOQ	<LLOQ	<LLOQ	<LLOQ	<LLOQ	<LLOQ	<LLOQ	5.96	<LLOQ	<LLOQ	<LLOQ	<LLOQ	<LLOQ	<LLOQ	<LLOQ	<LLOQ	<LLOQ	<LLOQ	<LLOQ
M03	7.14	6.83	14.50	9.70	9.09	6.88	12.22	7.23	10.45	8.90	19.19	10.32	17.77	11.11	9.09	6.90	5.92	5.55	9.38	5.26
M04	20.39	21.09	<LLOQ	5.96	<LLOQ	6.02	6.70	8.01	<LLOQ	7.28	<LLOQ	<LLOQ	<LLOQ	8.21	29.90	34.13	6.60	6.01	<LLOQ	5.06
M05	<LLOQ	5.14	<LLOQ	<LLOQ	<LLOQ	<LLOQ	<LLOQ	<LLOQ	<LLOQ	<LLOQ	<LLOQ	<LLOQ	<LLOQ	<LLOQ	<LLOQ	<LLOQ	<LLOQ	<LLOQ	<LLOQ	<LLOQ
M06	<LLOQ	<LLOQ	<LLOQ	<LLOQ	<LLOQ	<LLOQ	<LLOQ	5.62	<LLOQ	5.15	<LLOQ	5.90	<LLOQ	6.32	<LLOQ	5.12	<LLOQ	5.71	<LLOQ	<LLOQ
M07	<LLOQ	<LLOQ	5.26	<LLOQ	<LLOQ	<LLOQ	<LLOQ	<LLOQ	<LLOQ	5.18	<LLOQ	<LLOQ	5.79	<LLOQ	5.05	<LLOQ	<LLOQ	<LLOQ	<LLOQ	<LLOQ
M08	<LLOQ	5.79	10.03	5.82	<LLOQ	<LLOQ	6.51	8.22	<LLOQ	5.75	7.55	8.21	5.20	7.28	<LLOQ	<LLOQ	<LLOQ	<LLOQ	<LLOQ	<LLOQ
M09	10.78	12.25	14.94	14.27	7.97	9.20	12.73	15.39	13.59	14.43	15.11	14.04	9.37	9.45	13.68	10.61	11.50	10.22	12.86	12.01
M10	<LLOQ	<LLOQ	<LLOQ	5.46	<LLOQ	<LLOQ	<LLOQ	<LLOQ	<LLOQ	5.26	5.60	7.28	7.34	5.47	<LLOQ	<LLOQ	<LLOQ	<LLOQ	<LLOQ	<LLOQ
M11	<LLOQ	<LLOQ	<LLOQ	<LLOQ	<LLOQ	<LLOQ	<LLOQ	<LLOQ	<LLOQ	<LLOQ	<LLOQ	<LLOQ	<LLOQ	<LLOQ	<LLOQ	<LLOQ	<LLOQ	<LLOQ	<LLOQ	<LLOQ
M12	<LLOQ	<LLOQ	<LLOQ	5.31	<LLOQ	<LLOQ	6.07	5.04	<LLOQ	5.01	<LLOQ	<LLOQ	<LLOQ	5.07	<LLOQ	<LLOQ	<LLOQ	<LLOQ	<LLOQ	<LLOQ
M13	14.88	12.22	49.13	36.10	59.36	46.87	57.99	54.88	17.99	16.91	21.06	12.80	12.95	10.27	24.12	25.83	10.88	9.53	8.21	5.55
M14	6.89	8.28	<LLOQ	7.53	<LLOQ	5.32	8.32	8.96	5.57	7.14	11.47	11.12	5.92	7.80	<LLOQ	6.26	<LLOQ	6.05	<LLOQ	<LLOQ
M15	<LLOQ	<LLOQ	<LLOQ	<LLOQ	<LLOQ	<LLOQ	<LLOQ	<LLOQ	6.38	<LLOQ	<LLOQ	<LLOQ	<LLOQ	<LLOQ	<LLOQ	<LLOQ	<LLOQ	<LLOQ	<LLOQ	<LLOQ
M16	53.95	56.39	60.46	62.92	60.38	72.61	66.11	70.35	55.39	56.10	72.67	75.30	56.92	63.37	62.39	67.09	34.51	38.44	49.82	52.08
M17	12.08	11.45	<LLOQ	9.80	<LLOQ	6.94	5.77	13.46	10.22	10.68	17.91	22.01	38.73	35.99	37.51	32.38	15.79	15.80	5.16	<LLOQ
M18	<LLOQ	<LLOQ	<LLOQ	<LLOQ	<LLOQ	<LLOQ	<LLOQ	5.09	<LLOQ	<LLOQ	<LLOQ	<LLOQ	<LLOQ	<LLOQ	<LLOQ	<LLOQ	<LLOQ	<LLOQ	<LLOQ	<LLOQ
M19	<LLOQ	<LLOQ	6.48	14.79	14.29	19.30	8.95	13.42	17.82	21.36	83.08	83.42	89.41	88.78	78.93	77.73	8.28	8.79	<LLOQ	<LLOQ
M20	6.27	5.14	7.73	5.63	6.66	<LLOQ	10.32	5.41	<LLOQ	<LLOQ	<LLOQ	<LLOQ	<LLOQ	6.81	<LLOQ	<LLOQ	<LLOQ	<LLOQ	<LLOQ	<LLOQ

	CpG21		CpG22		CpG23		CpG24		CpG25		CpG26		CpG27		CpG27 +1		CpG27 +1	
Sample	PCR #1	PCR #2	PCR #1	PCR #2	PCR #1	PCR #2	PCR #1	PCR #2	PCR #1	PCR #2	PCR #1	PCR #2	PCR #1	PCR #2	PCR #1	PCR #2	PCR #1	PCR #2
M01	59.35	58.33	74.66	73.39	63.38	64.02	22.60	21.95	56.86	58.37	59.44	58.74	75.46	85.44	65.68	70.44	80.09	84.41
M02	<LLOQ	<LLOQ	<LLOQ	<LLOQ	<LLOQ	<LLOQ	<LLOQ	<LLOQ	<LLOQ	5.13	<LLOQ	<LLOQ	14.83	<LLOQ	<LLOQ	<LLOQ	5.24	5.64
M03	<LLOQ	<LLOQ	7.97	6.67	5.96	<LLOQ	<LLOQ	<LLOQ	<LLOQ	<LLOQ	<LLOQ	5.15	5.08	22.50	<LLOQ	7.28	7.50	16.07
M04	6.44	6.32	<LLOQ	<LLOQ	5.52	<LLOQ	<LLOQ	<LLOQ	<LLOQ	5.08	7.08	6.96	13.82	20.07	14.74	13.73	43.05	50.41
M05	<LLOQ	<LLOQ	<LLOQ	<LLOQ	<LLOQ	<LLOQ	<LLOQ	<LLOQ	<LLOQ	<LLOQ	<LLOQ	<LLOQ	<LLOQ	8.22	<LLOQ	<LLOQ	6.14	6.39
M06	<LLOQ	<LLOQ	5.00	<LLOQ	<LLOQ	<LLOQ	<LLOQ	<LLOQ	<LLOQ	5.69	<LLOQ	<LLOQ	<LLOQ	7.88	<LLOQ	<LLOQ	<LLOQ	6.43
M07	<LLOQ	<LLOQ	20.08	20.84	<LLOQ	<LLOQ	<LLOQ	<LLOQ	<LLOQ	5.21	<LLOQ	<LLOQ	10.22	7.63	<LLOQ	5.68	<LLOQ	8.81
M08	<LLOQ	<LLOQ	5.10	<LLOQ	<LLOQ	<LLOQ	<LLOQ	<LLOQ	<LLOQ	<LLOQ	<LLOQ	<LLOQ	23.51	7.76	46.60	21.16	29.68	29.02
M09	20.21	15.07	12.32	10.65	12.67	10.05	7.80	5.79	10.92	10.33	19.84	18.65	30.05	37.27	34.35	27.99	21.52	32.45
M10	<LLOQ	<LLOQ	<LLOQ	<LLOQ	<LLOQ	<LLOQ	<LLOQ	<LLOQ	<LLOQ	<LLOQ	<LLOQ	<LLOQ	13.29	5.09	<LLOQ	<LLOQ	<LLOQ	<LLOQ
M11	<LLOQ	<LLOQ	<LLOQ	<LLOQ	<LLOQ	<LLOQ	<LLOQ	<LLOQ	<LLOQ	<LLOQ	<LLOQ	<LLOQ	<LLOQ	10.57	<LLOQ	<LLOQ	<LLOQ	5.25
M12	<LLOQ	<LLOQ	<LLOQ	<LLOQ	<LLOQ	<LLOQ	<LLOQ	<LLOQ	<LLOQ	<LLOQ	<LLOQ	<LLOQ	6.89	6.64	<LLOQ	<LLOQ	<LLOQ	<LLOQ
M13	8.38	11.03	31.39	33.41	28.68	27.92	<LLOQ	7.77	12.62	15.07	10.02	6.25	13.47	6.98	11.77	9.62	19.77	13.54
M14	<LLOQ	<LLOQ	5.65	<LLOQ	6.01	<LLOQ	<LLOQ	<LLOQ	<LLOQ	5.74	10.40	<LLOQ	25.78	12.18	14.85	6.47	22.38	17.90
M15	<LLOQ	<LLOQ	<LLOQ	<LLOQ	<LLOQ	<LLOQ	<LLOQ	<LLOQ	<LLOQ	<LLOQ	<LLOQ	<LLOQ	<LLOQ	<LLOQ	<LLOQ	<LLOQ	6.13	<LLOQ
M16	56.68	56.27	64.27	65.56	53.03	55.53	37.37	36.12	62.28	56.80	58.90	58.98	73.29	77.35	61.50	67.56	73.66	86.56
M17	6.68	6.87	5.55	6.40	6.36	7.61	<LLOQ	<LLOQ	<LLOQ	<LLOQ	7.65	5.14	13.19	16.94	15.15	15.60	6.56	12.32
M18	<LLOQ	<LLOQ	<LLOQ	<LLOQ	<LLOQ	<LLOQ	<LLOQ	<LLOQ	<LLOQ	<LLOQ	<LLOQ	<LLOQ	9.33	10.10	<LLOQ	<LLOQ	<LLOQ	<LLOQ
M19	<LLOQ	<LLOQ	<LLOQ	5.16	<LLOQ	<LLOQ	<LLOQ	<LLOQ	5.25	5.82	<LLOQ	<LLOQ	5.65	12.24	<LLOQ	<LLOQ	7.21	8.16
M20	7.09	7.87	5.91	<LLOQ	<LLOQ	<LLOQ	<LLOQ	<LLOQ	<LLOQ	<LLOQ	<LLOQ	<LLOQ	14.17	13.42	<LLOQ	<LLOQ	<LLOQ	5.49

Supplementary Table 5 and 6: enh3 inter methylation levels [%] in melanoma metastasis samples determined by PSQ

	CpG5		CpG6		CpG7		CpG8		CpG11		CpG12		CpG13		CpG14		CpG15	
Sample	PCR #1	PCR #2	PCR #1	PCR #2	PCR #1	PCR #2	PCR #1	PCR #2	PCR #1	PCR #2	PCR #1	PCR #2	PCR #1	PCR #2	PCR #1	PCR #2	PCR #1	PCR #2
M01	55.30	55.00	54.81	56.48	67.22	69.33	52.23	55.59	68.50	78.62	72.76	80.92	67.90	73.92	60.54	64.68	78.42	82.15
M02	6.19	5.47	<LLOQ	<LLOQ	10.62	8.52	<LLOQ	<LLOQ	<LLOQ	<LLOQ	<LLOQ	<LLOQ	<LLOQ	<LLOQ	7.68	<LLOQ	15.55	8.31
M03	<LLOQ	<LLOQ	<LLOQ	<LLOQ	<LLOQ	<LLOQ	<LLOQ	<LLOQ	<LLOQ	<LLOQ	<LLOQ	<LLOQ	<LLOQ	<LLOQ	8.10	<LLOQ	12.71	7.57
M04	14.87	15.89	24.00	24.28	36.92	42.18	13.34	15.45	7.60	8.86	23.75	28.26	8.57	13.81	11.35	13.80	48.35	50.35
M05	21.71	17.94	<LLOQ	6.76	27.87	28.64	27.95	33.15	56.56	60.57	56.47	61.84	29.64	31.19	20.56	17.98	51.54	53.88
M06	<LLOQ	<LLOQ	<LLOQ	<LLOQ	<LLOQ	<LLOQ	<LLOQ	<LLOQ	<LLOQ	<LLOQ	<LLOQ	<LLOQ	<LLOQ	<LLOQ	<LLOQ	<LLOQ	7.89	<LLOQ
M07	<LLOQ	<LLOQ	<LLOQ	5.04	6.53	8.30	<LLOQ	5.44	<LLOQ	<LLOQ	<LLOQ	<LLOQ	<LLOQ	<LLOQ	<LLOQ	<LLOQ	28.33	22.55
M08	14.95	16.78	<LLOQ	12.56	24.72	28.63	44.00	66.00	5.44	<LLOQ	17.71	16.32	8.73	<LLOQ	6.61	6.10	78.73	70.47
M09	27.70	31.05	24.71	29.24	51.90	49.37	21.76	28.62	16.43	17.18	21.84	23.06	14.63	17.04	13.76	15.80	66.72	61.49
M10	8.07	5.04	<LLOQ	<LLOQ	9.85	6.17	<LLOQ	<LLOQ	<LLOQ	<LLOQ	<LLOQ	<LLOQ	<LLOQ	<LLOQ	6.10	<LLOQ	14.66	10.51
M11	<LLOQ	<LLOQ	<LLOQ	<LLOQ	<LLOQ	<LLOQ	<LLOQ	<LLOQ	<LLOQ	<LLOQ	<LLOQ	<LLOQ	<LLOQ	<LLOQ	<LLOQ	<LLOQ	6.83	5.64
M12	<LLOQ	<LLOQ	<LLOQ	<LLOQ	<LLOQ	<LLOQ	<LLOQ	<LLOQ	<LLOQ	<LLOQ	<LLOQ	<LLOQ	<LLOQ	<LLOQ	<LLOQ	<LLOQ	5.41	8.91
M13	23.16	38.10	41.34	48.35	56.39	62.22	32.57	34.40	64.11	68.13	69.20	71.55	39.65	42.38	33.74	38.13	82.59	82.01
M14	9.72	6.11	8.63	7.76	23.32	17.55	6.92	5.98	<LLOQ	<LLOQ	<LLOQ	5.76	<LLOQ	<LLOQ	5.86	6.08	11.13	11.30
M15	5.15	<LLOQ	<LLOQ	<LLOQ	8.19	6.78	<LLOQ	<LLOQ	<LLOQ	<LLOQ	<LLOQ	<LLOQ	<LLOQ	<LLOQ	<LLOQ	<LLOQ	14.07	13.70
M16	53.35	55.16	53.93	51.14	65.77	66.69	52.03	49.32	79.34	80.03	84.26	82.46	61.10	60.80	57.39	55.65	84.11	83.94
M17	30.78	26.31	19.38	18.22	51.11	47.62	28.63	39.38	28.13	29.74	26.16	28.08	11.22	14.28	8.63	10.22	54.42	51.74
M18	<LLOQ	<LLOQ	<LLOQ	<LLOQ	<LLOQ	5.43	<LLOQ	<LLOQ	<LLOQ	<LLOQ	<LLOQ	<LLOQ	<LLOQ	<LLOQ	<LLOQ	<LLOQ	13.22	7.82
M19	<LLOQ	<LLOQ	6.39	6.07	13.96	11.56	<LLOQ	<LLOQ	11.43	10.01	11.52	10.76	<LLOQ	<LLOQ	<LLOQ	<LLOQ	6.68	7.90
M20	12.80	11.38	<LLOQ	11.10	23.96	21.68	6.14	10.65	<LLOQ	<LLOQ	5.18	<LLOQ	<LLOQ	<LLOQ	<LLOQ	<LLOQ	12.21	14.23

	CpG16		CpG17		CpG18		CpG25		CpG26		CpG27		CpG37		CpG38		CpG39	
Sample	PCR #1	PCR #2	PCR #1	PCR #2	PCR #1	PCR #2	PCR #1	PCR #2	PCR #1	PCR #2	PCR #1	PCR #2	PCR #1	PCR #2	PCR #1	PCR #2	PCR #1	PCR #2
M01	66.62	60.48	80.28	82.59	74.36	67.83	17.93	18.17	17.98	23.82	5.63	<LLOQ	62.36	62.44	50.97	56.39	28.61	33.34
M02	6.41	<LLOQ	7.91	5.99	9.41	<LLOQ	<LLOQ	<LLOQ	<LLOQ	<LLOQ	<LLOQ	<LLOQ	<LLOQ	<LLOQ	<LLOQ	<LLOQ	<LLOQ	<LLOQ
M03	7.47	<LLOQ	12.97	7.93	16.92	9.22	<LLOQ	<LLOQ	<LLOQ	<LLOQ	<LLOQ	<LLOQ	8.95	12.25	5.19	11.92	<LLOQ	5.65
M04	62.12	56.52	85.97	87.32	67.09	60.97	<LLOQ	<LLOQ	<LLOQ	<LLOQ	<LLOQ	9.20	36.18	35.38	15.54	16.52	9.98	6.53
M05	58.56	50.43	86.39	81.77	65.76	60.41	<LLOQ	<LLOQ	<LLOQ	<LLOQ	<LLOQ	<LLOQ	<LLOQ	9.72	<LLOQ	8.62	<LLOQ	5.21
M06	<LLOQ	<LLOQ	<LLOQ	<LLOQ	<LLOQ	<LLOQ	<LLOQ	<LLOQ	<LLOQ	<LLOQ	<LLOQ	<LLOQ	<LLOQ	8.62	<LLOQ	6.78	<LLOQ	<LLOQ
M07	21.48	21.25	38.18	38.57	27.64	27.51	<LLOQ	<LLOQ	<LLOQ	<LLOQ	<LLOQ	<LLOQ	23.56	31.96	20.15	24.71	5.10	6.61
M08	53.81	62.89	85.19	86.44	56.86	67.31	<LLOQ	<LLOQ	<LLOQ	<LLOQ	14.21	8.65	7.11	7.22	7.14	<LLOQ	<LLOQ	6.92
M09	49.28	48.51	76.28	75.33	53.55	55.51	<LLOQ	<LLOQ	12.84	10.14	13.88	12.48	16.32	18.18	5.98	9.44	7.78	8.15
M10	<LLOQ	<LLOQ	6.04	<LLOQ	6.78	<LLOQ	<LLOQ	<LLOQ	<LLOQ	<LLOQ	6.08	<LLOQ	<LLOQ	6.06	<LLOQ	5.42	<LLOQ	<LLOQ
M11	<LLOQ	<LLOQ	<LLOQ	<LLOQ	<LLOQ	<LLOQ	<LLOQ	<LLOQ	<LLOQ	<LLOQ	<LLOQ	<LLOQ	<LLOQ	<LLOQ	<LLOQ	<LLOQ	<LLOQ	<LLOQ
M12	<LLOQ	<LLOQ	<LLOQ	<LLOQ	<LLOQ	<LLOQ	<LLOQ	<LLOQ	<LLOQ	<LLOQ	<LLOQ	<LLOQ	<LLOQ	5.26	<LLOQ	<LLOQ	<LLOQ	<LLOQ
M13	62.26	62.01	84.14	88.75	67.21	65.91	<LLOQ	<LLOQ	6.16	6.79	7.57	6.93	54.29	40.93	53.92	40.74	6.28	11.94
M14	<LLOQ	<LLOQ	6.07	6.87	7.29	<LLOQ	<LLOQ	<LLOQ	<LLOQ	<LLOQ	5.11	5.62	<LLOQ	6.85	<LLOQ	<LLOQ	<LLOQ	<LLOQ
M15	42.43	41.18	54.09	52.88	51.08	49.02	<LLOQ	<LLOQ	<LLOQ	<LLOQ	<LLOQ	<LLOQ	<LLOQ	<LLOQ	<LLOQ	<LLOQ	<LLOQ	<LLOQ
M16	65.10	64.54	84.37	79.94	69.74	68.48	25.36	26.71	45.00	49.43	40.69	38.62	62.73	56.79	57.62	42.85	53.05	45.54
M17	35.78	33.99	59.65	61.20	36.63	38.04	<LLOQ	<LLOQ	<LLOQ	<LLOQ	<LLOQ	6.40	<LLOQ	6.69	<LLOQ	<LLOQ	<LLOQ	<LLOQ
M18	9.06	7.29	15.42	11.86	13.16	12.23	<LLOQ	<LLOQ	<LLOQ	<LLOQ	<LLOQ	<LLOQ	<LLOQ	5.68	<LLOQ	<LLOQ	<LLOQ	<LLOQ
M19	<LLOQ	<LLOQ	77.77	80.05	31.67	34.27	<LLOQ	<LLOQ	<LLOQ	<LLOQ	<LLOQ	5.26	<LLOQ	<LLOQ	<LLOQ	<LLOQ	<LLOQ	<LLOQ
M20	<LLOQ	6.00	8.38	8.41	21.29	26.00	<LLOQ	<LLOQ	<LLOQ	<LLOQ	10.97	7.57	62.76	55.33	52.55	44.49	31.76	26.29

Supplementary Table 7 and 8: enh4 inter methylation levels [%] in Melanoma metastasis samples determined by PSQ

	CpG18		CpG19		CpG20		CpG21		CpG22		CpG23		CpG24	
Sample	PCR #1	PCR #2	PCR #1	PCR #2	PCR #1	PCR #2	PCR #1	PCR #2	PCR #1	PCR #2	PCR #1	PCR #2	PCR #1	PCR #2
M01	89.17	85.06	82.86	77.69	88.89	83.47	82.33	79.29	90.86	85.64	94.69	>ULOQ	86.52	89.11
M02	<LLOQ	<LLOQ	<LLOQ	<LLOQ	<LLOQ	<LLOQ	<LLOQ	<LLOQ	<LLOQ	<LLOQ	<LLOQ	<LLOQ	<LLOQ	<LLOQ
M03	7.64	7.91	5.01	6.82	7.63	8.21	5.75	6.19	<LLOQ	<LLOQ	10.16	10.79	7.79	9.58
M04	5.97	5.64	5.08	5.85	14.03	9.16	8.45	5.54	40.73	36.90	5.22	<LLOQ	5.49	7.11
M05	57.78	58.40	66.05	55.97	54.48	46.82	25.43	17.55	46.84	45.23	91.90	92.08	25.17	21.52
M06	<LLOQ	<LLOQ	<LLOQ	<LLOQ	<LLOQ	<LLOQ	<LLOQ	<LLOQ	<LLOQ	<LLOQ	20.27	25.92	6.22	9.20
M07	6.41	7.66	12.44	15.15	<LLOQ	<LLOQ	11.66	9.47	29.65	28.35	32.39	34.48	8.45	10.12
M08	13.40	18.63	7.96	8.27	11.95	14.32	9.15	6.76	<LLOQ	6.35	91.65	92.32	13.74	15.08
M09	53.93	48.52	60.78	51.65	65.85	57.97	31.52	20.15	68.51	64.55	50.90	51.42	27.06	22.80
M10	<LLOQ	<LLOQ	<LLOQ	<LLOQ	<LLOQ	5.23	<LLOQ	<LLOQ	26.69	31.18	9.39	6.45	7.98	<LLOQ
M11	5.90	8.52	<LLOQ	<LLOQ	<LLOQ	6.33	<LLOQ	<LLOQ	<LLOQ	<LLOQ	7.12	<LLOQ	7.72	<LLOQ
M12	6.92	8.05	<LLOQ	<LLOQ	7.22	7.24	<LLOQ	<LLOQ	<LLOQ	<LLOQ	6.98	6.60	9.53	<LLOQ
M13	32.37	33.65	38.34	36.70	41.72	39.02	37.24	38.09	67.37	66.67	39.82	31.90	14.97	13.65
M14	<LLOQ	6.50	<LLOQ	<LLOQ	5.49	5.86	<LLOQ	5.61	<LLOQ	5.23	7.42	5.45	9.44	6.00
M15	38.47	34.07	31.48	27.23	18.45	19.97	15.58	15.46	12.07	12.35	52.73	46.47	22.11	18.93
M16	86.82	84.18	80.97	78.98	86.16	85.21	76.08	79.28	82.05	76.52	86.74	89.57	80.74	79.93
M17	80.91	86.04	78.01	79.01	82.18	80.69	66.42	63.99	65.24	62.22	10.83	8.82	9.20	7.67
M18	<LLOQ	<LLOQ	<LLOQ	<LLOQ	<LLOQ	<LLOQ	<LLOQ	<LLOQ	<LLOQ	<LLOQ	17.99	17.18	<LLOQ	<LLOQ
M19	77.08	73.68	60.16	59.29	71.84	71.42	63.89	57.20	77.39	68.51	>ULOQ	>ULOQ	55.87	56.38
M20	<LLOQ	<LLOQ	<LLOQ	<LLOQ	<LLOQ	<LLOQ	<LLOQ	<LLOQ	<LLOQ	<LLOQ	5.52	<LLOQ	<LLOQ	<LLOQ

	CpG11		CpG12		CpG13		CpG14		CpG15		CpG16		CpG17	
Sample	PCR #1	PCR #2	PCR #1	PCR #2	PCR #1	PCR #2	PCR #1	PCR #2	PCR #1	PCR #2	PCR #1	PCR #2	PCR #1	PCR #2
M01	60.24	64.43	86.83	87.05	83.68	85.23	80.58	80.17	80.99	78.03	90.06	85.37	>ULOQ	>ULOQ
M02	<LLOQ	<LLOQ	<LLOQ	<LLOQ	<LLOQ	<LLOQ	<LLOQ	<LLOQ	<LLOQ	<LLOQ	<LLOQ	<LLOQ	<LLOQ	<LLOQ
M03	6.35	<LLOQ	8.19	8.68	5.62	<LLOQ	6.39	7.16	<LLOQ	5.03	<LLOQ	<LLOQ	<LLOQ	16.47
M04	<LLOQ	<LLOQ	34.36	31.86	23.28	31.07	7.79	7.04	26.20	19.34	<LLOQ	6.10	12.09	7.75
M05	7.20	<LLOQ	34.78	29.96	17.02	13.10	53.74	58.46	70.85	67.97	40.46	40.59	19.98	19.31
M06	<LLOQ	<LLOQ	5.91	<LLOQ	<LLOQ	<LLOQ	<LLOQ	<LLOQ	12.41	7.07	<LLOQ	<LLOQ	<LLOQ	<LLOQ
M07	<LLOQ	<LLOQ	<LLOQ	<LLOQ	<LLOQ	5.17	<LLOQ	<LLOQ	34.90	34.35	/	17.92	8.70	7.86
M08	9.09	5.56	81.46	79.35	13.45	11.87	76.13	80.14	7.06	7.20	6.43	6.20	17.73	18.18
M09	9.04	9.21	20.60	20.49	22.28	27.94	60.26	65.34	51.35	47.12	52.42	50.96	27.99	23.24
M10	<LLOQ	<LLOQ	6.75	5.87	6.74	<LLOQ	<LLOQ	<LLOQ	<LLOQ	<LLOQ	<LLOQ	<LLOQ	5.00	5.29
M11	6.82	<LLOQ	6.75	<LLOQ	<LLOQ	<LLOQ	5.99	<LLOQ	<LLOQ	<LLOQ	<LLOQ	<LLOQ	8.22	9.86
M12	6.36	<LLOQ	9.53	<LLOQ	<LLOQ	<LLOQ	<LLOQ	<LLOQ	<LLOQ	<LLOQ	<LLOQ	<LLOQ	8.92	6.66
M13	<LLOQ	<LLOQ	33.25	33.96	12.08	14.43	10.71	10.28	50.04	43.08	63.78	64.51	39.19	38.29
M14	<LLOQ	<LLOQ	5.49	<LLOQ	5.59	5.73	<LLOQ	6.98	5.87	5.61	6.49	6.64	8.06	9.34
M15	10.49	12.89	17.73	20.71	23.62	22.40	68.61	65.63	11.38	9.05	16.79	13.84	23.05	24.44
M16	56.25	59.15	76.92	80.85	73.67	77.89	77.09	78.80	78.12	77.12	89.21	87.72	94.81	88.76
M17	<LLOQ	<LLOQ	20.99	14.58	20.38	15.58	33.52	31.01	62.05	60.89	65.97	64.87	57.91	51.96
M18	<LLOQ	<LLOQ	<LLOQ	<LLOQ	<LLOQ	<LLOQ	<LLOQ	<LLOQ	<LLOQ	<LLOQ	<LLOQ	5.23	<LLOQ	<LLOQ
M19	48.18	53.10	65.12	64.21	42.09	35.56	79.76	84.21	70.74	63.95	54.53	50.34	94.41	81.69
M20	<LLOQ	<LLOQ	<LLOQ	<LLOQ	<LLOQ	<LLOQ	<LLOQ	<LLOQ	9.40	6.43	6.71	8.34	<LLOQ	6.45

Supplementary Table 9 and 10: enh5 inter methylation levels [%] in melanoma metastasis samples determined by PSQ

	CpG12		CpG13		CpG14		CpG15		CpG16		CpG17		CpG20		CpG21		CpG22	
Sample	PCR #1	PCR #2	PCR #1	PCR #2	PCR #1	PCR #2	PCR #1	PCR #2	PCR #1	PCR #2	PCR #1	PCR #2	PCR #1	PCR #2	PCR #1	PCR #2	PCR #1	PCR #2
M01	38.00	37.35	25.60	29.67	35.34	40.33	44.71	52.66	32.57	35.43	72.86	71.31	52.14	49.99	78.98	77.46	64.02	55.62
M02	<LLOQ	<LLOQ	<LLOQ	<LLOQ	<LLOQ	<LLOQ	<LLOQ	<LLOQ	<LLOQ	<LLOQ	<LLOQ	<LLOQ	<LLOQ	<LLOQ	<LLOQ	<LLOQ	<LLOQ	<LLOQ
M03	<LLOQ	7.20	<LLOQ	<LLOQ	<LLOQ	5.73	<LLOQ	<LLOQ	<LLOQ	6.04	8.14	8.99	<LLOQ	<LLOQ	5.84	<LLOQ	<LLOQ	<LLOQ
M04	<LLOQ	<LLOQ	<LLOQ	<LLOQ	6.34	5.35	<LLOQ	<LLOQ	<LLOQ	<LLOQ	16.54	14.55	<LLOQ	<LLOQ	8.18	9.54	5.17	6.27
M05	<LLOQ	<LLOQ	<LLOQ	5.06	<LLOQ	<LLOQ	20.87	18.69	<LLOQ	<LLOQ	19.25	27.90	5.16	5.05	34.82	37.42	29.82	24.98
M06	<LLOQ	6.25	<LLOQ	<LLOQ	<LLOQ	<LLOQ	<LLOQ	<LLOQ	<LLOQ	<LLOQ	<LLOQ	6.24	<LLOQ	<LLOQ	<LLOQ	5.66	<LLOQ	<LLOQ
M07	<LLOQ	<LLOQ	<LLOQ	<LLOQ	<LLOQ	<LLOQ	<LLOQ	<LLOQ	<LLOQ	<LLOQ	<LLOQ	5.28	<LLOQ	<LLOQ	<LLOQ	<LLOQ	5.07	<LLOQ
M08	8.21	6.64	<LLOQ	10.48	53.53	52.28	5.29	7.63	<LLOQ	5.52	<LLOQ	22.51	<LLOQ	<LLOQ	5.85	<LLOQ	<LLOQ	<LLOQ
M09	<LLOQ	7.77	6.19	9.62	6.11	6.86	8.93	13.33	<LLOQ	6.06	10.51	16.31	9.14	8.90	14.94	15.86	12.18	11.61
M10	<LLOQ	<LLOQ	<LLOQ	<LLOQ	<LLOQ	<LLOQ	<LLOQ	<LLOQ	<LLOQ	<LLOQ	<LLOQ	6.26	<LLOQ	<LLOQ	<LLOQ	<LLOQ	<LLOQ	<LLOQ
M11	6.70	5.55	<LLOQ	<LLOQ	<LLOQ	<LLOQ	5.06	<LLOQ	<LLOQ	<LLOQ	7.90	7.78	<LLOQ	<LLOQ	<LLOQ	5.44	<LLOQ	<LLOQ
M12	<LLOQ	<LLOQ	<LLOQ	<LLOQ	<LLOQ	<LLOQ	<LLOQ	<LLOQ	<LLOQ	<LLOQ	<LLOQ	<LLOQ	<LLOQ	<LLOQ	<LLOQ	5.05	<LLOQ	<LLOQ
M13	5.33	7.44	<LLOQ	7.22	<LLOQ	7.54	6.20	6.09	<LLOQ	<LLOQ	14.32	16.06	5.94	5.59	10.92	8.69	6.67	5.01
M14	<LLOQ	8.37	<LLOQ	6.30	<LLOQ	7.40	<LLOQ	5.44	<LLOQ	<LLOQ	5.81	10.58	5.08	<LLOQ	8.68	6.26	5.64	<LLOQ
M15	<LLOQ	<LLOQ	<LLOQ	<LLOQ	<LLOQ	<LLOQ	<LLOQ	<LLOQ	<LLOQ	<LLOQ	<LLOQ	<LLOQ	<LLOQ	<LLOQ	<LLOQ	<LLOQ	<LLOQ	<LLOQ
M16	48.91	49.23	38.53	37.24	43.36	42.78	49.84	50.54	35.76	37.28	76.10	73.69	52.99	42.91	79.46	77.62	69.55	51.31
M17	10.51	7.46	7.33	8.63	6.28	6.03	18.54	15.92	<LLOQ	<LLOQ	15.72	15.39	<LLOQ	<LLOQ	5.01	6.61	<LLOQ	<LLOQ
M18	<LLOQ	<LLOQ	7.71	5.26	5.83	<LLOQ	<LLOQ	<LLOQ	<LLOQ	<LLOQ	10.83	<LLOQ	<LLOQ	<LLOQ	5.00	6.73	<LLOQ	<LLOQ
M19	13.31	13.47	9.62	9.14	29.64	26.97	24.15	24.25	9.51	8.48	19.68	19.28	6.95	5.78	14.82	15.79	14.41	11.80
M20	8.64	10.11	6.05	<LLOQ	<LLOQ	<LLOQ	5.58	<LLOQ	<LLOQ	<LLOQ	8.70	8.53	<LLOQ	<LLOQ	<LLOQ	6.17	<LLOQ	<LLOQ

	CpG23		CpG24		CpG25		CpG26		CpG27		CpG27+1	
Sample	PCR #1	PCR #2	PCR #1	PCR #2	PCR #1	PCR #2	PCR #1	PCR #2	PCR #1	PCR #2	PCR #1	PCR #2
M01	73.84	75.74	83.29	81.22	53.76	50.47	67.37	61.83	84.44	79.35	6.18	6.23
M02	<LLOQ	5.02	<LLOQ	5.67	<LLOQ	<LLOQ	<LLOQ	<LLOQ	5.34	<LLOQ	<LLOQ	<LLOQ
M03	<LLOQ	<LLOQ	<LLOQ	<LLOQ	<LLOQ	<LLOQ	<LLOQ	<LLOQ	<LLOQ	<LLOQ	<LLOQ	<LLOQ
M04	17.97	15.26	39.32	33.26	17.00	14.51	<LLOQ	<LLOQ	35.86	31.89	5.88	5.44
M05	52.64	51.37	79.79	75.92	<LLOQ	<LLOQ	<LLOQ	<LLOQ	<LLOQ	<LLOQ	<LLOQ	<LLOQ
M06	<LLOQ	<LLOQ	<LLOQ	<LLOQ	<LLOQ	<LLOQ	<LLOQ	<LLOQ	<LLOQ	5.31	<LLOQ	<LLOQ
M07	15.08	18.16	32.12	34.17	<LLOQ	<LLOQ	<LLOQ	<LLOQ	<LLOQ	<LLOQ	<LLOQ	<LLOQ
M08	<LLOQ	<LLOQ	<LLOQ	<LLOQ	<LLOQ	7.45	<LLOQ	<LLOQ	6.55	<LLOQ	<LLOQ	<LLOQ
M09	20.31	21.36	34.34	31.50	15.69	17.45	19.61	21.26	36.51	32.90	<LLOQ	<LLOQ
M10	<LLOQ	<LLOQ	<LLOQ	<LLOQ	<LLOQ	<LLOQ	<LLOQ	<LLOQ	<LLOQ	<LLOQ	<LLOQ	<LLOQ
M11	<LLOQ	<LLOQ	<LLOQ	<LLOQ	<LLOQ	<LLOQ	<LLOQ	<LLOQ	<LLOQ	<LLOQ	<LLOQ	<LLOQ
M12	<LLOQ	<LLOQ	<LLOQ	<LLOQ	<LLOQ	<LLOQ	<LLOQ	<LLOQ	<LLOQ	<LLOQ	<LLOQ	<LLOQ
M13	6.29	10.22	6.03	9.93	15.78	16.73	21.52	20.93	35.48	34.07	<LLOQ	<LLOQ
M14	<LLOQ	<LLOQ	<LLOQ	5.65	<LLOQ	<LLOQ	<LLOQ	<LLOQ	<LLOQ	<LLOQ	<LLOQ	<LLOQ
M15	<LLOQ	<LLOQ	<LLOQ	<LLOQ	<LLOQ	<LLOQ	<LLOQ	<LLOQ	<LLOQ	<LLOQ	<LLOQ	<LLOQ
M16	67.51	71.20	71.14	73.22	38.78	42.74	<LLOQ	5.71	66.49	70.68	10.85	11.60
M17	9.19	7.76	23.84	24.67	5.04	<LLOQ	<LLOQ	<LLOQ	8.32	5.78	<LLOQ	<LLOQ
M18	<LLOQ	<LLOQ	<LLOQ	<LLOQ	<LLOQ	<LLOQ	<LLOQ	<LLOQ	<LLOQ	<LLOQ	<LLOQ	<LLOQ
M19	13.70	7.54	16.55	20.39	6.08	5.11	10.52	7.11	15.90	11.83	<LLOQ	<LLOQ
M20	16.39	17.17	33.29	32.62	<LLOQ	<LLOQ	<LLOQ	<LLOQ	7.97	9.78	<LLOQ	<LLOQ

Supplementary Table 11 and 12: MGMT promoter methylation levels [%] in melanoma metastasis samples determined by PSQ

	CpG72		CpG73		CpG74		CpG75		CpG76		CpG77		CpG78		CpG79		CpG80	
Sample	PCR #1	PCR #2	PCR #1	PCR #2	PCR #1	PCR #2	PCR #1	PCR #2	PCR #1	PCR #2	PCR #1	PCR #2	PCR #1	PCR #2	PCR #1	PCR #2	PCR #1	PCR #2
M01	<LLOQ	<LLOQ	<LLOQ	<LLOQ	<LLOQ	<LLOQ	<LLOQ	<LLOQ	<LLOQ	<LLOQ	<LLOQ	<LLOQ	<LLOQ	<LLOQ	<LLOQ	<LLOQ	<LLOQ	<LLOQ
M02	42.87	32.98	37.80	29.22	58.62	68.88	58.51	63.53	49.32	53.60	31.23	20.62	59.58	55.38	92.05	>ULOQ	76.72	77.00
M03	7.59	7.31	8.83	7.32	6.89	<LLOQ	8.65	7.73	6.51	7.55	<LLOQ	<LLOQ	5.92	6.80	25.72	34.08	27.28	28.18
M04	72.82	68.07	80.84	80.20	92.80	91.43	88.64	85.18	49.91	51.68	87.14	86.85	21.71	25.10	46.09	49.43	57.21	62.18
M05	<LLOQ	<LLOQ	<LLOQ	<LLOQ	<LLOQ	<LLOQ	<LLOQ	<LLOQ	<LLOQ	<LLOQ	<LLOQ	<LLOQ	<LLOQ	<LLOQ	<LLOQ	<LLOQ	<LLOQ	<LLOQ
M06	<LLOQ	<LLOQ	<LLOQ	<LLOQ	<LLOQ	<LLOQ	<LLOQ	<LLOQ	<LLOQ	<LLOQ	<LLOQ	<LLOQ	<LLOQ	<LLOQ	<LLOQ	<LLOQ	<LLOQ	<LLOQ
M07	<LLOQ	<LLOQ	<LLOQ	<LLOQ	<LLOQ	<LLOQ	<LLOQ	<LLOQ	<LLOQ	<LLOQ	<LLOQ	<LLOQ	<LLOQ	<LLOQ	<LLOQ	5.02	<LLOQ	<LLOQ
M08	<LLOQ	<LLOQ	<LLOQ	<LLOQ	<LLOQ	<LLOQ	<LLOQ	<LLOQ	<LLOQ	<LLOQ	<LLOQ	<LLOQ	<LLOQ	<LLOQ	<LLOQ	<LLOQ	<LLOQ	<LLOQ
M09	9.34	8.86	11.53	12.26	7.44	7.38	8.22	9.58	9.61	12.02	<LLOQ	7.53	<LLOQ	<LLOQ	10.67	13.46	12.69	17.37
M10	<LLOQ	<LLOQ	<LLOQ	<LLOQ	<LLOQ	<LLOQ	<LLOQ	<LLOQ	<LLOQ	6.06	<LLOQ	<LLOQ	<LLOQ	<LLOQ	<LLOQ	<LLOQ	<LLOQ	<LLOQ
M11	<LLOQ	<LLOQ	<LLOQ	<LLOQ	<LLOQ	5.50	5.63	<LLOQ	7.60	9.82	6.55	6.86	6.94	9.95	44.60	51.74	34.95	38.21
M12	<LLOQ	<LLOQ	<LLOQ	<LLOQ	5.74	<LLOQ	<LLOQ	<LLOQ	5.45	<LLOQ	7.33	<LLOQ	6.29	<LLOQ	32.64	37.74	22.02	21.75
M13	54.00	45.50	51.47	42.38	53.61	50.25	51.21	46.30	58.09	54.63	52.46	46.98	55.22	52.77	58.92	62.60	42.55	42.80
M14	22.72	24.02	51.68	38.74	66.34	57.92	81.94	80.52	93.65	>ULOQ	89.90	84.47	92.26	92.30	>ULOQ	>ULOQ	76.08	72.21
M15	<LLOQ	<LLOQ	<LLOQ	<LLOQ	<LLOQ	<LLOQ	<LLOQ	<LLOQ	<LLOQ	<LLOQ	<LLOQ	<LLOQ	<LLOQ	<LLOQ	<LLOQ	<LLOQ	<LLOQ	<LLOQ
M16	<LLOQ	<LLOQ	<LLOQ	<LLOQ	<LLOQ	<LLOQ	<LLOQ	<LLOQ	<LLOQ	<LLOQ	<LLOQ	<LLOQ	<LLOQ	<LLOQ	<LLOQ	<LLOQ	<LLOQ	<LLOQ
M17	18.27	17.03	20.17	22.23	26.80	28.36	21.78	25.74	20.71	20.93	13.31	13.64	14.02	19.20	13.07	19.61	14.15	17.83
M18	<LLOQ	<LLOQ	<LLOQ	<LLOQ	<LLOQ	<LLOQ	<LLOQ	<LLOQ	<LLOQ	<LLOQ	<LLOQ	<LLOQ	<LLOQ	<LLOQ	<LLOQ	6.53	<LLOQ	<LLOQ
M19	<LLOQ	<LLOQ	<LLOQ	<LLOQ	<LLOQ	<LLOQ	<LLOQ	<LLOQ	<LLOQ	<LLOQ	<LLOQ	<LLOQ	<LLOQ	<LLOQ	<LLOQ	<LLOQ	<LLOQ	<LLOQ
M20	>ULOQ	92.85	89.45	89.88	92.32	91.81	50.44	52.76	54.52	56.24	80.34	80.90	15.79	22.09	93.30	>ULOQ	75.69	68.95

	CpG81		CpG82		CpG83	
Sample	PCR #1	PCR #2	PCR #1	PCR #2	PCR #1	PCR #2
M01	<LLOQ	<LLOQ	<LLOQ	<LLOQ	<LLOQ	<LLOQ
M02	84.78	75.16	85.16	79.84	85.64	81.33
M03	34.53	33.28	28.31	27.59	31.82	29.97
M04	83.42	71.14	94.42	84.69	64.14	60.93
M05	<LLOQ	<LLOQ	<LLOQ	<LLOQ	<LLOQ	<LLOQ
M06	<LLOQ	<LLOQ	<LLOQ	<LLOQ	<LLOQ	<LLOQ
M07	<LLOQ	<LLOQ	<LLOQ	<LLOQ	<LLOQ	<LLOQ
M08	<LLOQ	<LLOQ	<LLOQ	<LLOQ	<LLOQ	<LLOQ
M09	11.42	14.47	13.48	20.77	7.86	8.52
M10	<LLOQ	<LLOQ	<LLOQ	<LLOQ	<LLOQ	<LLOQ
M11	38.6	36.96	36.01	37.95	26.41	22.33
M12	41.61	36.11	17.32	16.65	50.55	46.89
M13	45.79	38.49	52.95	47.72	46.55	41.98
M14	52.98	44.55	89.38	84.74	82.25	72.47
M15	<LLOQ	<LLOQ	<LLOQ	<LLOQ	<LLOQ	<LLOQ
M16	<LLOQ	<LLOQ	<LLOQ	<LLOQ	<LLOQ	<LLOQ
M17	16.68	16.58	25.51	31.47	20.37	25.12
M18	5.33	5.64	6.53	7.19	13.52	16.59
M19	<LLOQ	<LLOQ	<LLOQ	<LLOQ	<LLOQ	<LLOQ
M20	87.99	72.19	66.64	65.17	86.1	78.56

Supplementary Table 13: enh6 intra methylation levels [%] in melanoma metastasis samples determined by PSQ

	CpG8		CpG9		CpG10	
Sample	PCR #1	PCR #2	PCR #1	PCR #2	PCR #1	PCR #2
M01	>ULOQ	94.38	89.06	87.66	84.02	80.96
M02	5.37	5.12	8.10	16.00	7.54	9.30
M03	18.55	15.92	42.01	38.18	21.22	18.78
M04	56.05	62.58	73.88	72.20	53.80	54.17
M05	83.30	84.74	88.59	83.58	80.16	73.95
M06	81.20	87.00	79.53	75.37	66.84	67.58
M07	69.37	71.16	78.77	76.74	71.38	67.05
M08	>ULOQ	>ULOQ	93.33	93.19	82.05	85.59
M09	61.14	67.07	83.18	83.12	79.04	83.51
M10	>ULOQ	>ULOQ	90.09	88.19	80.70	76.89
M11	8.19	14.07	8.13	15.00	8.10	14.25
M12	12.08	12.40	14.70	26.70	9.44	12.63
M13	72.83	66.97	87.65	87.70	77.20	83.03
M14	9.08	7.03	12.86	9.56	9.64	<LLOQ
M15	>ULOQ	94.20	89.80	92.52	82.90	83.14
M16	>ULOQ	>ULOQ	92.13	85.70	85.25	77.18
M17	41.18	37.73	85.79	84.25	79.58	77.91
M18	<LLOQ	<LLOQ	11.73	17.23	9.08	10.81
M19	>ULOQ	>ULOQ	91.63	90.05	87.54	85.86
M20	<LLOQ	8.70	20.62	21.16	12.63	17.20

Supplementary Table 14 and 15: enh7 intra methylation levels [%] in melanoma metastasis samples determined by PSQ

	CpG1		CpG2		CpG3		CpG7		CpG8		CpG9		CpG10		CpG11		CpG12	
Sample	PCR #1	PCR #2	PCR #1	PCR #2	PCR #1	PCR #2	PCR #1	PCR #2	PCR #1	PCR #2	PCR #1	PCR #2	PCR #1	PCR #2	PCR #1	PCR #2	PCR #1	PCR #2
M01	66.36	73.91	52.24	51.93	89.45	89.43	>ULOQ	92.95	88.27	87.57	82.67	85.79	77.12	74.16	>ULOQ	>ULOQ	79.14	82.76
M02	<LLOQ	5.19	7.77	5.86	<LLOQ	<LLOQ	<LLOQ	<LLOQ	<LLOQ	<LLOQ	<LLOQ	<LLOQ	<LLOQ	<LLOQ	12.52	10.76	7.71	6.96
M03	19.15	22.68	9.32	8.24	10.88	11.29	9.27	9.40	5.73	<LLOQ	11.84	6.12	17.69	11.29	21.60	10.93	11.74	<LLOQ
M04	12.55	8.98	8.99	5.43	<LLOQ	<LLOQ	43.23	39.82	<LLOQ	<LLOQ	41.86	44.72	70.48	66.34	66.71	66.58	49.78	41.75
M05	64.12	70.97	70.77	72.80	54.76	56.08	87.17	85.15	71.49	70.94	80.24	77.85	75.03	70.73	92.17	85.96	75.83	79.43
M06	46.28	45.27	35.76	25.51	45.77	44.97	66.60	69.22	60.64	62.03	58.09	54.41	64.96	62.42	84.87	84.27	57.75	65.14
M07	30.87	36.63	20.50	17.72	16.27	13.08	74.04	73.11	20.02	17.41	19.02	15.83	48.64	56.87	69.44	63.77	55.22	63.05
M08	71.19	74.48	75.03	78.27	91.24	90.74	94.90	>ULOQ	81.98	87.51	84.39	75.73	71.04	63.73	>ULOQ	88.90	78.11	85.21
M09	51.05	49.87	52.07	52.14	34.61	38.94	71.25	71.49	57.21	60.46	52.14	60.08	53.27	60.43	72.56	76.40	65.17	74.50
M10	65.40	71.00	83.79	87.62	91.67	93.69	93.87	>ULOQ	89.57	90.36	88.05	83.31	77.91	75.33	94.31	>ULOQ	80.32	78.64
M11	11.29	8.49	12.22	8.54	6.65	<LLOQ	7.83	7.52	7.71	8.53	6.63	5.21	5.63	<LLOQ	5.76	7.65	<LLOQ	5.93
M12	16.21	9.89	7.47	5.31	5.77	6.92	<LLOQ	5.21	5.00	<LLOQ	<LLOQ	5.12	7.03	<LLOQ	7.64	5.02	6.31	<LLOQ
M13	34.18	37.12	31.84	30.24	26.27	18.45	39.53	44.93	15.72	9.86	28.94	31.02	31.32	32.58	52.21	49.23	67.26	65.23
M14	8.02	10.68	8.64	11.15	5.23	5.78	5.66	5.45	6.31	6.64	6.08	<LLOQ	5.62	<LLOQ	8.19	<LLOQ	6.23	<LLOQ
M15	67.50	65.30	5.80	8.22	<LLOQ	<LLOQ	14.66	11.66	57.74	63.75	45.67	27.25	73.36	74.95	94.84	94.71	45.93	55.99
M16	62.54	68.70	58.31	65.01	81.18	83.04	90.30	92.85	86.93	88.16	83.45	76.07	77.30	75.10	91.59	94.44	78.22	80.85
M17	14.83	12.00	7.55	9.02	<LLOQ	<LLOQ	12.45	17.07	<LLOQ	<LLOQ	5.30	<LLOQ	55.51	55.79	64.59	65.72	49.15	56.22
M18	<LLOQ	<LLOQ	5.75	5.25	<LLOQ	<LLOQ	<LLOQ	<LLOQ	<LLOQ	<LLOQ	<LLOQ	<LLOQ	6.54	<LLOQ	9.89	5.80	7.04	9.05
M19	69.31	76.03	73.99	79.24	86.56	78.52	>ULOQ	>ULOQ	88.72	88.56	83.11	78.99	79.82	73.85	>ULOQ	94.30	81.85	80.56
M20	10.53	8.38	7.30	6.16	<LLOQ	<LLOQ	5.07	<LLOQ	<LLOQ	<LLOQ	<LLOQ	<LLOQ	26.05	24.90	30.84	38.11	8.88	6.00

	CpG13		CpG19		CpG20		CpG21		CpG22	
Sample	PCR #1	PCR #2	PCR #1	PCR #2	PCR #1	PCR #2	PCR #1	PCR #2	PCR #1	PCR #2
M01	88.56	83.37	>ULOQ	93.37	94.75	93.49	>ULOQ	>ULOQ	91.29	92.91
M02	5.04	5.63	<LLOQ	<LLOQ	6	10.94	<LLOQ	6.08	<LLOQ	<LLOQ
M03	12.34	<LLOQ	6.87	7.98	18.41	22.28	8.58	11.28	7.85	9.64
M04	39.95	28.05	62.4	67.28	86.09	94.1	82.27	89.52	81.89	87.19
M05	79.78	81.32	94.09	92.38	94.83	92.82	88.06	90.53	84.85	87.02
M06	63.57	66.09	67.15	70.32	81.69	77.67	71.5	76.26	66.92	65.41
M07	51.48	53.38	87.58	86.1	94.72	93.58	85.88	89.42	86.27	83.65
M08	79.58	85.69	87.92	94.27	>ULOQ	>ULOQ	89.38	94.82	93.93	85.18
M09	70.12	76.69	84.11	85.23	91.63	93.89	90.66	88.4	87.38	85.14
M10	66.32	69.42	>ULOQ	94.64	>ULOQ	>ULOQ	>ULOQ	94.47	94.55	89.91
M11	5.36	5.78	10.09	6.63	18.72	14.42	11.68	8.89	8.88	<LLOQ
M12	5.79	<LLOQ	6.73	5.74	15.27	19.92	7.62	11.75	8.88	5.89
M13	66.48	70.73	74.73	77.93	90.43	90.35	76.93	84.93	77.67	82.16
M14	5.46	5.51	6.31	22.82	9.41	30.81	8.09	24.98	<LLOQ	19.27
M15	55.18	64.36	>ULOQ	91.75	>ULOQ	>ULOQ	90.8	93.96	92.56	90.87
M16	82.01	83.78	90.82	93.48	93.15	>ULOQ	92.41	>ULOQ	92.02	91.62
M17	45.89	50.24	72.86	72.53	91.71	89.11	42.84	47.9	77.5	70.02
M18	7.22	7.11	5.67	10.5	14.12	21.96	6.17	11.9	6.15	6.55
M19	78.69	81.18	90.2	93.87	93.35	93.87	49.1	57.72	90.76	87.92
M20	7.72	6.33	37.05	37.36	49.39	51.8	13.06	19.29	39.01	38.79

Supplementary Table 16: enh8 intra methylation levels [%] in melanoma metastasis samples determined by PSQ

	CpG2		CpG3		CpG4		CpG6		CpG7		CpG10		CpG11		CpG12		CpG13	
Sample	PCR #1	PCR #2	PCR #1	PCR #2	PCR #1	PCR #2	PCR #1	PCR #2	PCR #1	PCR #2	PCR #1	PCR #2	PCR #1	PCR #2	PCR #1	PCR #2	PCR #1	PCR #2
M01	66.37	70.15	83.50	86.04	94.32	>ULOQ	89.13	83.85	>ULOQ	>ULOQ	>ULOQ	94.15	65.97	58.96	93.48	>ULOQ	60.75	46.99
M02	<LLOQ	<LLOQ	<LLOQ	5.29	<LLOQ	<LLOQ	<LLOQ	<LLOQ	<LLOQ	<LLOQ	<LLOQ	<LLOQ	<LLOQ	<LLOQ	<LLOQ	<LLOQ	<LLOQ	<LLOQ
M03	9.41	6.11	15.98	7.26	13.71	5.01	7.98	12.36	7.75	10.36	<LLOQ	<LLOQ	<LLOQ	<LLOQ	5.99	<LLOQ	<LLOQ	<LLOQ
M04	7.03	5.20	22.80	24.43	15.62	17.84	75.01	73.26	82.26	85.85	<LLOQ	6.79	22.37	27.72	8.94	12.40	6.85	<LLOQ
M05	64.69	64.81	41.37	48.23	41.75	41.03	86.95	81.32	>ULOQ	91.64	46.42	47.82	57.04	53.79	78.95	86.75	55.53	>ULOQ
M06	58.76	54.40	48.43	53.46	45.17	35.97	75.43	66.83	80.41	78.48	62.23	59.22	36.98	38.22	59.23	61.90	35.21	24.76
M07	34.13	31.34	57.75	56.53	24.00	27.57	51.88	55.82	58.13	64.82	40.49	42.66	16.28	10.67	9.62	12.88	9.77	7.37
M08	71.05	70.76	86.25	84.70	81.66	81.25	83.58	78.86	>ULOQ	>ULOQ	81.20	88.95	62.40	52.47	88.75	87.42	61.67	42.77
M09	55.04	56.05	66.35	65.52	64.53	59.67	63.87	55.35	70.26	74.59	72.92	71.37	39.26	37.31	63.88	64.84	34.45	25.45
M10	72.28	76.23	83.19	87.74	>ULOQ	94.64	88.87	84.01	>ULOQ	>ULOQ	94.85	93.27	62.61	49.94	91.66	91.53	59.23	42.25
M11	6.33	5.78	7.46	5.74	<LLOQ	<LLOQ	8.74	5.52	9.86	6.15	8.63	9.14	<LLOQ	6.46	6.56	9.88	<LLOQ	<LLOQ
M12	<LLOQ	<LLOQ	<LLOQ	5.22	<LLOQ	<LLOQ	<LLOQ	<LLOQ	5.26	<LLOQ	<LLOQ	<LLOQ	<LLOQ	<LLOQ	<LLOQ	<LLOQ	<LLOQ	<LLOQ
M13	34.68	26.85	32.17	29.41	32.58	33.18	38.40	43.81	44.39	53.71	44.76	48.62	26.01	25.34	36.64	48.24	29.58	20.83
M14	6.24	7.31	5.83	6.62	5.44	<LLOQ	6.88	7.07	7.67	8.00	6.89	5.56	<LLOQ	<LLOQ	34.33	33.57	25.02	18.00
M15	64.41	73.24	53.68	51.83	33.66	31.30	86.69	80.02	>ULOQ	>ULOQ	79.17	86.29	57.38	45.92	53.79	58.47	49.75	35.54
M16	71.91	76.60	80.56	85.67	87.59	83.28	89.17	88.08	>ULOQ	>ULOQ	>ULOQ	90.41	65.47	51.90	93.40	91.27	60.75	41.41
M17	<LLOQ	<LLOQ	<LLOQ	<LLOQ	5.80	<LLOQ	79.54	83.31	91.76	92.91	<LLOQ	5.32	9.24	9.62	18.84	19.91	7.65	7.74
M18	<LLOQ	<LLOQ	<LLOQ	<LLOQ	<LLOQ	<LLOQ	5.26	6.34	<LLOQ	10.42	<LLOQ	<LLOQ	<LLOQ	<LLOQ	<LLOQ	<LLOQ	<LLOQ	<LLOQ
M19	72.20	67.50	81.76	82.75	>ULOQ	>ULOQ	83.87	84.91	>ULOQ	>ULOQ	94.07	94.63	61.89	51.23	92.41	94.27	58.17	39.74
M20	<LLOQ	<LLOQ	7.52	5.30	6.68	<LLOQ	5.27	<LLOQ	<LLOQ	<LLOQ	<LLOQ	5.06	10.52	10.32	8.61	9.76	12.08	6.89

Supplementary Table 17: enh9 intra methylation levels [%] in melanoma metastasis samples determined by PSQ

	CpG6		CpG7		CpG8		CpG9		CpG10		CpG11	
Sample	PCR #1	PCR #2	PCR #1	PCR #2	PCR #1	PCR #2	PCR #1	PCR #2	PCR #1	PCR #2	PCR #1	PCR #2
M01	92.65	>ULOQ	91.42	93.03	71.54	67.14	74.91	72.67	67.95	63.33	>ULOQ	>ULOQ
M02	9.08	5.60	<LLOQ	<LLOQ	<LLOQ	<LLOQ	<LLOQ	<LLOQ	<LLOQ	<LLOQ	6.26	7.96
M03	26.13	26.05	29.82	36.40	13.79	15.28	15.66	14.08	34.95	35.00	35.80	47.14
M04	67.82	73.81	77.84	80.70	65.90	64.87	78.64	70.32	71.36	64.95	>ULOQ	>ULOQ
M05	86.77	93.59	81.18	87.96	75.63	69.97	78.49	74.46	75.49	65.19	>ULOQ	>ULOQ
M06	73.40	72.40	72.09	78.53	58.08	58.81	69.46	63.86	66.36	62.24	93.91	91.48
M07	42.21	49.31	57.78	69.31	50.40	50.96	54.25	54.55	60.69	54.63	43.74	47.95
M08	>ULOQ	>ULOQ	92.09	94.79	76.70	68.09	81.79	72.21	73.70	62.62	>ULOQ	>ULOQ
M09	61.05	55.42	73.59	72.17	63.54	58.18	68.42	62.16	72.55	63.11	93.91	91.79
M10	>ULOQ	>ULOQ	92.40	91.48	75.33	69.44	81.66	77.27	72.94	67.59	>ULOQ	>ULOQ
M11	10.30	7.02	12.23	9.54	7.43	<LLOQ	6.49	<LLOQ	9.01	7.19	13.01	10.98
M12	10.57	9.01	15.12	13.37	7.60	<LLOQ	<LLOQ	5.20	7.24	7.34	10.32	10.06
M13	65.15	63.97	78.75	75.00	70.51	64.49	70.16	69.19	69.35	63.91	90.18	>ULOQ
M14	49.45	39.48	50.40	44.60	35.39	31.48	15.01	14.51	36.56	31.25	51.40	50.84
M15	91.68	94.18	89.06	87.28	74.31	67.18	62.37	60.06	68.63	63.03	>ULOQ	95.00
M16	>ULOQ	>ULOQ	95.00	>ULOQ	70.81	75.17	77.75	79.87	68.04	73.31	>ULOQ	>ULOQ
M17	53.19	45.35	68.04	68.87	66.29	63.99	68.03	64.13	73.42	71.11	>ULOQ	>ULOQ
M18	8.09	5.18	7.18	5.89	9.50	8.01	7.17	8.04	18.49	17.08	15.54	17.63
M19	>ULOQ	>ULOQ	>ULOQ	94.55	70.76	65.82	76.74	74.39	71.23	61.74	>ULOQ	>ULOQ
M20	7.87	<LLOQ	9.69	7.90	9.42	8.30	11.73	9.02	33.13	34.16	45.66	51.96

8.3 Clinical data on melanoma metastasis samples

Supplementary Table 18: Clinical data on melanoma metastasis samples

Sample	Date of establishment	Operation	Histology	Stable cell line yes (1)	MGMT protexpr.	MGMT mRNA expr	dead (1) alive(0)
M01	10.09.2001	Brain Metastasis	Melanoma	1	0.00	4.20	1
M02	22.12.2011	Brain Metastasis	Melanoma	1	0.00	0.00	1
M03	01.02.2012	Brain Metastasis recurrence	Melanoma	1	0.20	0.00	1
M04	24.09.2013	Brain Metastasis	Melanoma	1	0.00	0.90	1
M05	30.06.2015	Brain Metastasis	Melanoma	1	0.19	0.38	1
M06	02.06.2006	Brain Metastasis	Melanoma	1	0.00	4.00	1
M07	17.05.2016	Brain Metastasis	Melanoma	1	0.14	0.66	1
M08	19.05.2016	Brain Metastasis	Melanoma	1	0.03	1.03	1
M09	06.10.2006	Brain Metastasis	Melanoma	1	0.00	1.50	1
M10	12.07.2007	Brain Metastasis	Melanoma	1	0.12	1.80	1
M11	11.02.2008	Brain Metastasis recurrence	Melanoma	1	0.00	0.00	1
M12	08.05.2008	Brain Metastasis recurrence	Melanoma	1	0.00	0.34	/
M13	28.11.2005	Brain Metastasis	Melanoma	1	0.20	0.90	1
M14	04.11.2009	Brain Metastasis	Melanoma	1	0.00	1.70	1
M15	24.01.2002	Brain Metastasis	Melanoma	1	0.40	1.70	1
M16	25.01.2001	Brain Metastasis	Melanoma	1	0.50	3.50	1
M17	12.10.2000	Brain Metastasis	Melanoma	1	0.00	0.00	1
M18	20.03.2000	Brain Metastasis	Melanoma	1	0.00	0.00	1
M19	07.08.2000	Brain Metastasis	Melanoma	1	0.50	1.00	/
M20	10.10.2002	Brain Metastasis	Melanoma	1	0.00	0.70	1

8.4 List of figures

8.5 List of tables

8.6 List of abbreviations

%	percent
°C	degrees Celsius
µg	microgram(s)
µL	microliter(s)
µM	micromolar
5-hmC	5-hydroxymethylcytosine
5-mC	5-methylcytosine
A	adenine
APS	adenosine 5’ phosphosulfate
ATP	adenosine triphosphate
BS	bisulfite sequencing
Btn	biotin label
C	cytosine
CAPS	chemically assisted pyridine borane sequencing
CpG	cytosine-phosphate-guanine dinucleotide
Ct	cycle threshold
dATP	deoxyadenosine triphosphate
dATPαS	deoxyadenosine alpha-thio triphosphate
dCTP	deoxycytidine triphosphate
dGTP	deoxyguanosine triphosphate
DNA	deoxyribonucleic acid
dTTP	deoxythymidine triphosphate
dXTP	deoxynucleoside triphosphate
G	guanine
HC	hippocampus
L	Liter(s)
LLOQ	lower limit of quantification
MGMT	O6-methylguanine-DNA methyltransferase
mRNA	messenger ribonucleic acid
NCBI	National Center for Biotechnology Information
NGS	next generation sequencing
NTC	no-template control
OS	overall survival
oxBS	oxidative bisulfite sequencing
PCR	polymerase chain reaction
PPi	pyrophosphate
PSQ	pyrosequencing
RNA	ribonucleic acid
rRNA	ribosomal ribonucleic acid
rcf	relative centrifugal force

SNP	single nucleotide polymorphism
T	temperature
T	thymine
Ta	annealing temperature
Tm	melting temperature
TMZ	temozolomide
U	uracil
ULOQ	upper limit of quantification